

Supporting Information

for

**Tetracyclic silaheterocycle formed through a pericyclic reaction cascade
including a two-fold intramolecular C–C bond activation**

Joschua Helmer,^[a] Olli J. Pakkanen,^[b] Chris Gendy,^[b] Alexander Hepp,^[a] Heikki M Tuononen,^{[b]*} Felicitas Lips^{[a]*}

^[a] Institut für Anorganische und Analytische Chemie, Corrensstraße 28-30, 48149 Münster (Germany)

^[b] Department of Chemistry, NanoScience Centre, P.O. Box 35, FI-40014 University of Jyväskylä (Finland)

Table of Contents

1. General Experimental Procedures	1
2. Synthesis and Characterization of 1–3, 8, 9, and 19'	2
2.1. Synthesis and Characterization of 1.....	2
2.2. Synthesis and Characterization of 2.....	8
2.3. Synthesis and Characterization of 3.....	15
2.4. Synthesis and Characterization of 8.....	24
2.5. Synthesis and Characterization of 9.....	31
2.6. Synthesis and Characterization of 19'	37
2.7. Synthesis and Characterization of 19.....	45
3. Details of Single Crystal X-ray Diffraction Analyses	53
3.1. Refinement Details.....	53
4. Computational Details.....	61
5. References	63

1. General Experimental Procedures

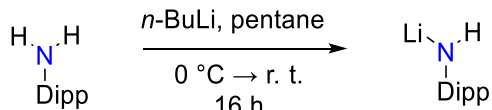
All reactions were performed with the use of modified Schlenk techniques with additional manipulations using an inert atmosphere MBraun glovebox. All solvents were obtained from commercial providers and dried over sodium benzophenone or calcium hydride, distilled, and stored over 4 Å molecular sieves prior to use. Silicon tetrabromide, *n*-butyllithium, 2,6-diisopropylaniline, and chloro(dimethyl)phenylsilane were purchased from Aldrich (Merck) and used without further purification. Ethene (2.5, 99.5%) was purchased from Westfalen AG and was used as received. 2,3-Dimethyl-1,3-butadiene was dried with CaH₂, vacuum distilled, and degassed (freeze-pump-thaw) three times prior to use. Activated magnesium (Mg*)^{S1,S2} and tribromosilane {N(SiMe₃)Dipp}SiBr₃^{S3} were prepared according to literature procedures.

All NMR data were obtained on Bruker Avance I and III spectrometers. The spectra were referenced to deuterated solvents (C₆D₆ or *d*₈-THF), according to an IUPAC recommendation, or internally to residual solvent resonances at 300 K. ¹H, ¹³C and ²⁹Si NMR chemical shifts are reported with respect to tetramethylsilane (TMS, δ = 0 ppm), whereas ammonia (NH₃, δ = 0 ppm) is used as a reference for ¹⁵N. Further explanation of the ²⁹Si NMR experiments: ²⁹Si{¹H}-DEPT19.5 = ²⁹Si proton decoupled NMR measurement with Distortionless Enhancement Polarization Transfer method, pulse angle 19.5°, coupling to 9 protons as polarization source with coupling ²J_{Si-H} = 7 Hz; ²⁹Si DEPT 24.1-NMR = ²⁹Si NMR measurement with Distortionless Enhancement Polarization Transfer method, pulse angle 24.1°, coupling to 6 protons as polarization source with coupling ²J_{Si-H} = 7 Hz; ²⁹Si{¹H}-IG = ²⁹Si proton decoupled Inverse Gated NMR measurement.

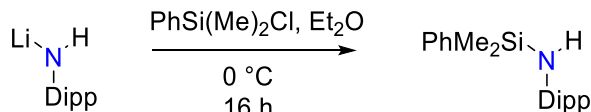
IR spectra were recorded as KBr pellets on a Shimadzu IR PRESTIGE 21 spectrometer. UV-Visible spectra were recorded as dilute *n*-hexane solutions in 1 mL quartz cuvettes using an Agilent Cary 100 spectrometer. Mass spectrometry was performed with a Varian MAT 212 Micromass Quattro LC-Z device. Melting points were measured in glass capillaries sealed under argon gas by using a Stuart Melting Point Apparatus SMP3 and are uncorrected.

2. Synthesis and Characterization of 1–3, 8, 9, and 19'

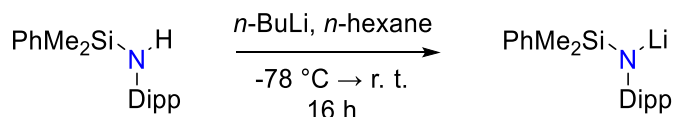
2.1. Synthesis and Characterization of 1



A solution of *n*-BuLi (1.6 M in *n*-hexane; 26 mL, 42 mmol, 1.0 equiv.) was added dropwise to a solution of DippNH₂ (8.0 mL, 42 mmol, 1.0 equiv.) in pentane (50 mL) at 0 °C. The reaction mixture was allowed to warm to room temperature and was stirred for 16 h. The colourless precipitate, LiDippNH, was filtered off, dried *in vacuo*, and used without further purification.



LiDippNH (7.0 g, 32 mmol, 1.0 eq.) was dissolved in Et₂O (150 mL) and cooled to 0 °C. Chloro(dimethyl)phenylsilane (6.4 mL, 32 mmol, 1.0 eq.) was added dropwise and the mixture was stirred overnight at 0 °C. The colourless precipitate was filtered off and the volatiles were removed *in vacuo* to give {N(SiMe₂Ph)Dipp}H as an orange oil that was used without further purification.



1

{N(SiMe₂Ph)Dipp}H (15.840 g, 50.9 mmol, 1.0 equiv.) was dissolved in *n*-hexane (50 mL) and *n*-BuLi (1.6 M in *n*-hexane; 31.8 mL, 50.9 mmol, 1.0 equiv.) was added slowly at -78 °C. The reaction mixture was allowed to warm to room temperature and was stirred for 16 h. The colourless precipitate was isolated *via* filtration and all volatile components are removed *in vacuo* to obtain {N(SiMe₂Ph)Dipp}Li **1** (14.882 g, 46.9 mmol, 92%) as a colourless precipitate. Single crystals of **1** were grown from a concentrated *n*-hexane solution at -32 °C.

¹H-NMR (d_8 -THF, 300 K, 400 MHz): δ [ppm] = 7.57–7.54 (2H, m, *ortho*-H_{Ph}), 7.15–7.06 (3H, m, *meta/para*-H_{Ph}), 6.73 (2H, m, *meta*-H_{Dipp}), 6.39–6.35 (1H, m, *para*-H_{Dipp}), 4.05 (2H, sept, $^3J_{\text{H-H}} = 6.9$ Hz, C-H(CH₃)₂), 0.99 (12H, d, $^3J_{\text{H-H}} = 6.9$ Hz, C-H(CH₃)₂), 0.17 (6H, s, Si(CH₃)₂).
⁷Li-NMR (d_8 -THF, 300 K, 155.5 MHz): δ [ppm] = -0.2 (NLi).

¹³C{¹H}-NMR (d_8 -THF, 300 K, 100.6 MHz): δ [ppm] = 157.4 (*ipso*-C_{Dipp}), 149.2 (*ipso*-C_{Ph}), 143.8 (*ortho*-C_{Dipp}), 134.5 (*ortho*-C_{Ph}), 127.5 (*meta*-C_{Ph}), 127.2 (*para*-C_{Ph}), 122.2 (*meta*-C_{Dipp}), 115.3 (*para*-C_{Dipp}), 27.2 (C-H(CH₃)₂), 25.3 (C-H(CH₃)₂), 3.0 (Si(CH₃)₂).

²⁹Si{¹H}-DEPT24.1-NMR (d_8 -THF, 300 K, 79.5 MHz): δ [ppm] = -29.1 ((Si(CH₃)₂).

²⁹Si{¹H}-IG-NMR (d_8 -THF, 300 K, 79.5 MHz): δ [ppm] = -29.1 ((Si(CH₃)₂).

IR (KBr pellet): $\tilde{\nu}$ [cm⁻¹] (intensity) = 438(s), 451(m), 476(vw), 532(m), 573(w), 669(m), 702(vs), 737(s), 756(s), 777(vs), 826(vs), 882(w), 924(vs), 997(vw), 1042(w), 1109(vs), 1142(vw), 1190(vs), 1236(vs), 1310(vs), 1362(vw), 1422(vs), 1445(m), 1460(m), 1587(w), 2868(s), 2924(s), 2961(vs), 3009(w), 3046(m), 3067(w).

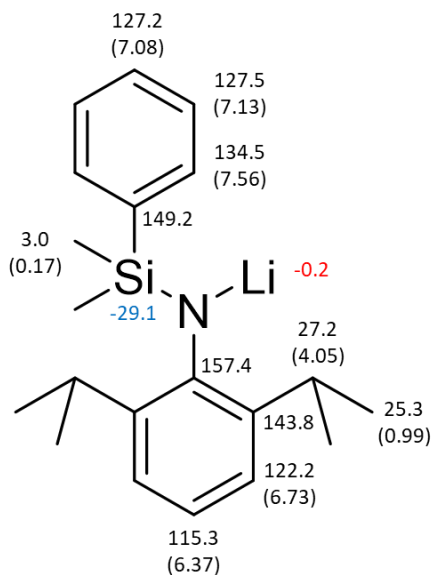


Figure S1. Assignment of chemical shifts to **1**; ¹H (in brackets), ⁷Li (red) ¹³C (black), and ²⁹Si (blue).

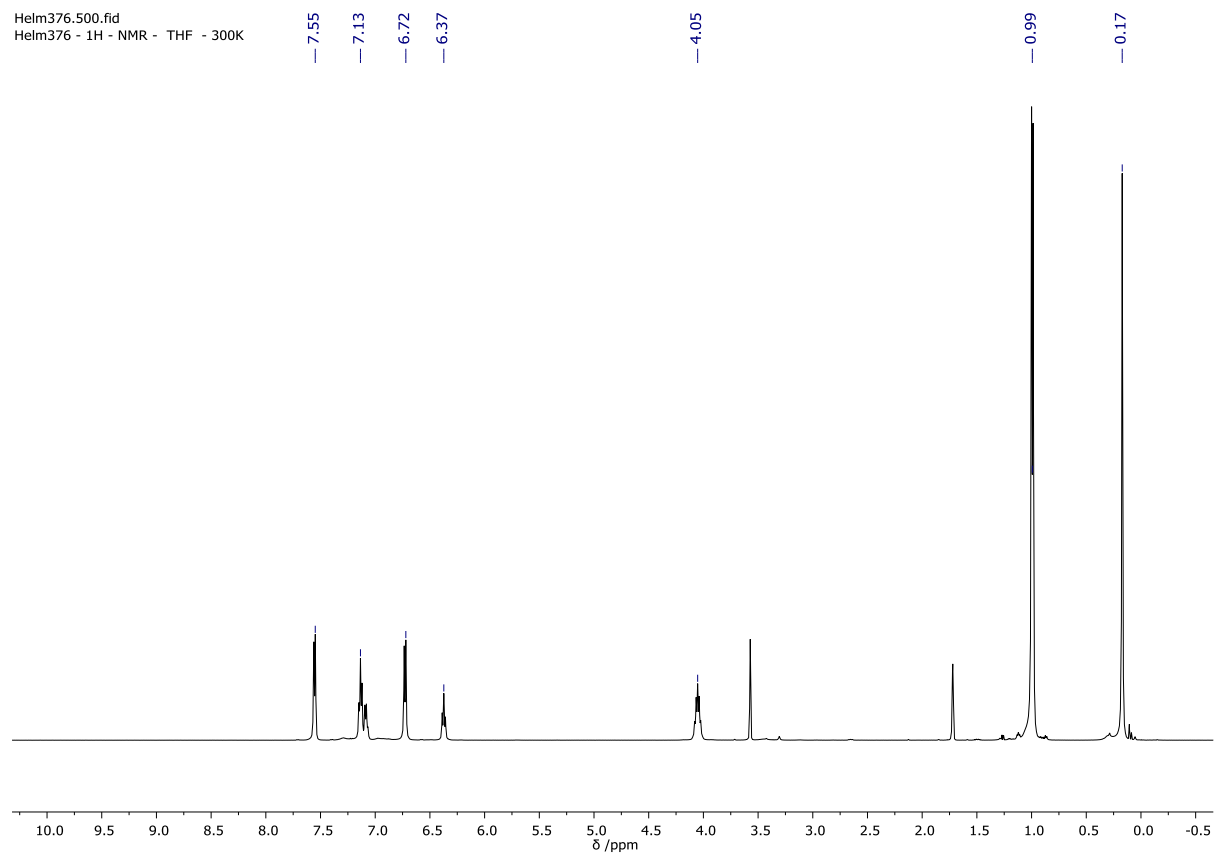


Figure S2. ¹H-NMR spectrum (*d*₈-THF, 300 K, 400 MHz) of **1**.

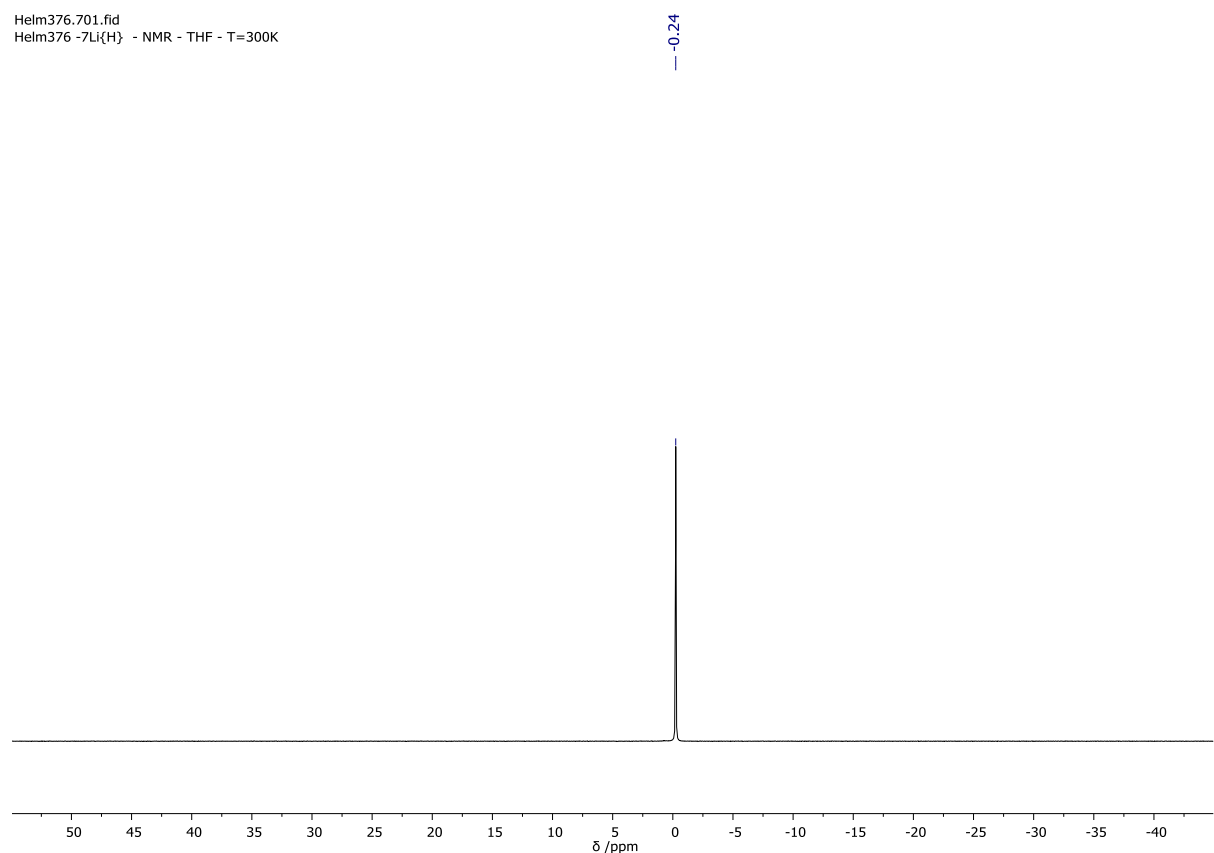


Figure S3. ⁷Li-NMR spectrum (*d*₈-THF, 300 K, 155.5 MHz) of **1**.

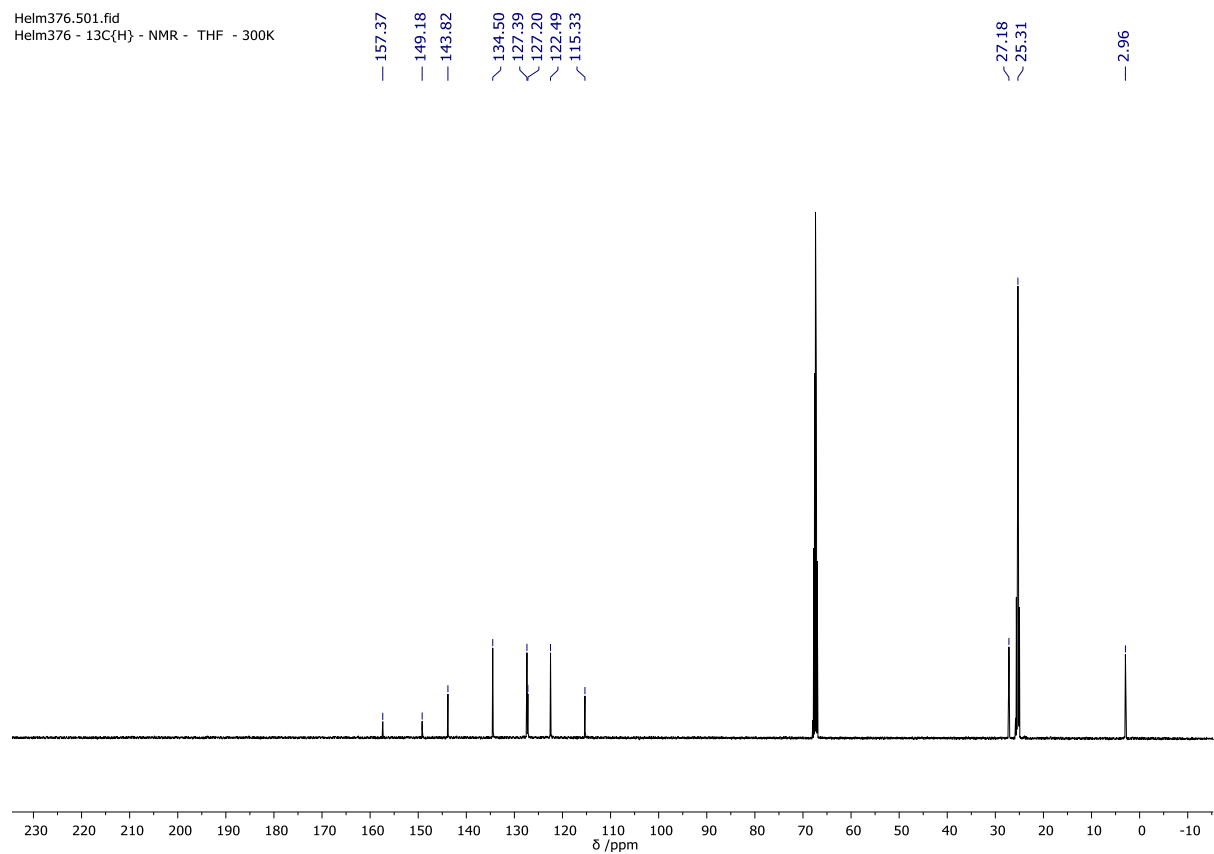


Figure S4. $^{13}\text{C}\{\text{H}\}$ -NMR spectrum (d_8 -THF, 300 K, 100 MHz) of **1**.

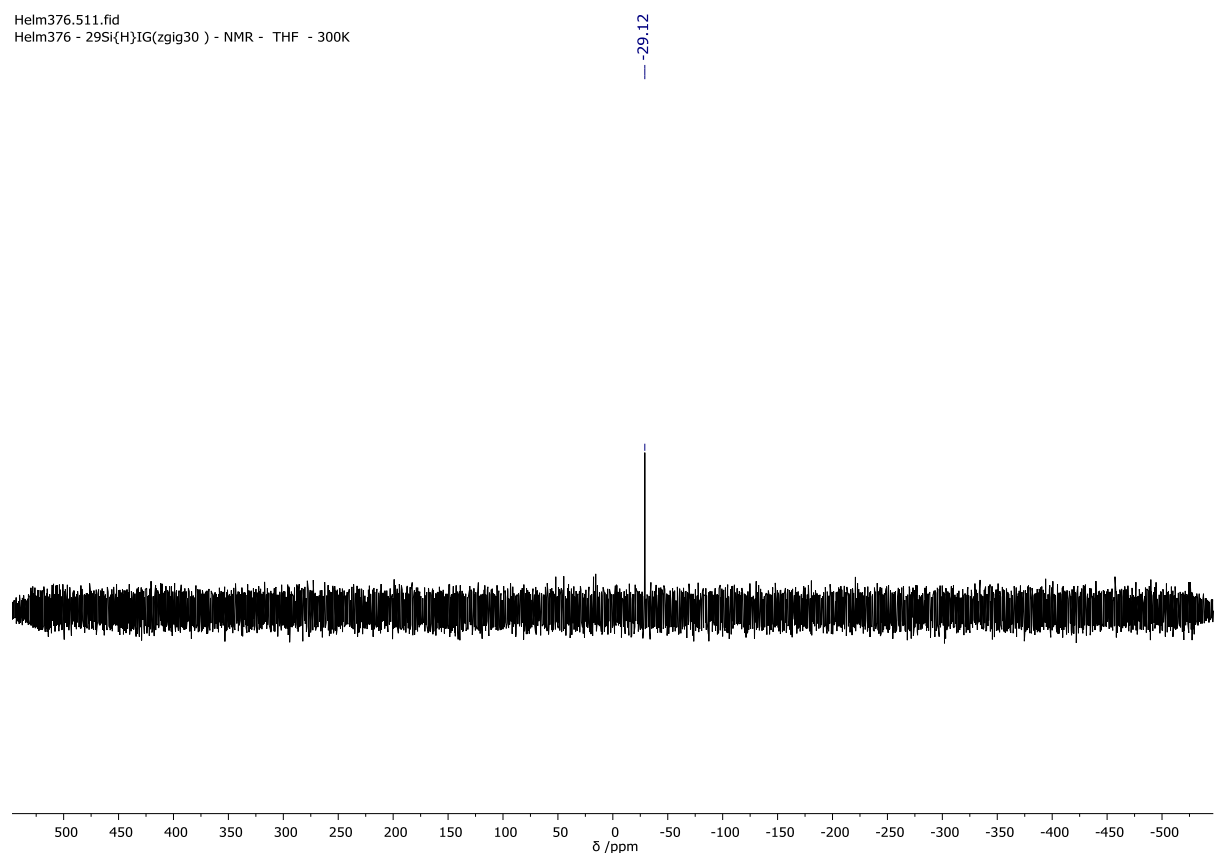


Figure S5. $^{29}\text{Si}\{\text{H}\}$ -IG-NMR spectrum (d_8 -THF, 300 K, 80 MHz) of **1**.

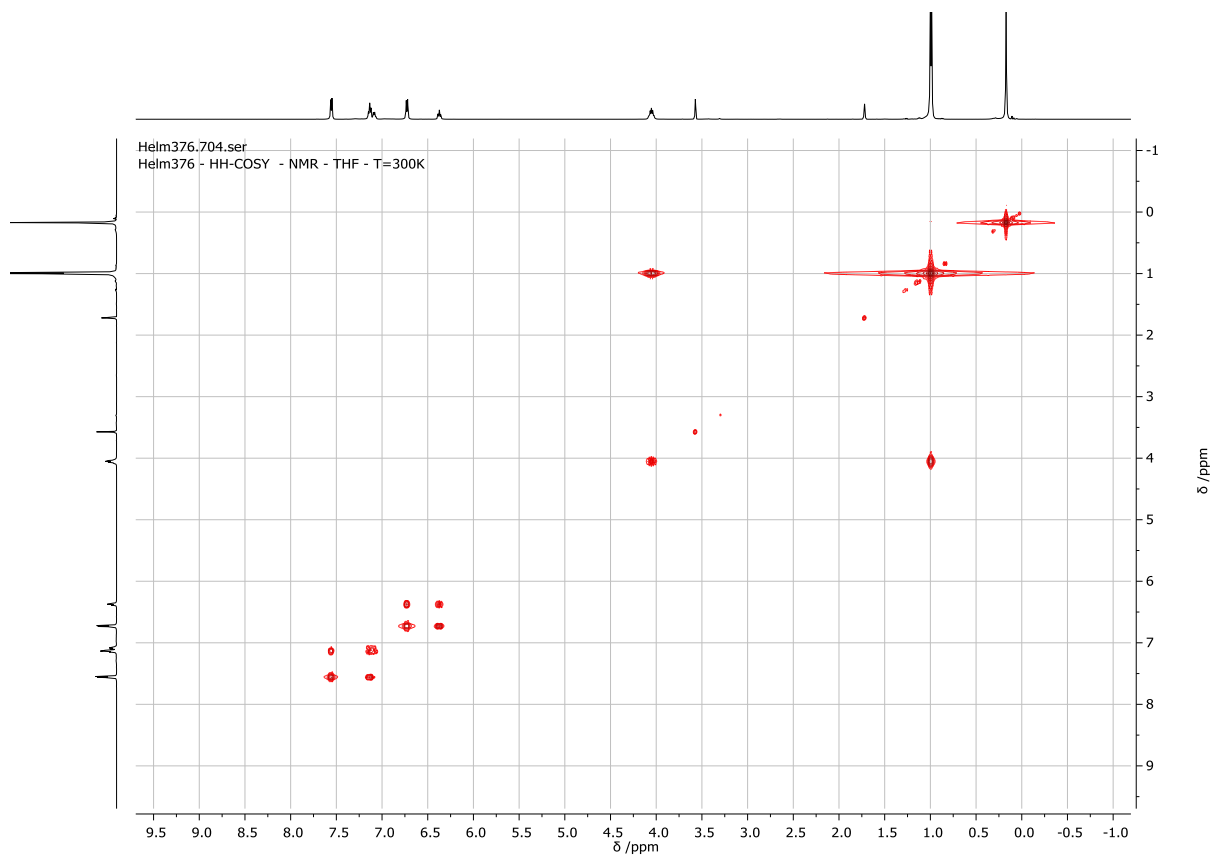


Figure S6. ^1H , ^1H -COSY-NMR spectrum (d_8 -THF, 300 K) of **1**.

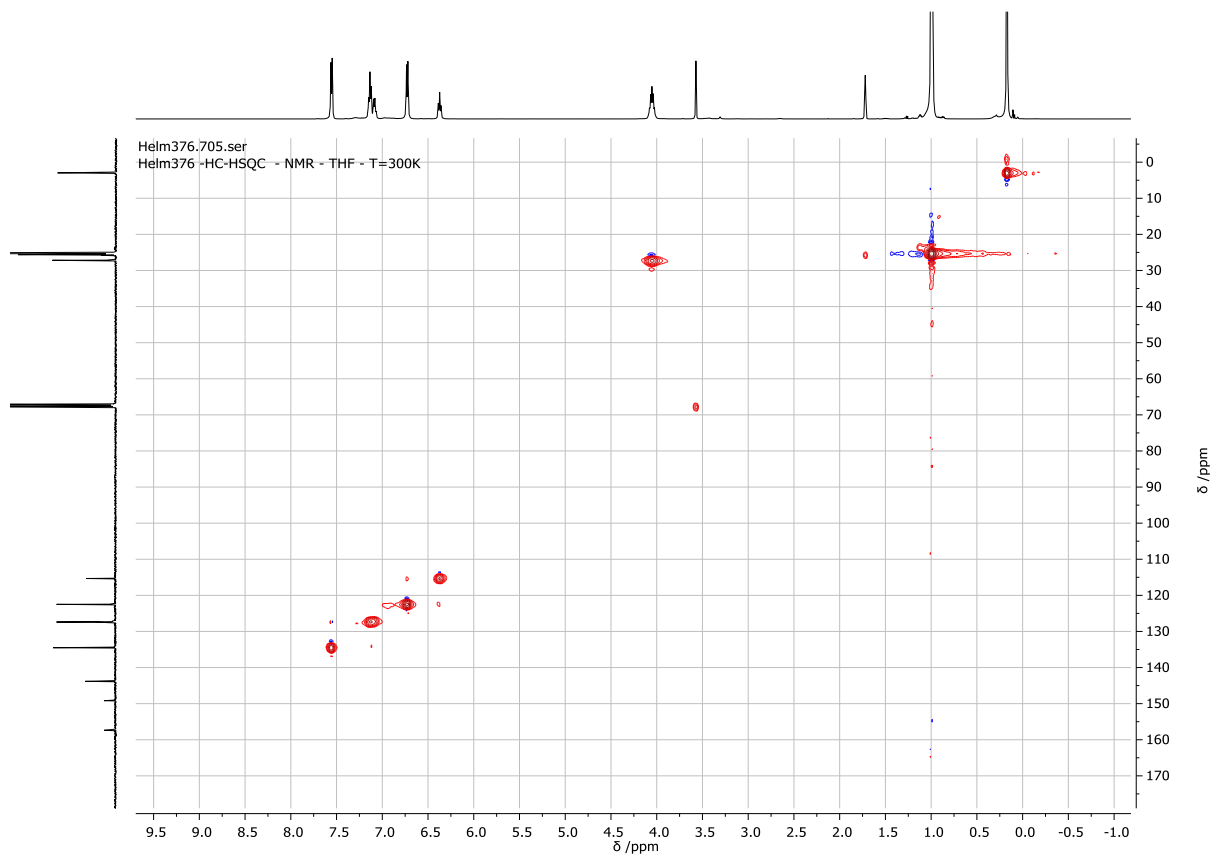
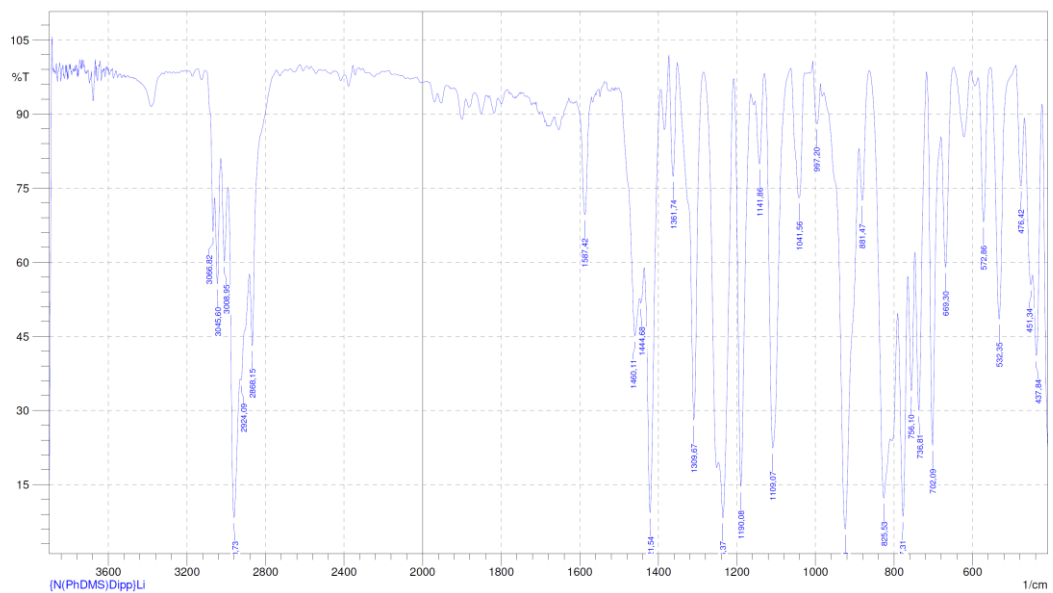


Figure S7. ^1H , ^{13}C -HSQC-NMR spectrum (d_8 -THF, 300 K) of **1**.



Comment:
N(PhDMS)DippLi

No. of Scans:

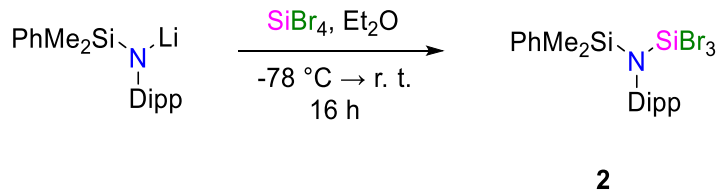
D:\Messdaten\Josch\N(PhDMS)DippLi\N(PhDMS)
DippLi1.smf

Resolution;
Apodization;

Date/Time: 10.01.2020 17:14:34
User: IR-Messung

Figure S8. IR spectrum (KBr pellet) of **1**.

2.2. Synthesis and Characterization of 2



$\{\text{N}(\text{SiMe}_2\text{Ph})\text{Dipp}\}\text{Li}$ (14.882 g, 46.9 mmol, 1.0 equiv.) was dissolved in Et_2O (100 ml) and slowly added to SiBr_4 (16.298 g, 5.82 ml, 1.0 equiv.) in Et_2O (50 ml) at -78°C . The reaction mixture was allowed to warm to room temperature and was stirred for 16 h. All volatile components were removed *in vacuo* and the colourless residue was extracted with *n*-hexane (100 ml) and filtrated to give $\{\text{N}(\text{SiMe}_2\text{Ph})\text{Dipp}\}\text{SiBr}_3$ **2** (21.050 g, 36.4 mmol, 78%). Colourless crystals of **2** were obtained from a concentrated *n*-hexane solution after storage at -32°C for 16 h.

$^1\text{H-NMR}$ (d_8 -THF, 300 K, 400 MHz): δ [ppm] = 7.63–7.59 (2H, m, *ortho*- H_{Ph}), 7.40–7.31 (3H, m, *meta/para*- H_{Ph}), 7.21–7.12 (3H, m, *meta/para*- H_{Dipp}), 3.42 (2H, sept, $^3J_{\text{H-H}} = 6.7$ Hz, $\text{C-H}(\text{CH}_3)_2$), 1.22 (6H, d, $^3J_{\text{H-H}} = 6.7$ Hz, $\text{C-H}(\text{CH}_3)_2$), 1.18 (6H, d, $^3J_{\text{H-H}} = 6.7$ Hz, $\text{C-H}(\text{CH}_3)_2$), 0.58 (6H, s, $\text{Si}(\text{CH}_3)_2$).

$^{13}\text{C}\{^1\text{H}\}$ -NMR (d_8 -THF, 300 K, 100.6 MHz): δ [ppm] = 147.4 (*ortho*- C_{Dipp}), 139.4 (*ipso*- C_{Dipp}), 135.4 (*ipso*- C_{Ph}), 135.0 (*ortho*- C_{Ph}), 130.2 (*para*- C_{Ph}), 127.9 (*meta*- C_{Ph}), 127.1 (*para*- C_{Dipp}), 124.7 (*meta*- C_{Dipp}), 28.3 ($\text{CH}(\text{CH}_3)_2$), 25.3 ($\text{CH}(\text{CH}_3)_2$), 24.2 ($\text{CH}(\text{CH}_3)_2$), 0.8 ($\text{Si}(\text{CH}_3)_2$).

$^{29}\text{Si}\{^1\text{H}\}$ -DEPT24.1-NMR (d_8 -THF, 300 K, 79.5 MHz): δ [ppm] = 2.3 ($(\text{Si}(\text{CH}_3)_2)$).

$^{29}\text{Si}\{^1\text{H}\}$ -IG-NMR (d_8 -THF, 300 K, 79.5 MHz): δ [ppm] = 2.3 ($(\text{Si}(\text{CH}_3)_2)$), -62.9 (SiBr_3).

IR (KBr pellet): $\tilde{\nu}$ [cm^{-1}] (intensity) = 430(s), 449(vs), 475(vs), 538(m), 604(w), 658(w), 700(s), 735(s), 781(vs), 802(vs), 833(s), 862(vs), 887(m), 961(vs), 968(s), 1045(m), 1098(s), 1115(s), 1163(vs), 1256(vs), 1316(m), 1339(vw), 1362(w), 1383(m), 1404(vw), 1433(s), 1458(s), 1508(vw), 1586(vw), 1653(vw), 1703(vw), 1817(vw), 1937(vw), 2357(vw), 2866(m), 2926(m), 2963(vs), 3028(vw), 3046(w), 3071(w).

EI-MS: $m/z = 577$ [$\{\text{N}(\text{SiMe}_2\text{Ph})\text{Dipp}\}\text{SiBr}_3$], 562 [$\{\text{N}(\cdot\text{SiMePh})\text{Dipp}\}\text{SiBr}_3$], 501 [$\{\text{N}(\cdot\text{SiMe}_2)\text{Dipp}\}\text{SiBr}_3$].

Melting point: 94 °C.

Elemental analysis: Calc.: H: 4.88, C: 41.54, N: 4.88; Found: H: 4.92, C: 41.50, N: 4.92.

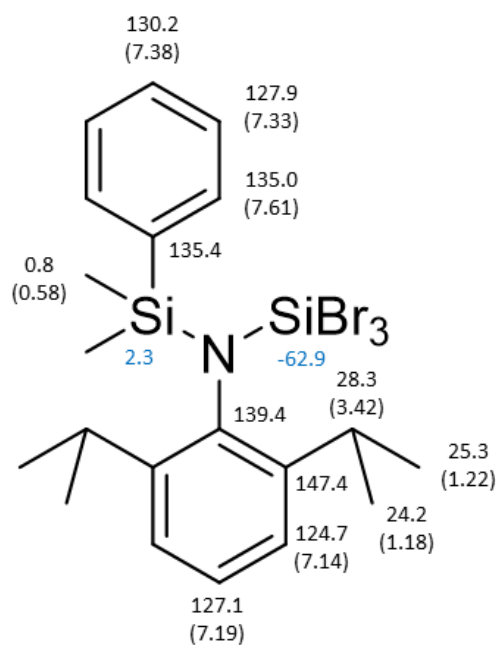


Figure S9. Assignment of chemical shifts to **2**; ^1H (in brackets), ^{13}C (black), and ^{29}Si (blue).

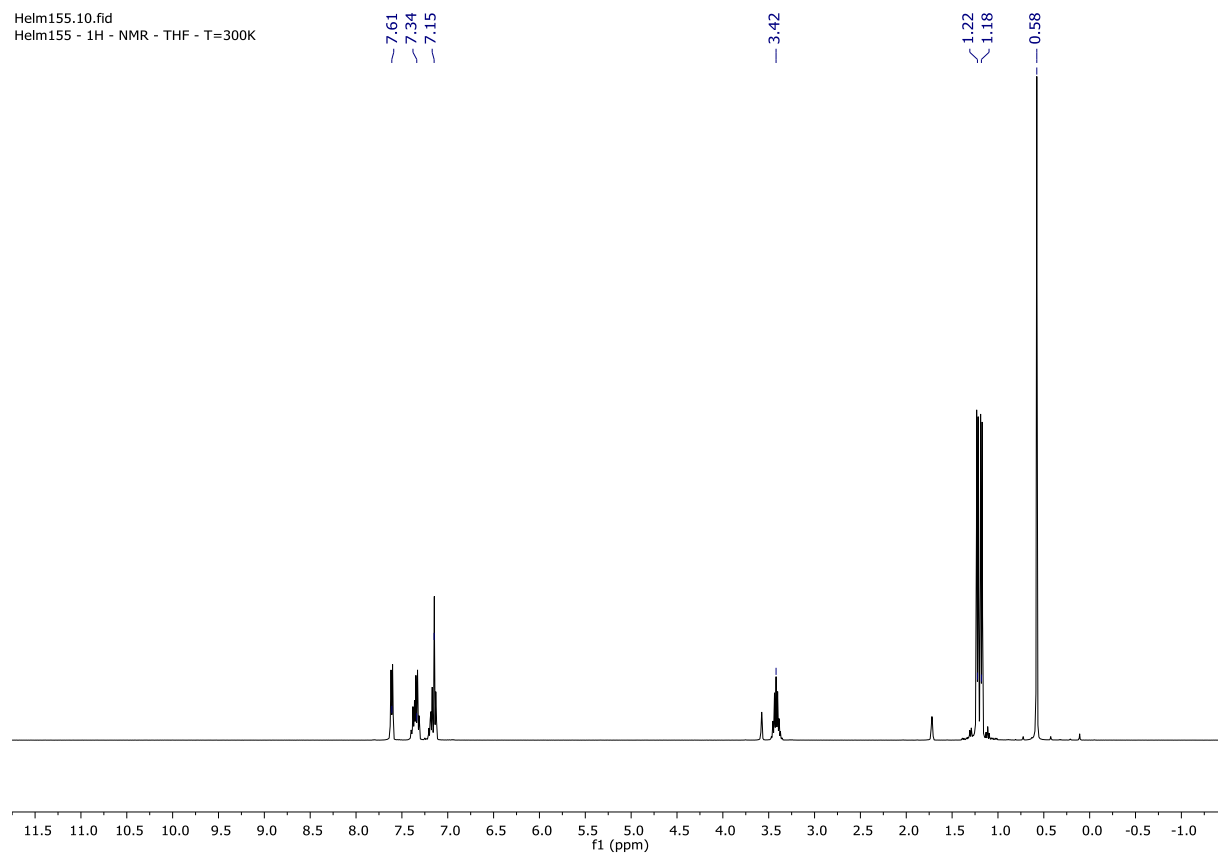


Figure S10. ^1H -NMR spectrum (d_8 -THF, 300 K, 400 MHz) of **2**.

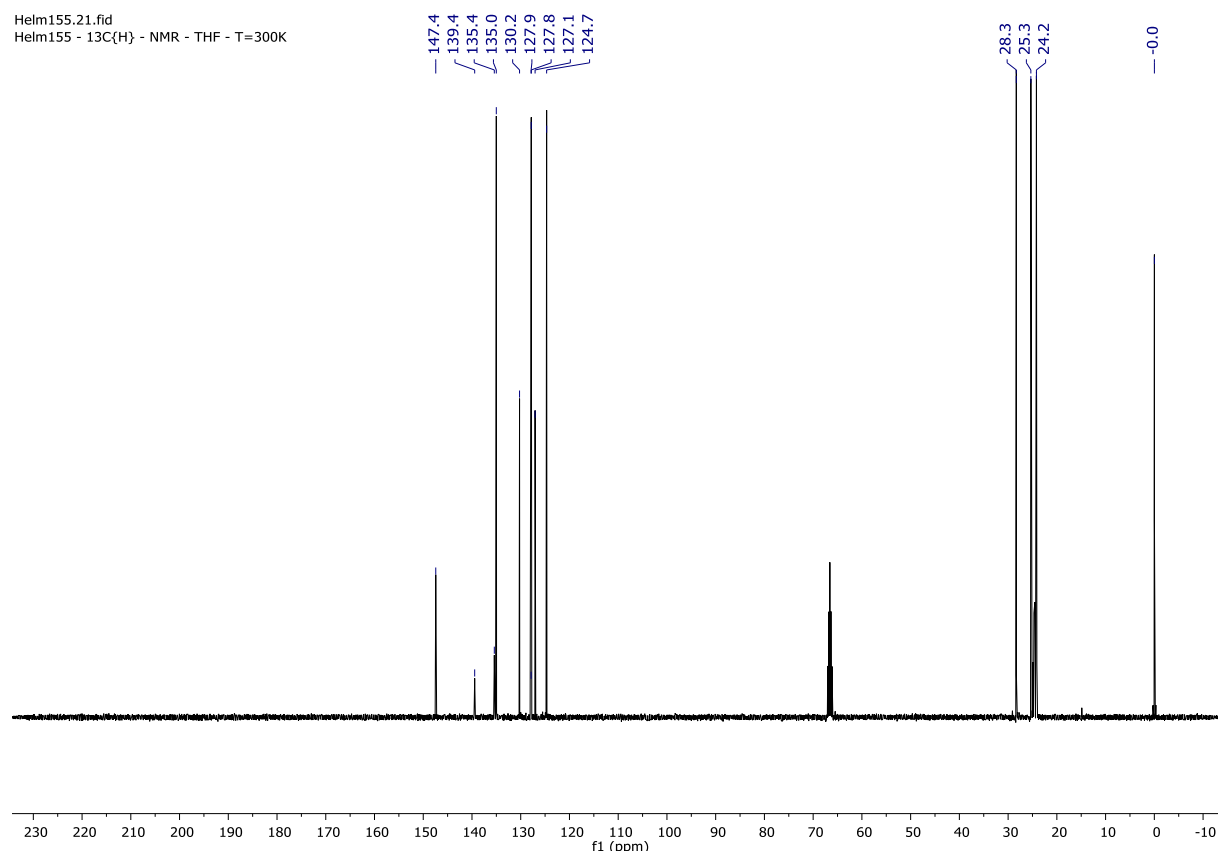


Figure S11. $^{13}\text{C}\{^1\text{H}\}$ -NMR spectrum (d_8 -THF, 300 K, 100 MHz) of **2**.

Helm155.23.fid
Helm155 - $^{29}\text{Si}\{\text{H}\}$ Dept24.1 - NMR - THF - T=300K

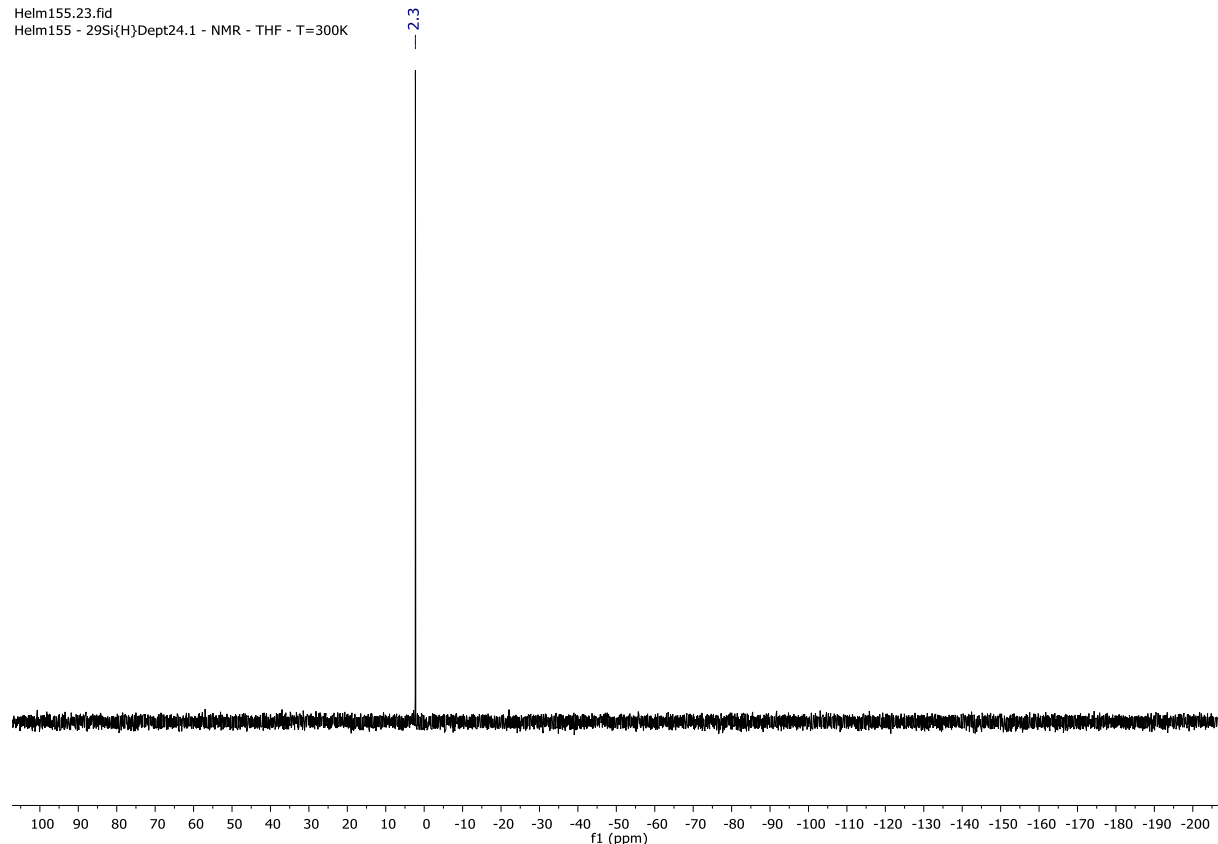


Figure S12. $^{29}\text{Si}\{\text{H}\}$ -DEPT24.1-NMR spectrum (d_8 -THF, 300 K, 80 MHz) of **2**.

Helm155.24.fid
Helm155 - $^{29}\text{Si}\{\text{H}\}$ IG - NMR - THF - T=300K

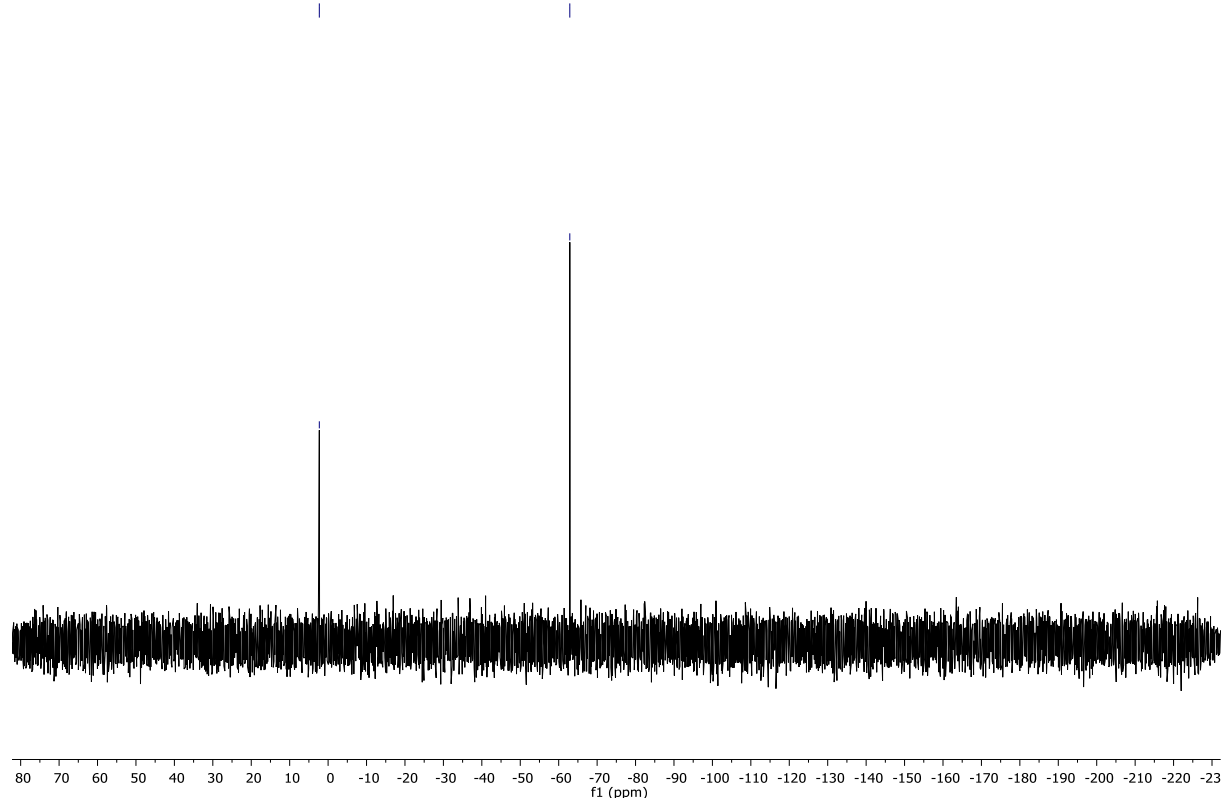


Figure S13. $^{29}\text{Si}\{\text{H}\}$ -IG-NMR spectrum (d_8 -THF, 300 K, 80 MHz) of **2**.

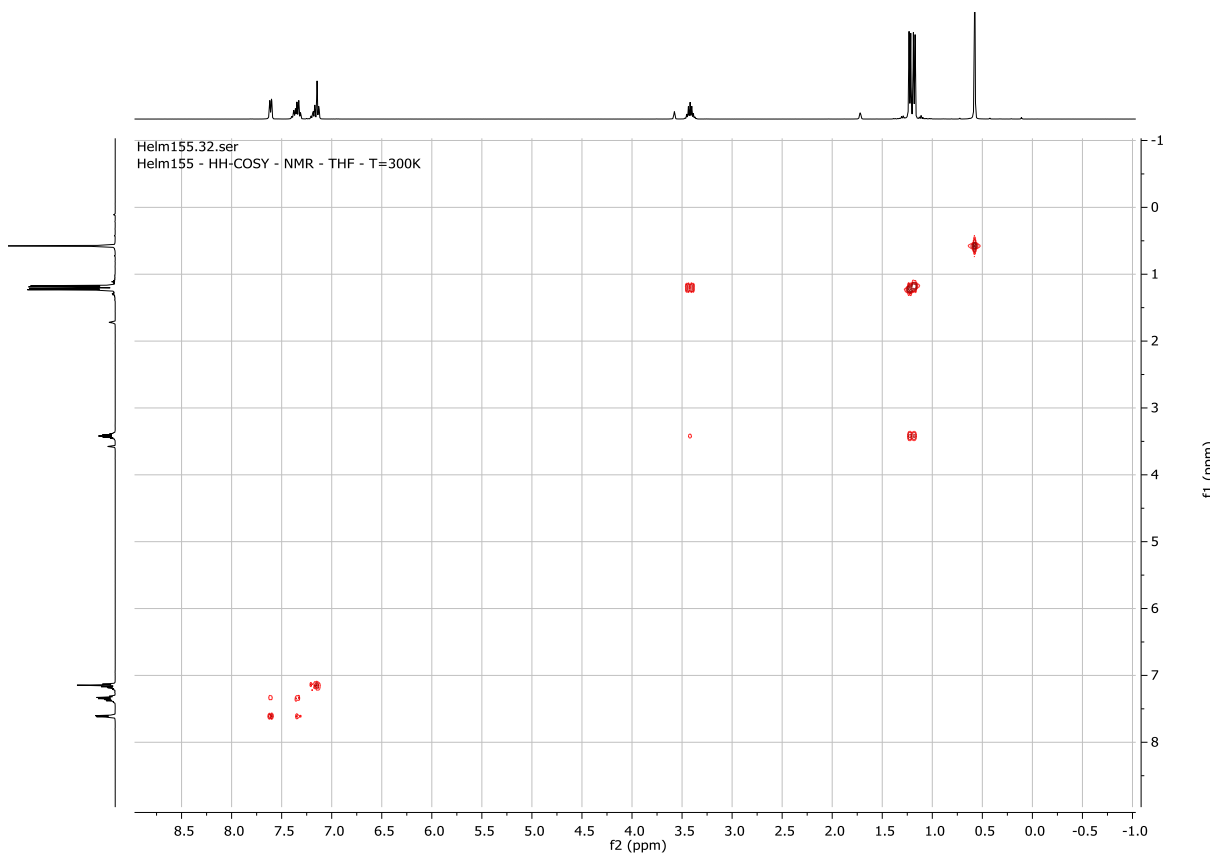


Figure S14. ^1H , ^1H -COSY-NMR spectrum (d_8 -THF, 300 K) of **2**.

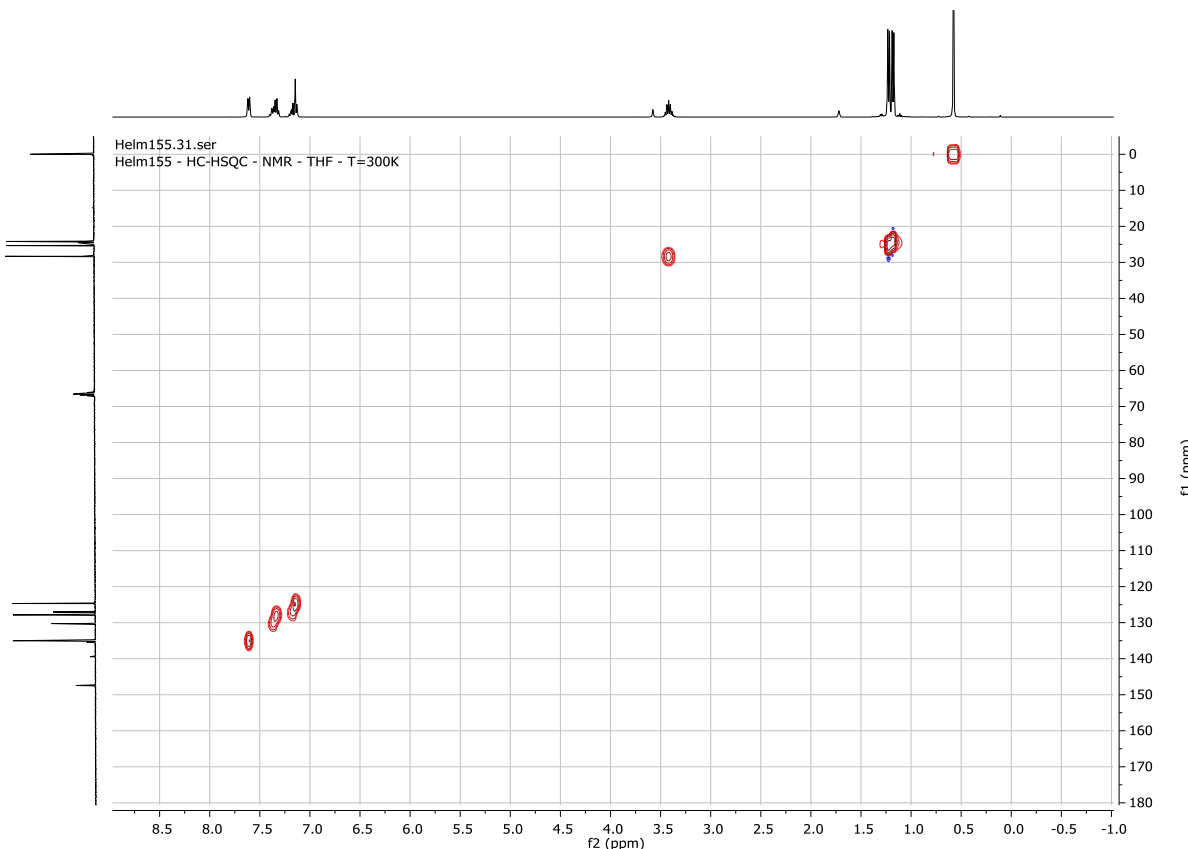


Figure S15. ^1H , ^{13}C -HSQC-NMR spectrum (d_8 -THF, 300 K) of **2**.

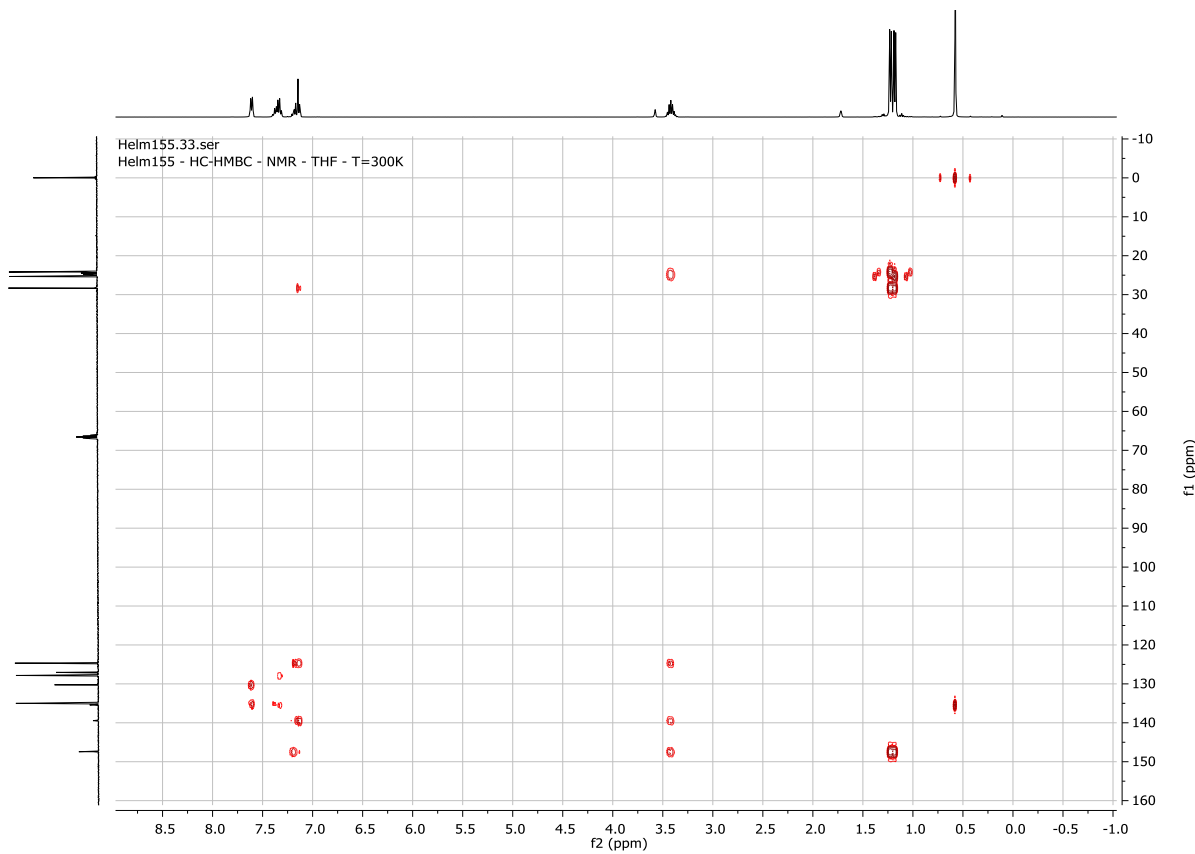


Figure S16. ^1H , ^{13}C -HMBC-NMR spectrum ($\text{d}_8\text{-THF}$, 300 K) of **2**.

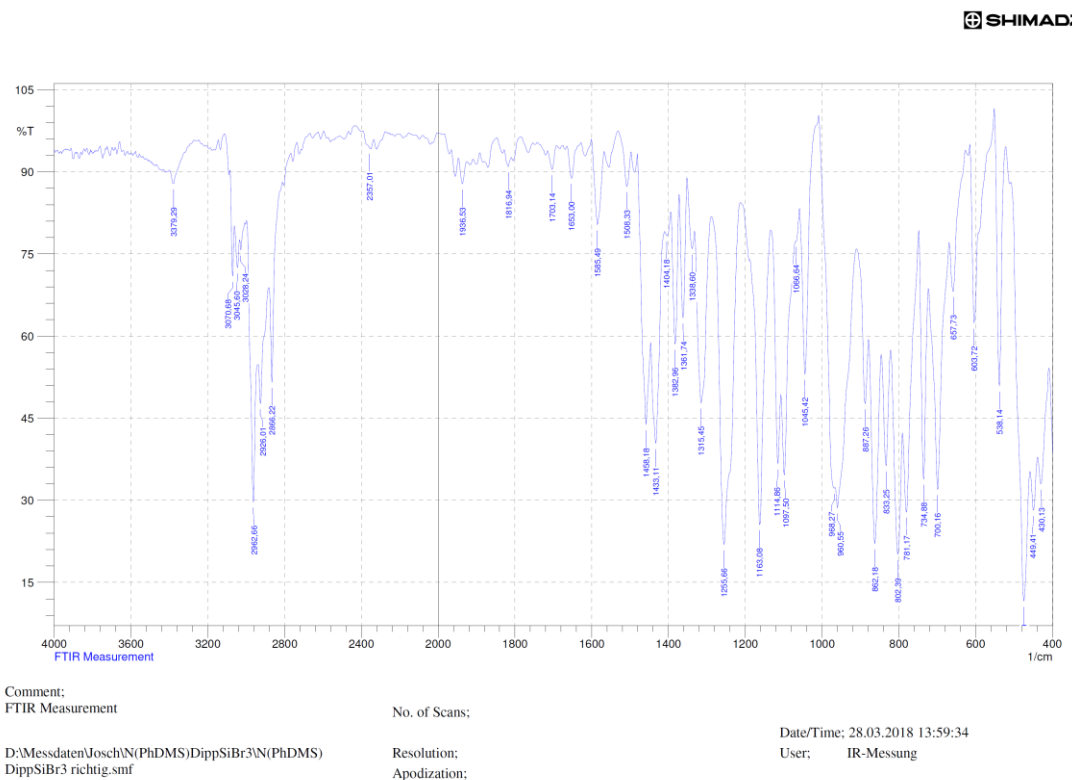


Figure S17. IR spectrum (KBr pellet) of **2**.

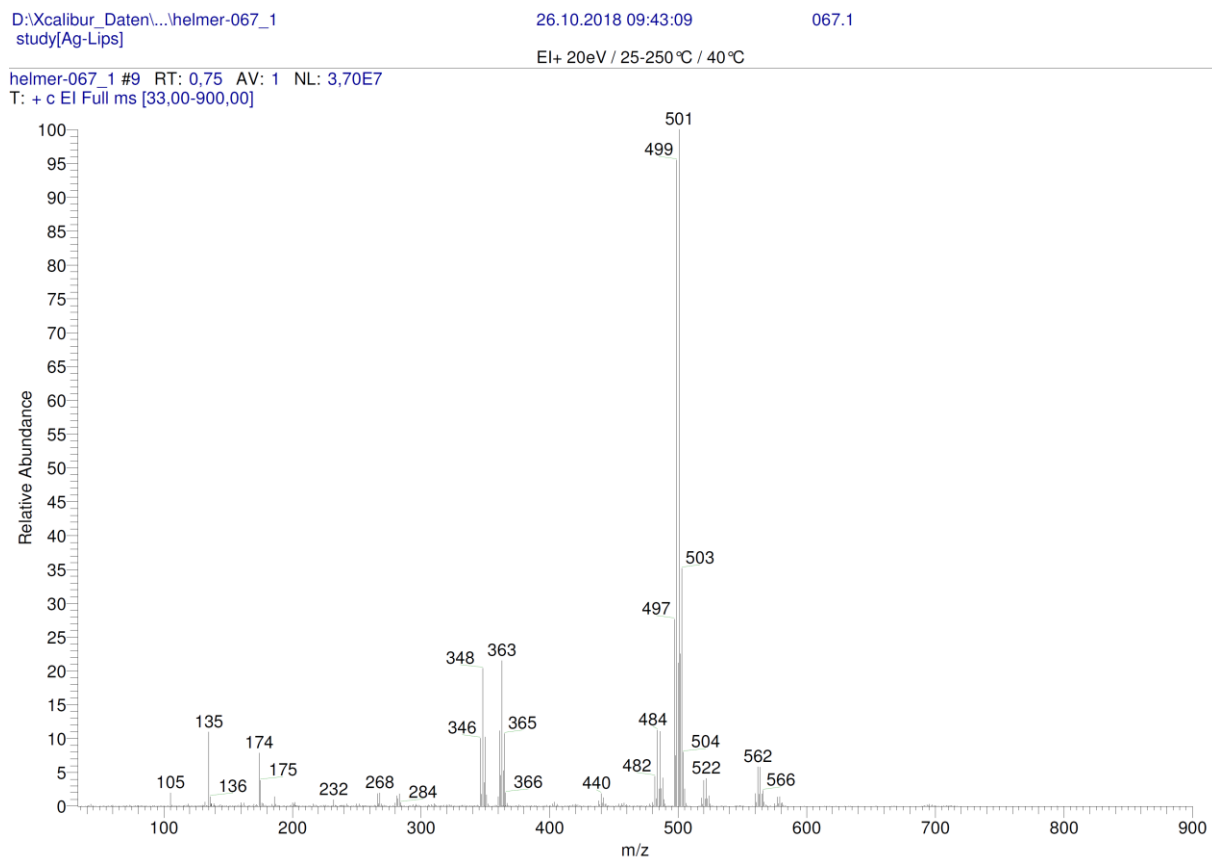


Figure S18. EI-MS spectrum of **2**.

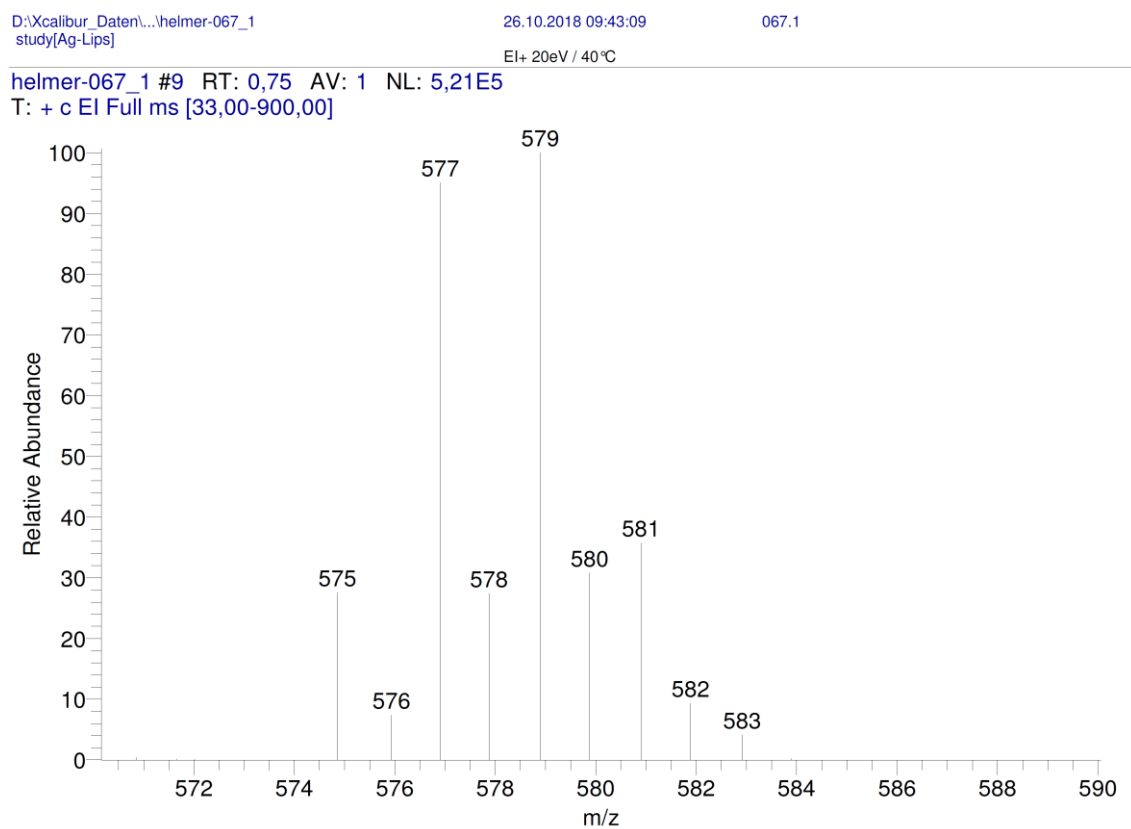
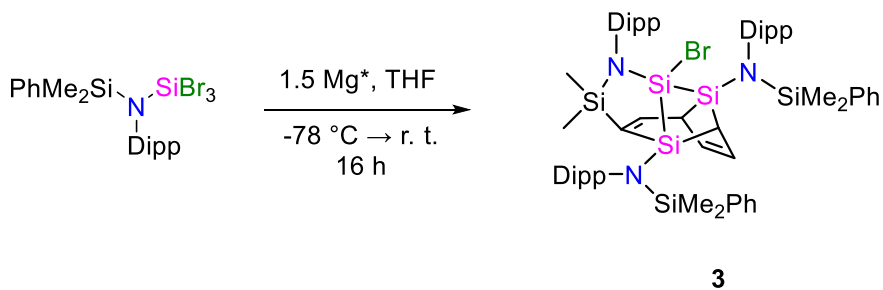


Figure S19. EI-MS spectrum of **2**.

2.3. Synthesis and Characterization of 3



$\{\text{N}(\text{PhDMS})\text{Dipp}\}\text{SiBr}_3$ (**2**) (1.157 g, 2.0 mmol, 1.0 equiv.) was dissolved in THF (15 ml) and slowly added to a suspension of Mg^* (0.073 g, 3.0 mmol, 1.5 equiv.) in THF (15 ml) at -78°C . The reaction mixture was allowed to warm to room temperature and stirred for 16 h. After addition of 1,4-dioxane (0.66 ml, 7.5 mmol, 3.75 equiv.), the deep yellow suspension was stirred for one hour and was filtrated. All volatile components were removed *in vacuo* and the yellow residue was extracted with *n*-hexane (50 ml) and filtrated. Compound **3** was obtained from a concentrated solution in *n*-hexane after storage at -32°C for 16 h. Single crystals of **3** were obtained from a concentrated solution in toluene at room temperature. Yield: 0.170 g, 0.16 mmol, 23%

$^1\text{H-NMR}$ (d_8 -THF, 210 K, 400 MHz): δ [ppm] = 8.16–8.09 (3H, m), 7.70–7.64 (2H, m), 7.60–7.55 (1H, m), 7.37–7.32 (1H, m), 7.30–7.25 (2H, m), 7.24–7.19 (3H, m), 7.17–7.02 (7H, m), 7.00–6.90 (3H, m), 6.82–6.79 (1H, m), 5.46–5.44 (1H, m), 4.93–4.91 (1H, m), 3.63–3.56 (2H, m), 3.53–3.44 (2H, m), 3.26–3.17 (1H, m), 2.90–2.81 (1H, m), 2.62–2.56 (1H, m), 2.04–2.01 (1H, m), 1.66–1.63 (3H, m), 1.39–1.36 (3H, m), 1.34–1.31 (3H, m), 1.29–1.26 (3H, m), 1.18–1.14 (3H, m), 1.08–1.01 (9H, m), 0.93–0.89 (3H, m), 0.86–0.82 (3H, m), 0.74–0.71 (3H, m), 0.49 (3H, s), 0.22 (3H, s), –0.10 (3H, m), –0.22 (3H, m), –0.38 (3H, m), –0.82 (3H, m). For assignment, see Figure S20.

$^{13}\text{C}\{^1\text{H}\}\text{-NMR}$ (d_8 -THF, 210 K, 100.6 MHz): δ [ppm] = 165.4, 148.5, 148.3, 148.3, 148.2, 147.8, 147.4, 142.2, 141.7, 141.3, 140.1, 139.4, 138.7, 136.1, 135.6, 135.6, 135.3, 135.3, 130.4, 129.8, 129.8, 129.4, 128.2, 128.2, 126.9, 126.6, 126.5, 126.1, 125.5, 125.4, 125.3, 125.2, 124.3, 124.1, 39.5, 31.0, 30.6, 29.1, 28.0, 27.7, 27.6, 27.6, 27.6, 27.3, 27.2, 27.2, 26.7, 26.6, 26.6, 25.9, 25.2, 24.4, 24.3, 22.6, 3.8, 2.5, 2.3, 1.3, –1.3., –3.1. For assignment, see Figure S20.

$^{29}\text{Si}\{^1\text{H}\}\text{DEPT24.1-NMR}$ (d_8 -THF, 300 K, 79.5 MHz): δ [pm] = 3.8, 0.5, –0.4. For assignment, see Figure S20.

$^{29}\text{Si}\{^1\text{H}\}\text{-IG-NMR}$ (d_8 -THF, 300 K, 79.5 MHz): δ [ppm] = 33.2, 3.8, 0.5, –0.4, –16.1, –33.9. For assignment, see Figure S20.

IR (KBr pellet): $\tilde{\nu}$ [cm⁻¹] (intensity) = 444(m), 542(vw), 557(vw), 590(vw), 606(vw), 654(vw), 698(s), 729(s), 793(vs), 812(s), 851(w), 880(vs), 914(vs), 939(vs), 970(vw), 1044(vw), 1072(vw), 1105(s), 1138(vw), 1167(vs), 1252(vs), 1312(m), 1360(vw), 1383(w), 1431(s), 1462(m), 1489(vw), 1522(vw), 1533(vw), 1549(vw), 1570(vw), 1589(vw), 1628(vw), 1665(vw), 1707(vw), 2866(m), 2926(m), 2963(vs), 3021(vw), 3053(w).

UV-Vis ($7.31 \cdot 10^{-5}$ mol/L in *n*-hexane): λ [nm] (ε [L·mol⁻¹·cm⁻¹]) = 259 (1086), 309 (422), 386 (45).

ESI-MS: m/z = 1096.45 [M+H]⁺.

Melting point: 161 °C.

Elemental analysis: Calc.: H: 7.73, C: 65.77, N: 3.83; Found: H: 7.45, C: 66.02, N: 3.51.

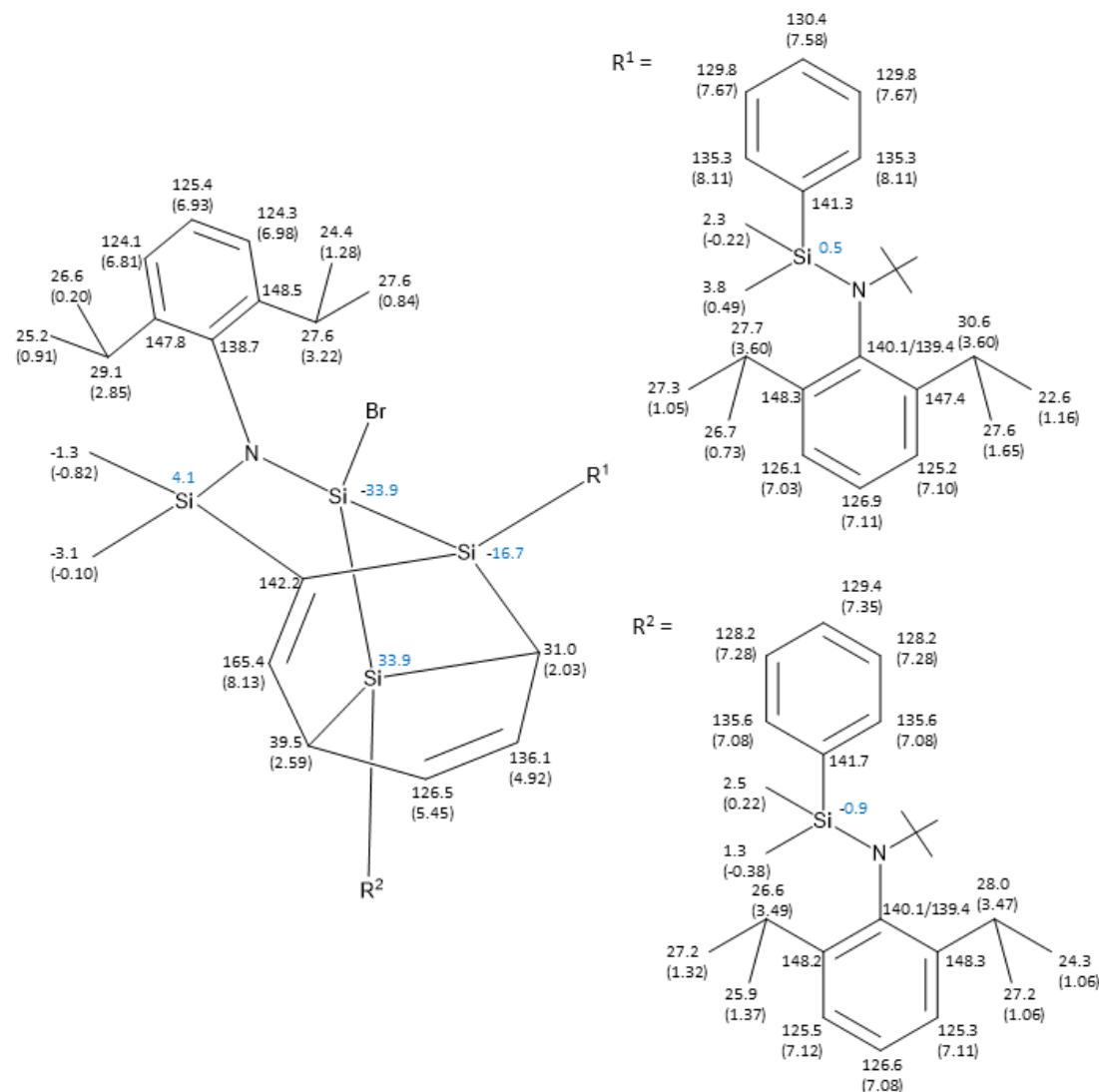


Figure S20. Assignment of chemical shifts to **3**; ¹H (in brackets), ¹³C (black), and ²⁹Si (blue).

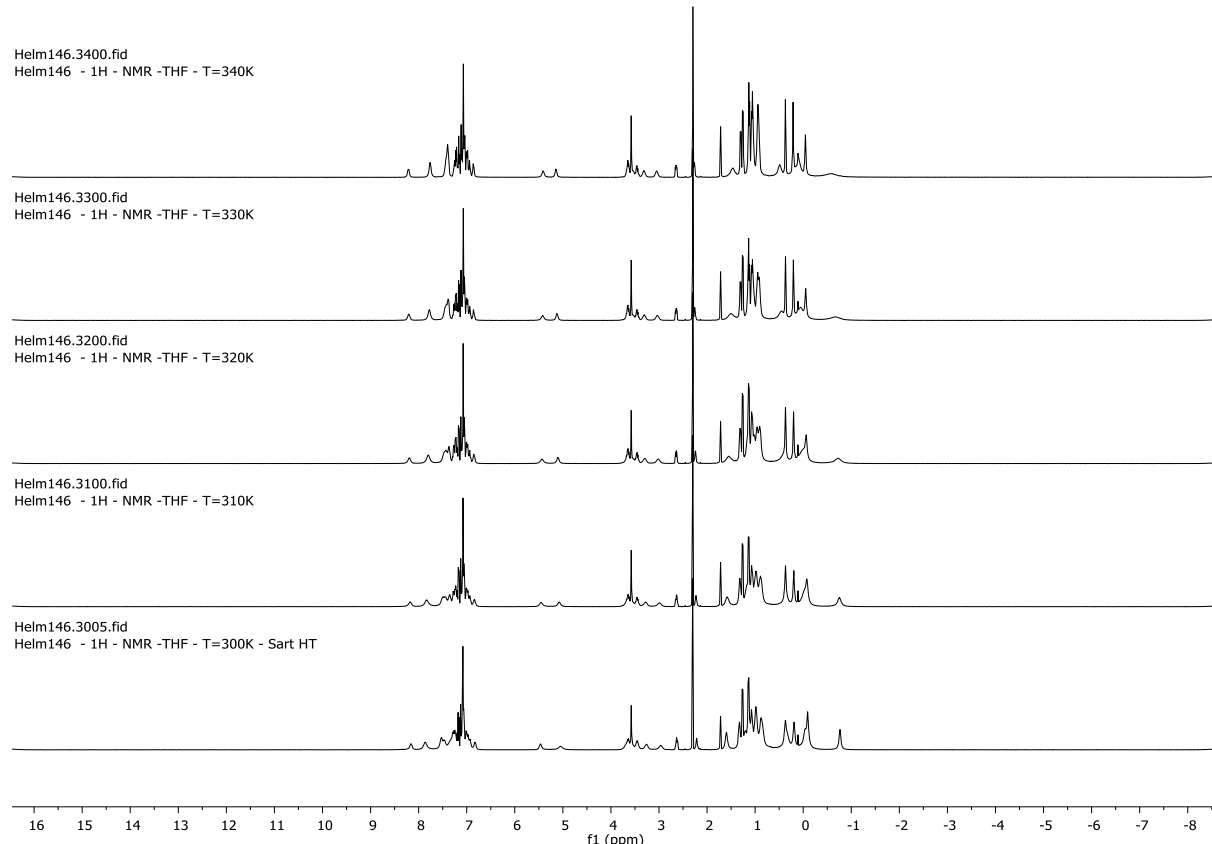


Figure S21. Variable temperature ¹H-NMR spectra (d₈-THF, 300–340 K, 400 MHz) of **3**.

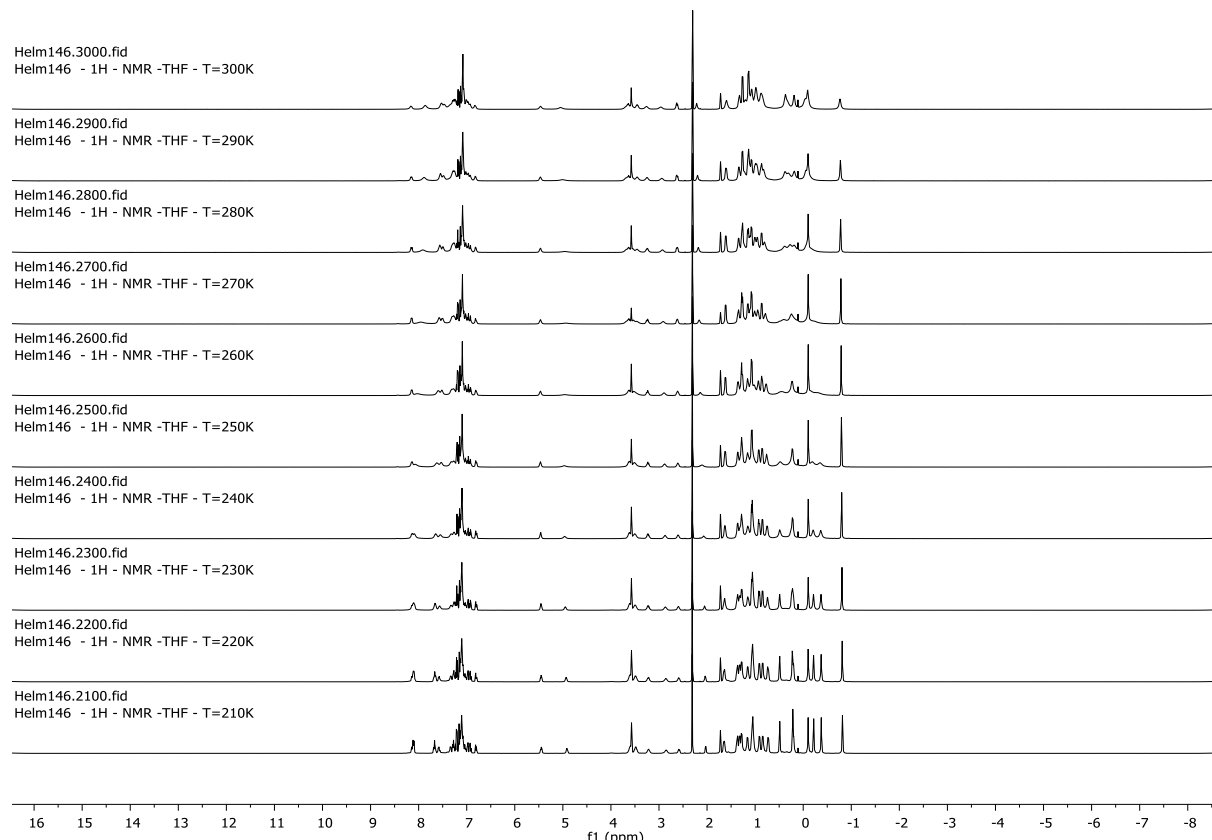


Figure S22. Variable temperature ¹H-NMR spectra (d₈-THF, 300–210 K, 400 MHz) of **3**.

Helm146.2105.fid
Helm146 - $^{13}\text{C}\{\text{H}\}$ - NMR -THF - T=210K

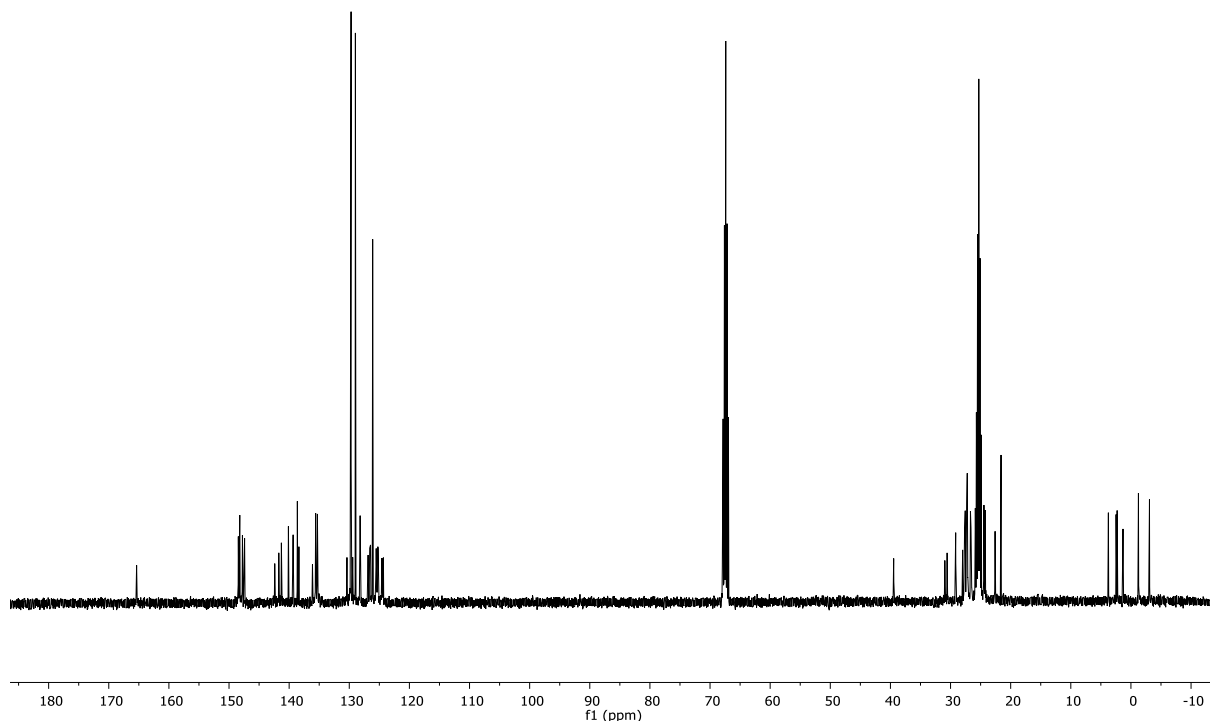


Figure S23. $^{13}\text{C}\{\text{H}\}$ -NMR spectrum (d_8 -THF, 210 K, 100 MHz) of **3**.

Helm146.2102.fid
Helm146 - $^{29}\text{Si}\{\text{H}\}$ -Dept24.1 - NMR -THF - T=210K

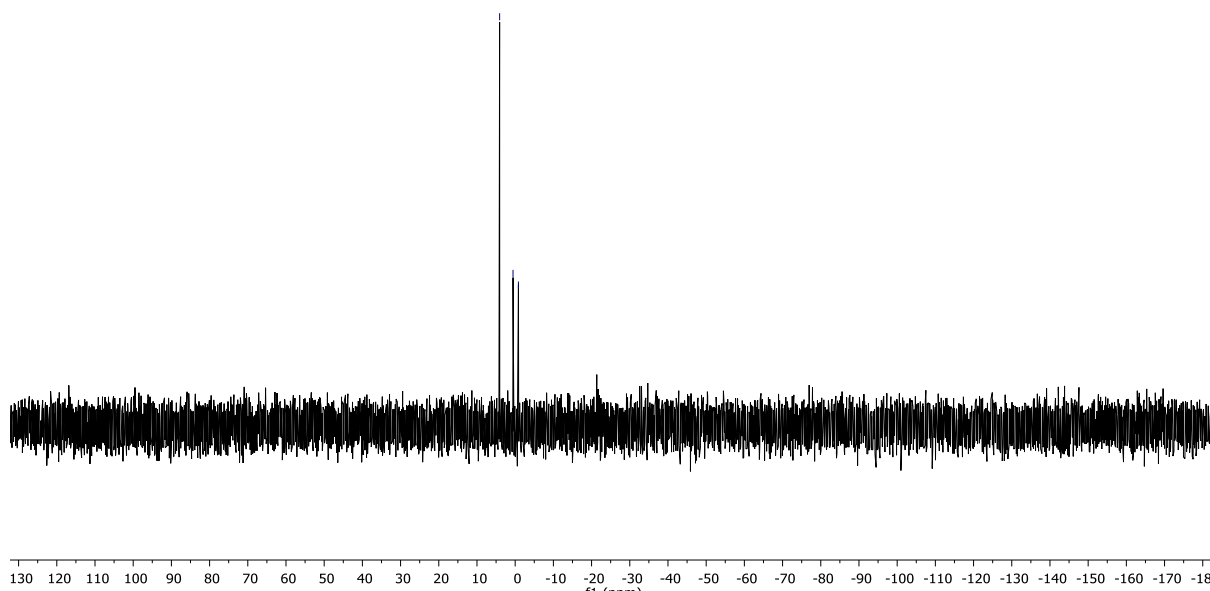


Figure S24. $^{29}\text{Si}\{\text{H}\}$ -DEPT24.1-NMR spectrum (d_8 -THF, 210 K, 80 MHz) of **3**.

Helm146.2103.fid
Helm146 - $^{29}\text{Si}\{\text{H}\}$ IG - NMR -THF - T=210K

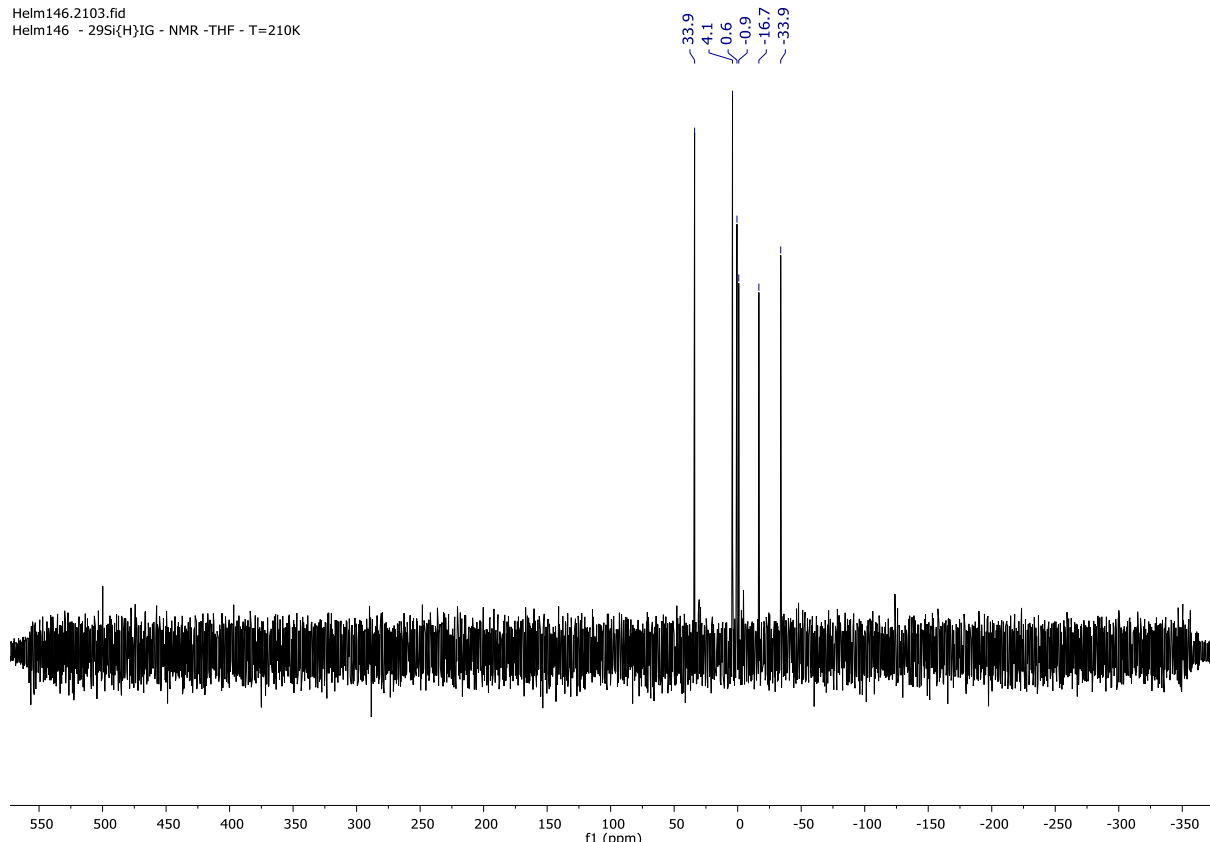


Figure S25. $^{29}\text{Si}\{\text{H}\}$ -IG-NMR spectrum (d_8 -THF, 210 K, 80 MHz) of **3**.

Helm146.3006.fid
Helm146 - $^{29}\text{Si}\{\text{H}\}$ IG - NMR -THF - T=300K

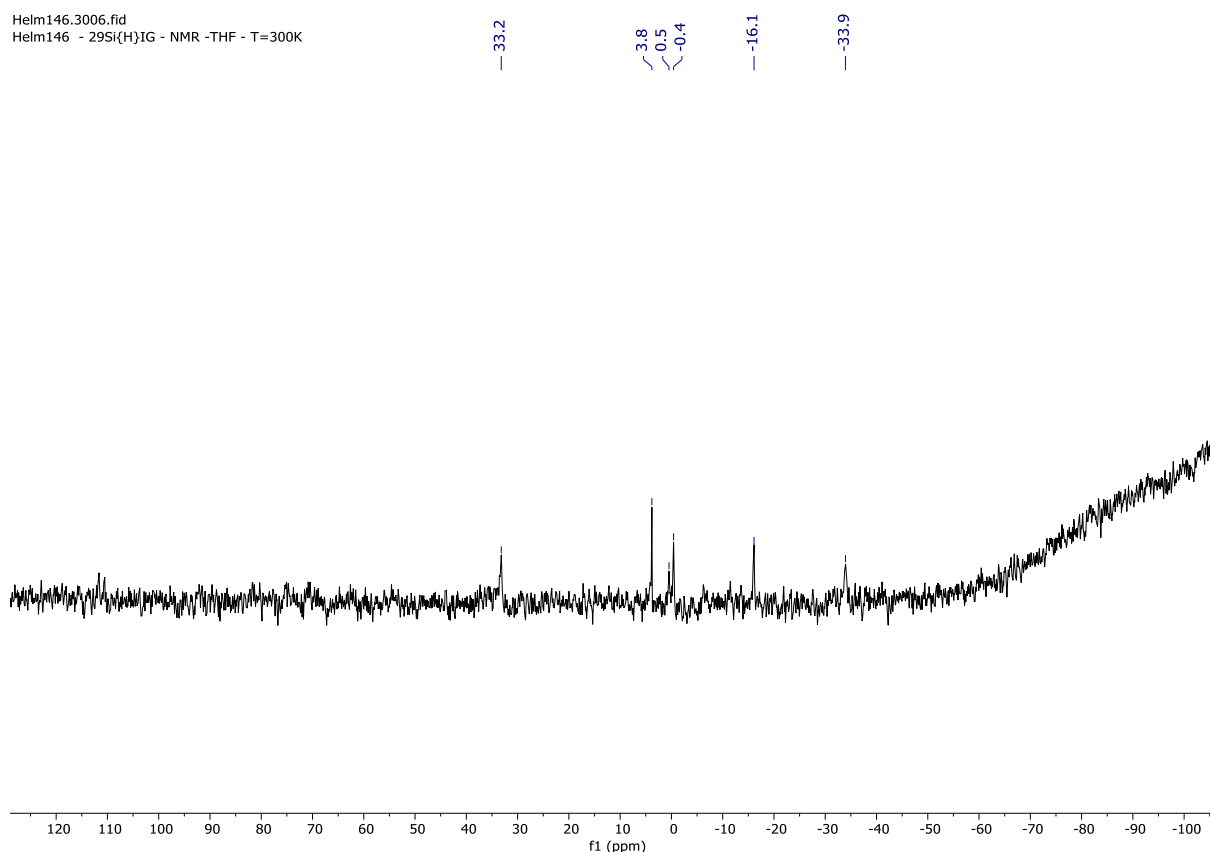


Figure S26. $^{29}\text{Si}\{\text{H}\}$ -IG-NMR spectrum (d_8 -THF, 300 K, 80 MHz) of **3**.

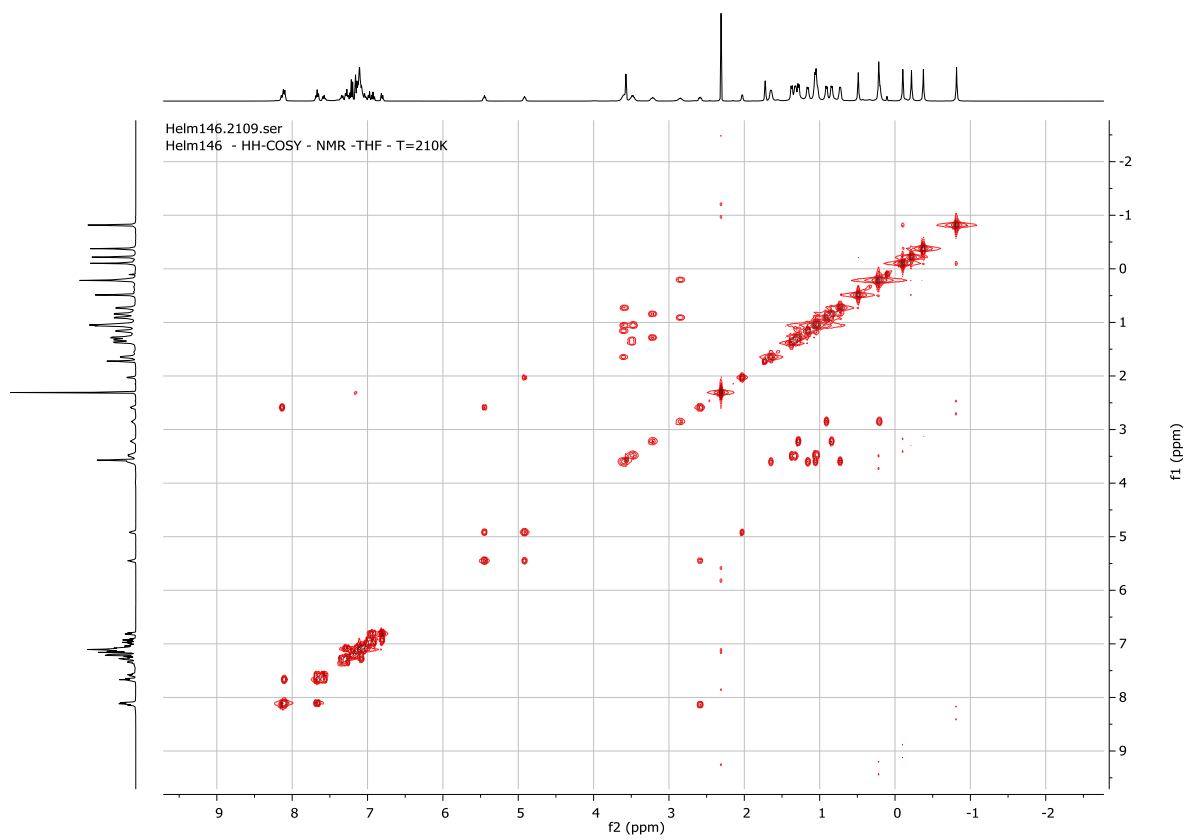


Figure S27. ^1H , ^1H -COSY-NMR spectrum (d_8 -THF, 210 K) of **3**.

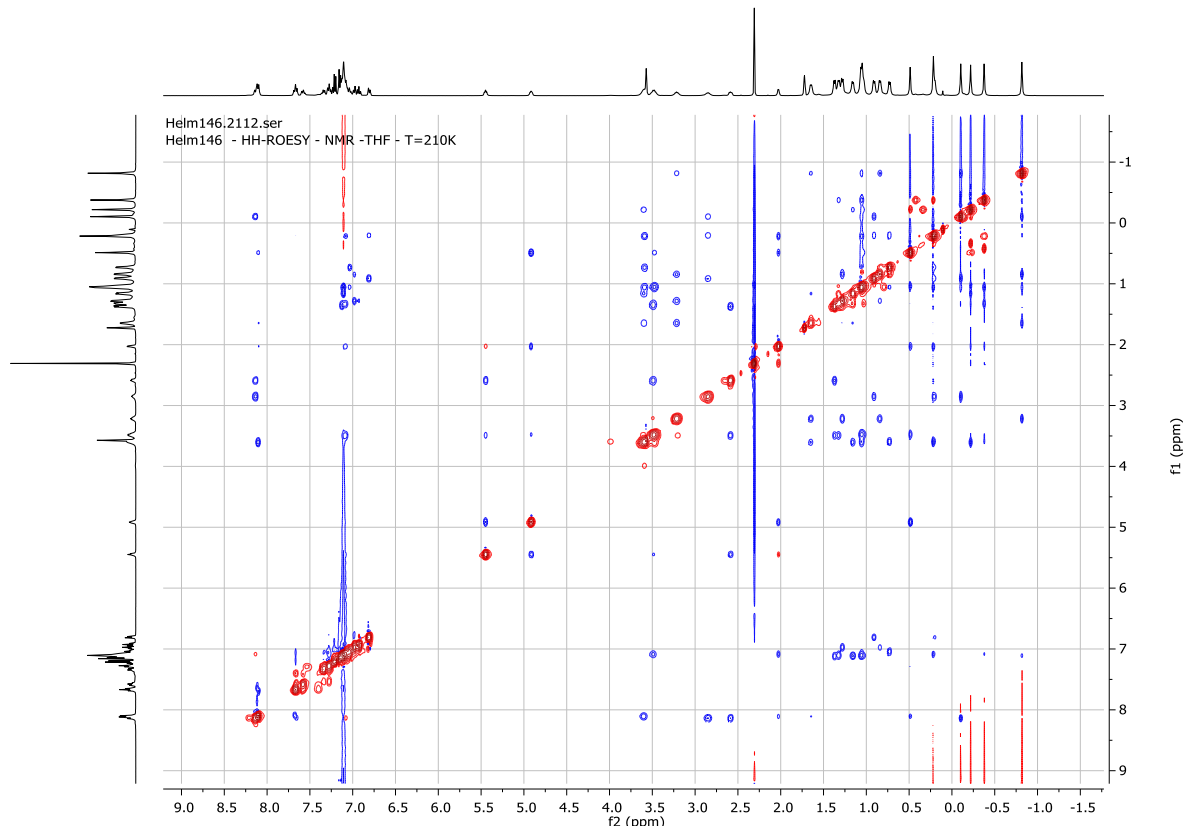


Figure S28. ^1H , ^1H -ROESY-NMR spectrum (d_8 -THF, 210 K) of **3**.

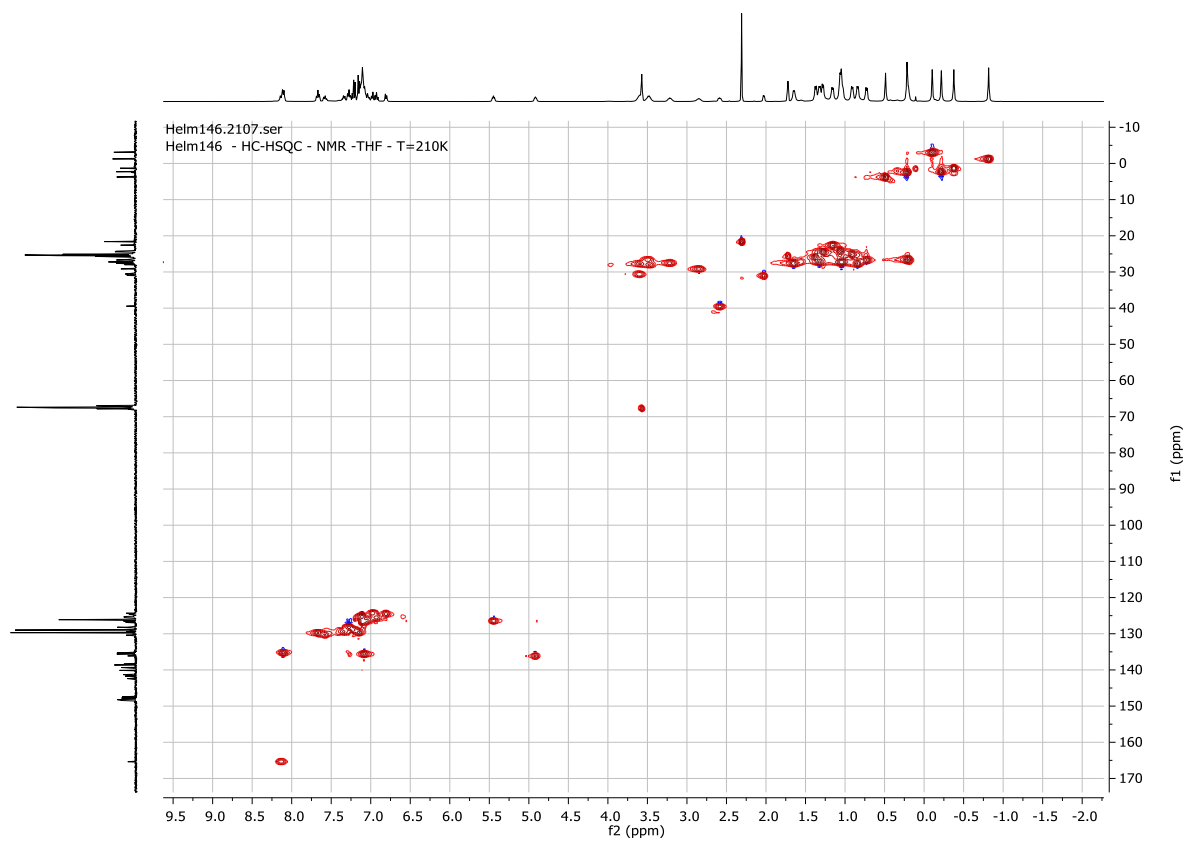


Figure S29. ^1H , ^{13}C -HSQC-NMR spectrum (d_8 -THF, 210 K) of 3.

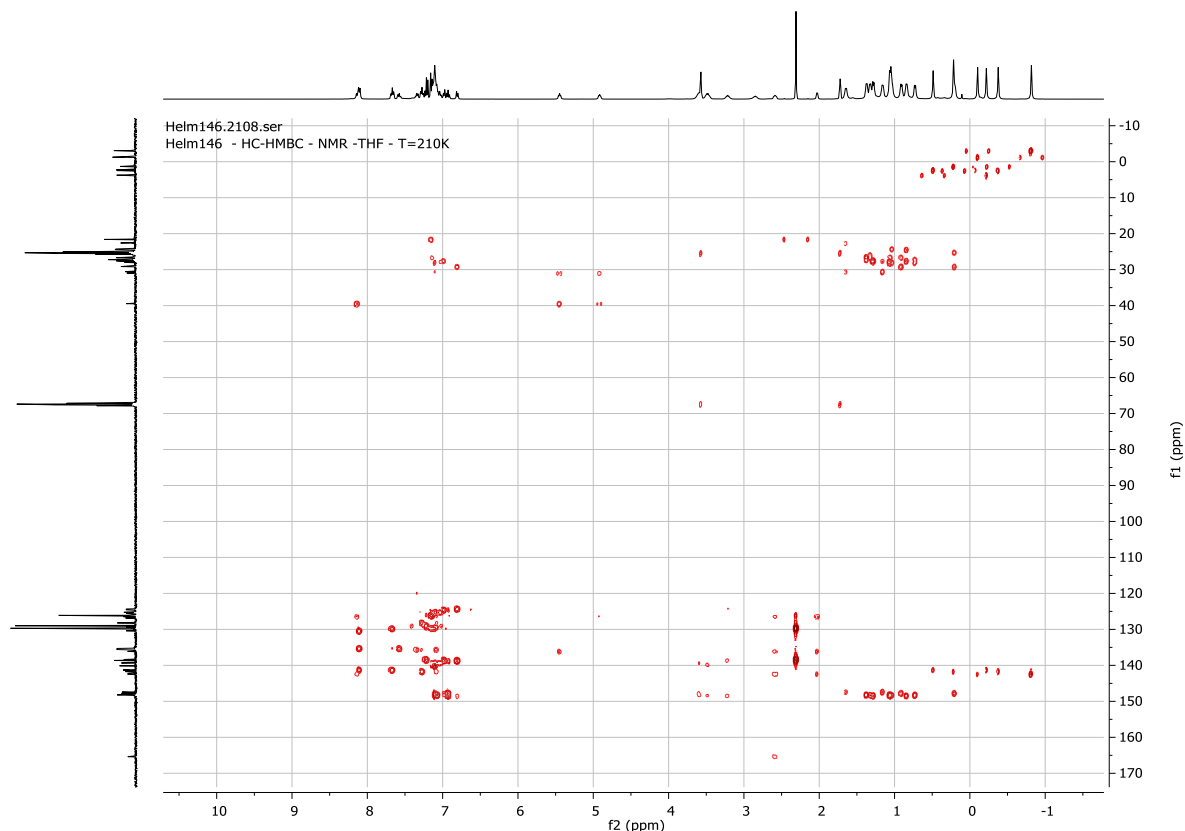


Figure S30. ^1H , ^{13}C -HMBC-NMR spectrum (d_8 -THF, 210 K) of 3.

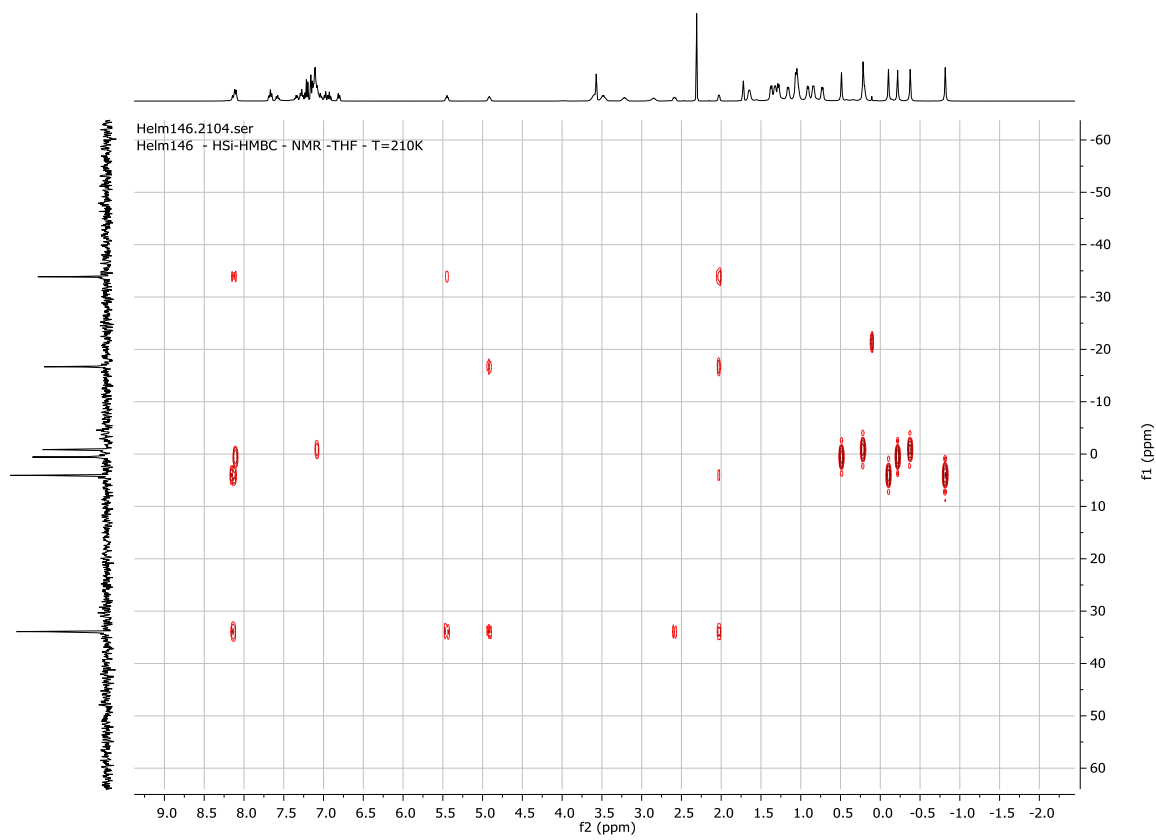


Figure S31. ^1H , ^{29}Si -HMBC-NMR spectrum (d_8 -THF, 210 K) of **3**.

SHIMADZU

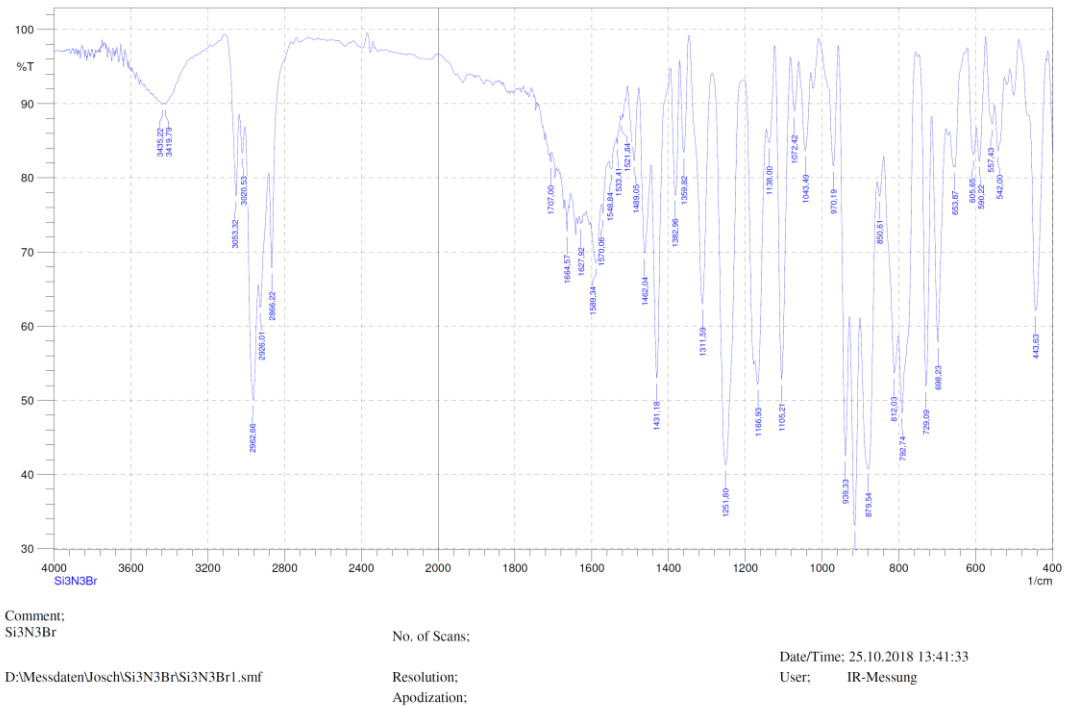


Figure S32. FT-IR spectrum (KBr pellet) of **3**.

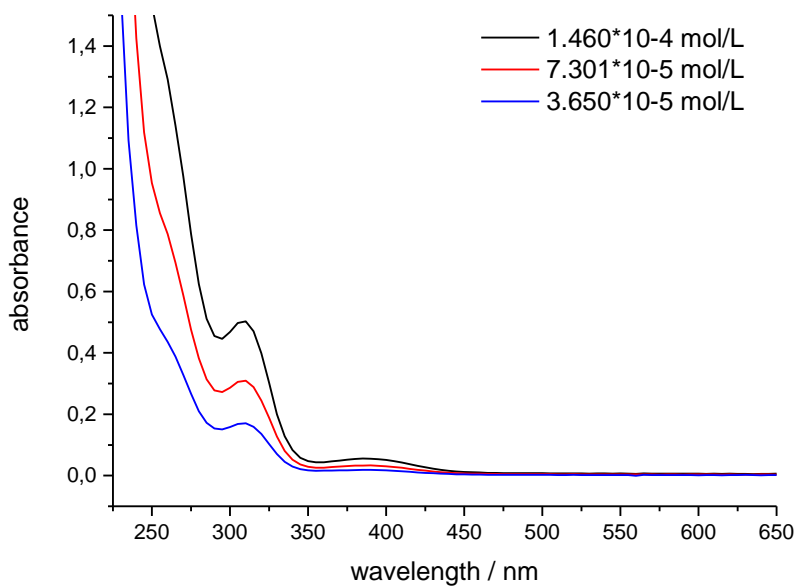


Figure S33. UV/Vis spectrum (*n*-hexane) of **3**.

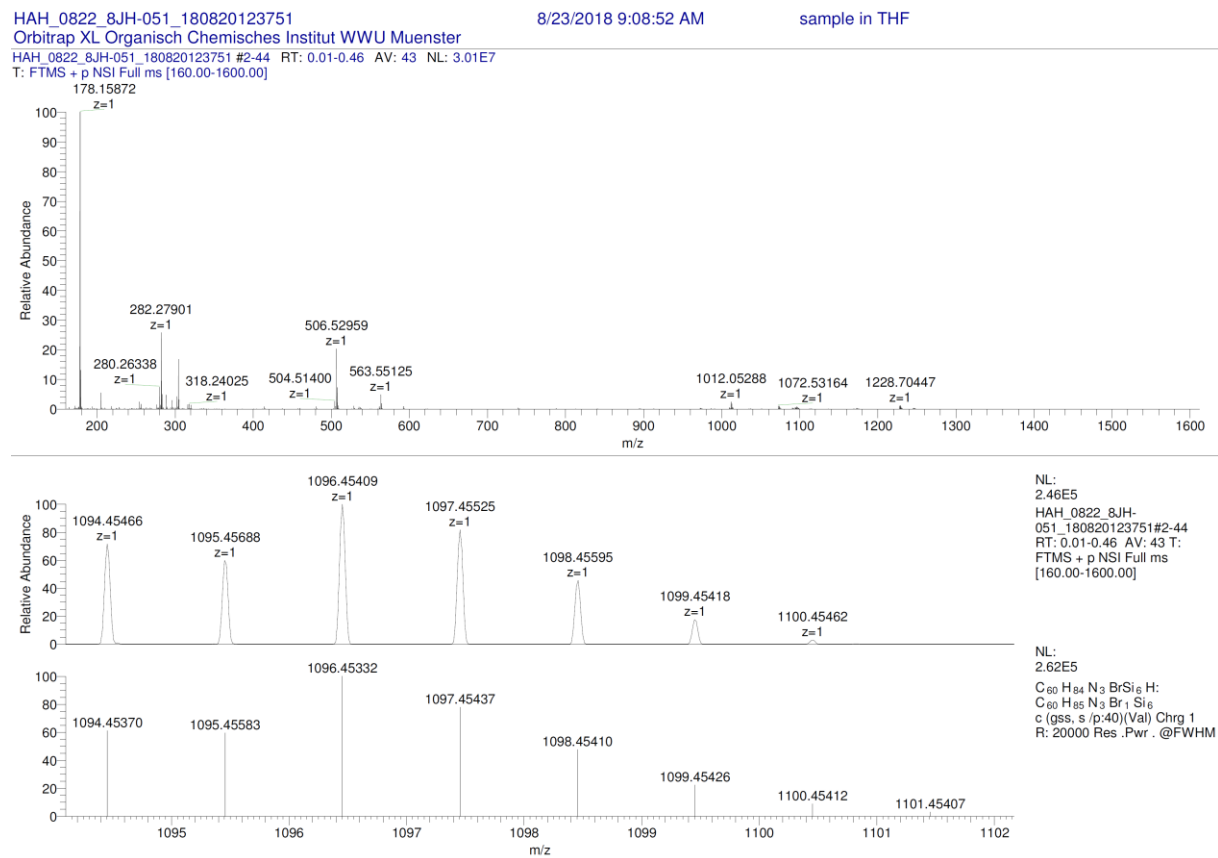
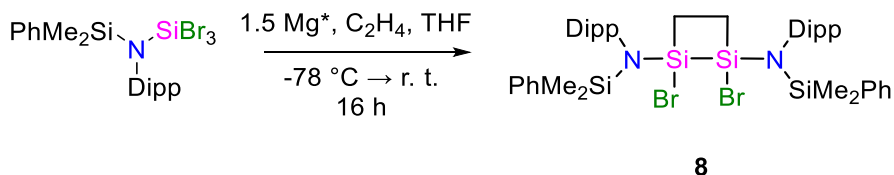


Figure S34. ESI-MS spectrum of **3**.

2.4. Synthesis and Characterization of 8



$[\text{N}\{\text{SiMe}_2\text{Ph}\}\text{Dipp}]\text{SiBr}_3$ **2** (2.892 g, 5.0 mmol, 1.0 equiv.) was dissolved in THF (30 ml) and slowly added to a suspension of Mg^* (0.182 g, 7.5 mmol, 1.5 equiv.) in THF (20 ml) at -78°C . The reaction mixture was degassed, and an ethylene atmosphere (1 bar) was introduced. The system was allowed to warm to room temperature and stirred for 16 h. After addition of 1,4-dioxane (3.0 ml, 33.4 mmol, 6.7 eq.), the solution was stirred for one hour at room temperature. The suspension was filtrated, and all volatiles were removed *in vacuo*. The bright yellow residue was extracted with *n*-hexane (3 x 20 ml) and filtrated. Colourless crystals of $[\text{N}\{(\text{SiMe}_2\text{Ph})\text{Dipp}\}\text{SiBrCH}_2]_2$ **8** (0.120 g, 0.14 mmol, 6%) formed from a concentrated *n*-hexane solution after storage at -32°C .

$^1\text{H-NMR}$ (C_6D_6 , 300 K, 400 MHz): δ [ppm] = 7.57–7.55 (4H, m, *ortho*- H_{Ph}), 7.20–7.17 (6H, m, *meta/para*- H_{Ph}), 7.07–7.03 (4H, m, *meta/para*- H_{Dipp}), 7.01–6.97 (2H, m, *meta*- H_{Dipp}), 3.89 (2H, sept, $^3J_{\text{H-H}} = 6.8$ Hz, $\text{C-H}(\text{CH}_3)_2$), 3.78 (2H, sept, $^3J_{\text{H-H}} = 6.8$ Hz, $\text{C-H}(\text{CH}_3)_2$), 1.20–1.17 (16 H, o.l., BrSiCH_2 , $\text{CH}(\text{CH}_3)_2$), 1.12 (6H, d, $^3J_{\text{H-H}} = 6.8$ Hz, $\text{CH}(\text{CH}_3)_2$), 0.95 (6H, d, $^3J_{\text{H-H}} = 6.8$ Hz, $\text{CH}(\text{CH}_3)_2$), 0.78 (6H, s, $\text{Si}(\text{CH}_3)_2\text{Ph}$), 0.70 (6H, s, $\text{Si}(\text{CH}_3)_2\text{Ph}$).

$^{13}\text{C}\{^1\text{H}\}\text{-NMR}$ (C_6D_6 , 300 K, 101 MHz): δ [ppm] = 148.2 (*ortho*- C_{Dipp}), 147.9 (*ortho*- C_{Dipp}), 139.1 (*ipso*- C_{Dipp}), 137.6 (*ipso*- C_{Ph}), 135.2 (*ortho*- C_{Ph}), 129.9 (*para*- C_{Ph}), 128.0 (*meta*- C_{Ph}), 126.7 (*para* C_{Dipp}), 125.1 (*meta*- C_{Dipp}), 124.9 (*meta*- C_{Dipp}), 28.5 ($\text{CH}(\text{CH}_3)_2$), 27.7 ($\text{CH}(\text{CH}_3)_2$), 27.6 ($\text{CH}(\text{CH}_3)_2$), 27.3 ($\text{CH}(\text{CH}_3)_2$), 24.6 ($\text{CH}(\text{CH}_3)_2$), 24.2 ($\text{CH}(\text{CH}_3)_2$), 15.3 (BrSiCH_2), 1.9 ($\text{Si}(\text{CH}_3)_2\text{Ph}$), 1.3 ($\text{Si}(\text{CH}_3)_2\text{Ph}$).

$^{29}\text{Si}\{^1\text{H}\}\text{-DEPT19.5-NMR}$ (C_6D_6 , 300 K, 80 MHz): δ [ppm] = 0.1 ($\text{Si}(\text{CH}_3)_2\text{Ph}$).

$^{29}\text{Si}\{^1\text{H}\}\text{-IG-NMR}$ (C_6D_6 , 300 K, 80 MHz): δ [ppm] = 15.2 (BrSiCH_2).

IR (KBr pellet): $\tilde{\nu}$ [cm^{-1}] (intensity) = 440(s), 473(s), 536(m), 594(vw), 627(w), 658(w), 702(vs), 733(m), 777(vs), 802(vs), 833(s), 872(vs), 891(vs), 928(vs), 970(w), 988(w), 1045(m), 1103(vs), 1163(vs), 1252(vs), 1316(s), 1362(w), 1383(m), 1431(vs), 1460(s), 1584(vw), 1653(vw), 1813(vw), 1873(vw), 2866(s), 2920(s), 2965(vs), 3019(w), 3053(m), 3071(w).

EI-MS: $m/z = 864$ $[[\text{N}\{(\text{SiMe}_2\text{Ph})\text{Dipp}\}\text{SiBrCH}_2]_2]$.

Melting point: 220 °C.

Elemental analysis: Calc.: H: 6.99, C: 58.31, N: 3.24; Found: H: 7.10, C: 57.60, N: 3.08.

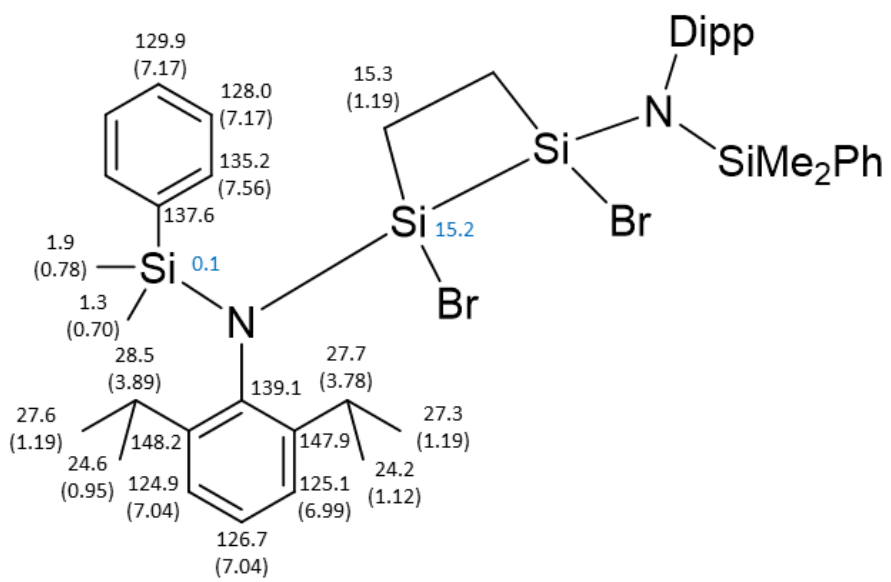


Figure S35. Assignment of chemical shifts to **8**; ¹H (in brackets), ¹³C (black), and ²⁹Si (blue).

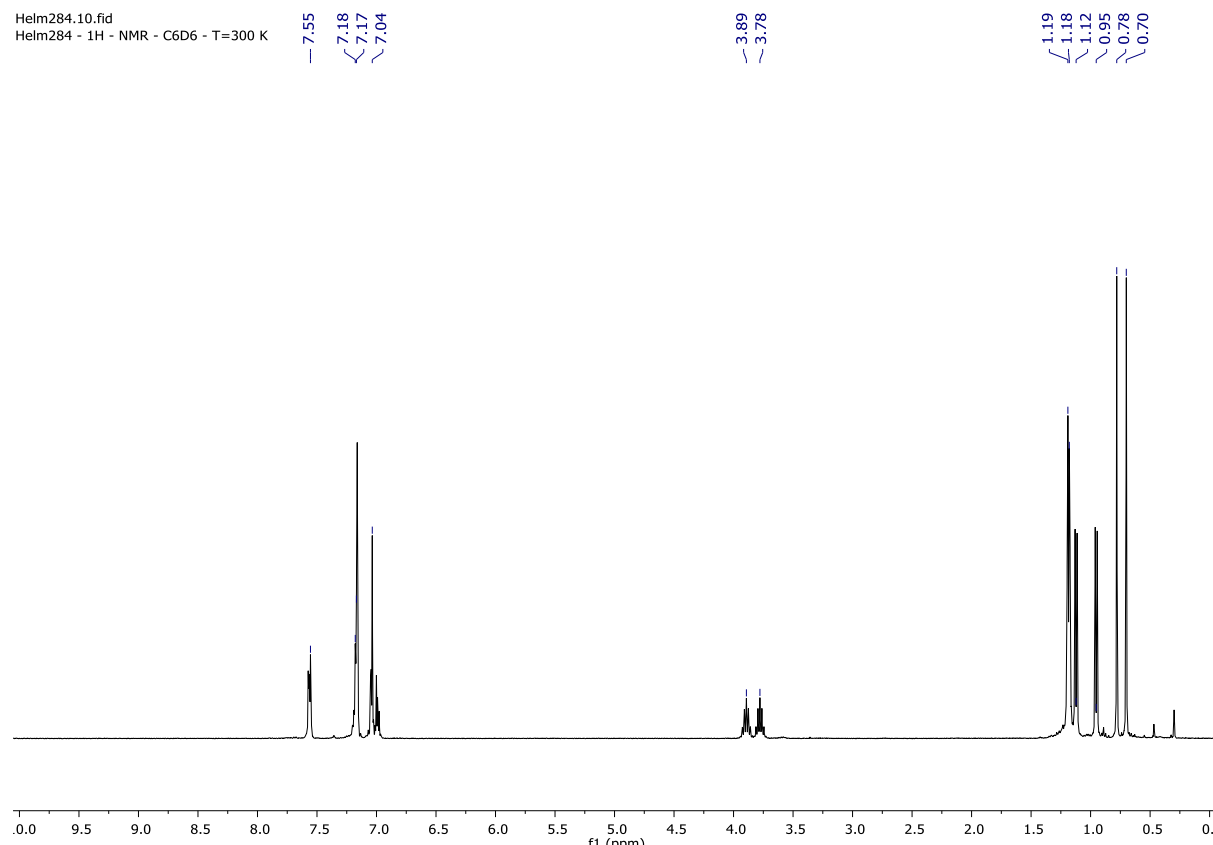


Figure S36. ¹H-NMR spectrum (C₆D₆, 300 K, 400 MHz) of **8**.

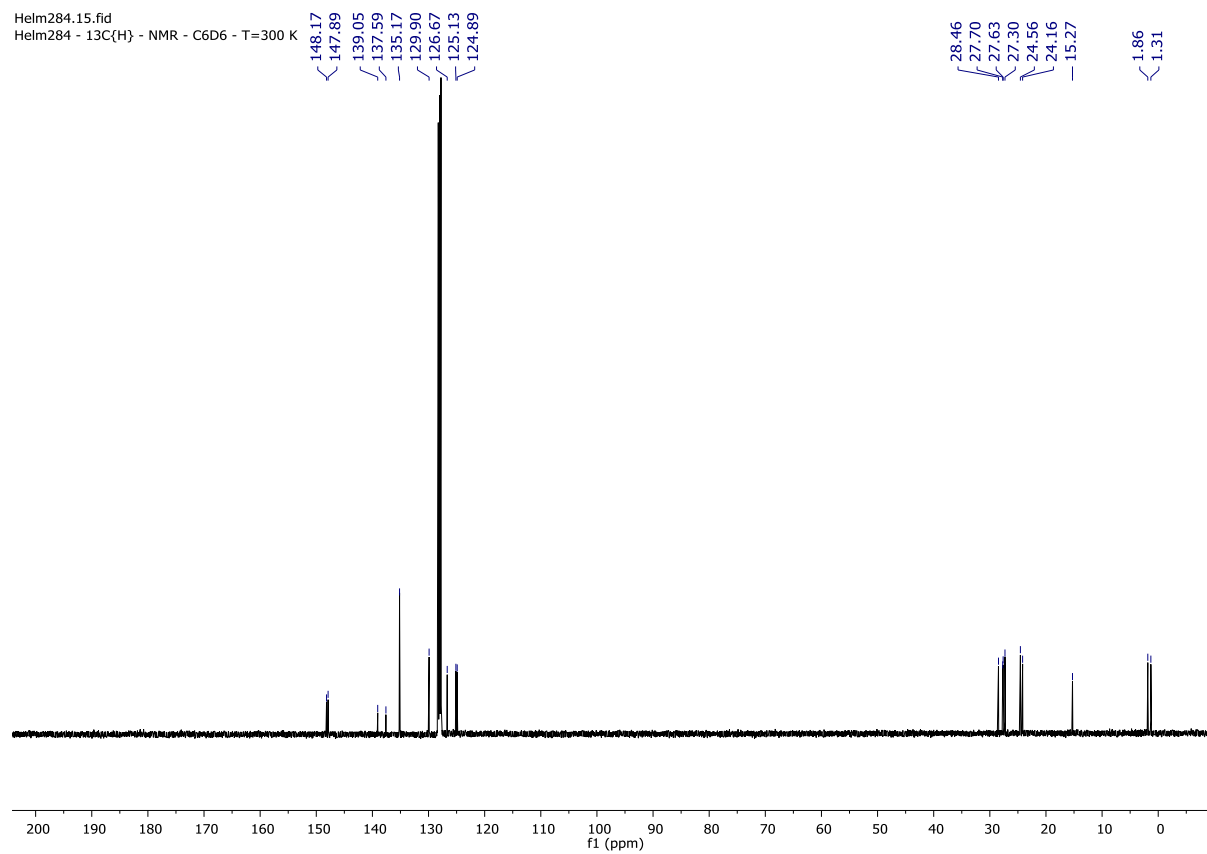


Figure S37. $^{13}\text{C}\{\text{H}\}$ -NMR spectrum (C_6D_6 , 300 K, 100 MHz) of **8**.

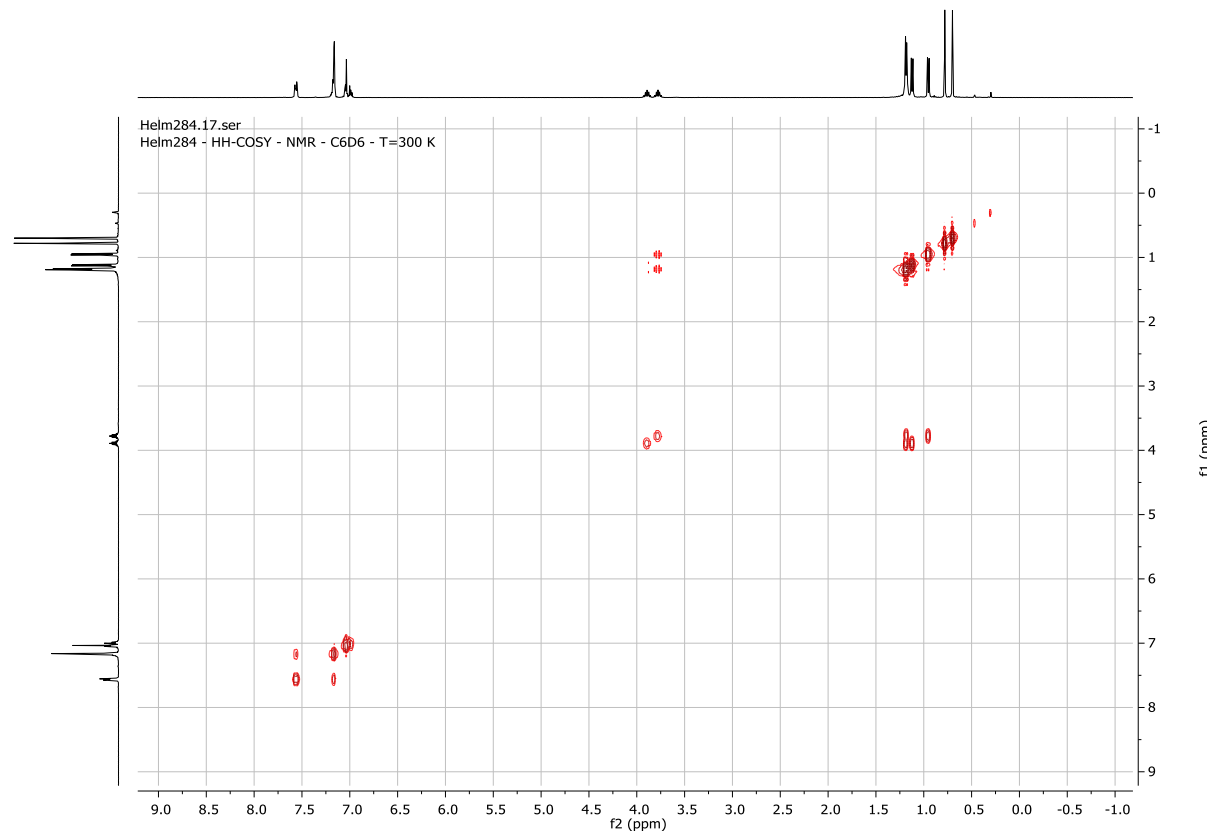


Figure S38. $^1\text{H},^1\text{H}$ -COSY-NMR spectrum (C_6D_6 , 300 K) of **8**.

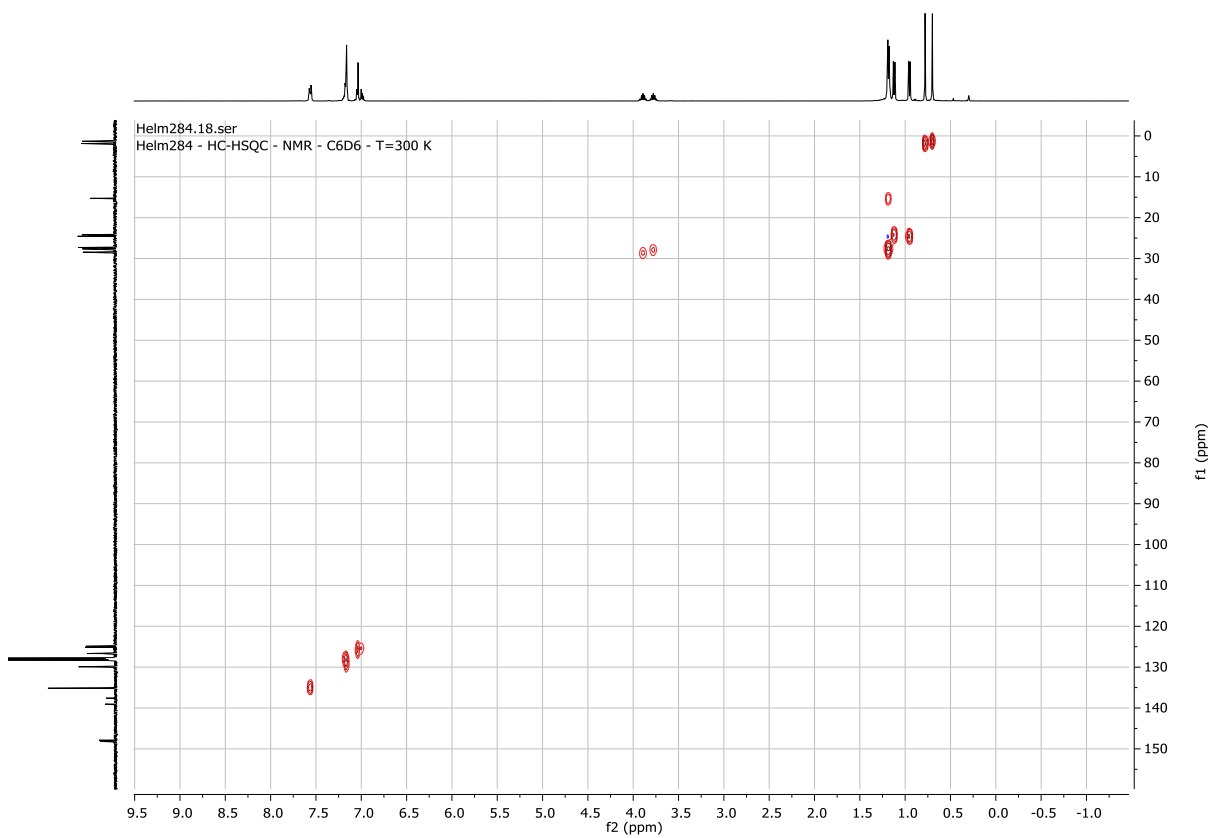


Figure S39. ¹H, ¹³C-HSQC-NMR spectrum (C_6D_6 , 300 K) of **8**.

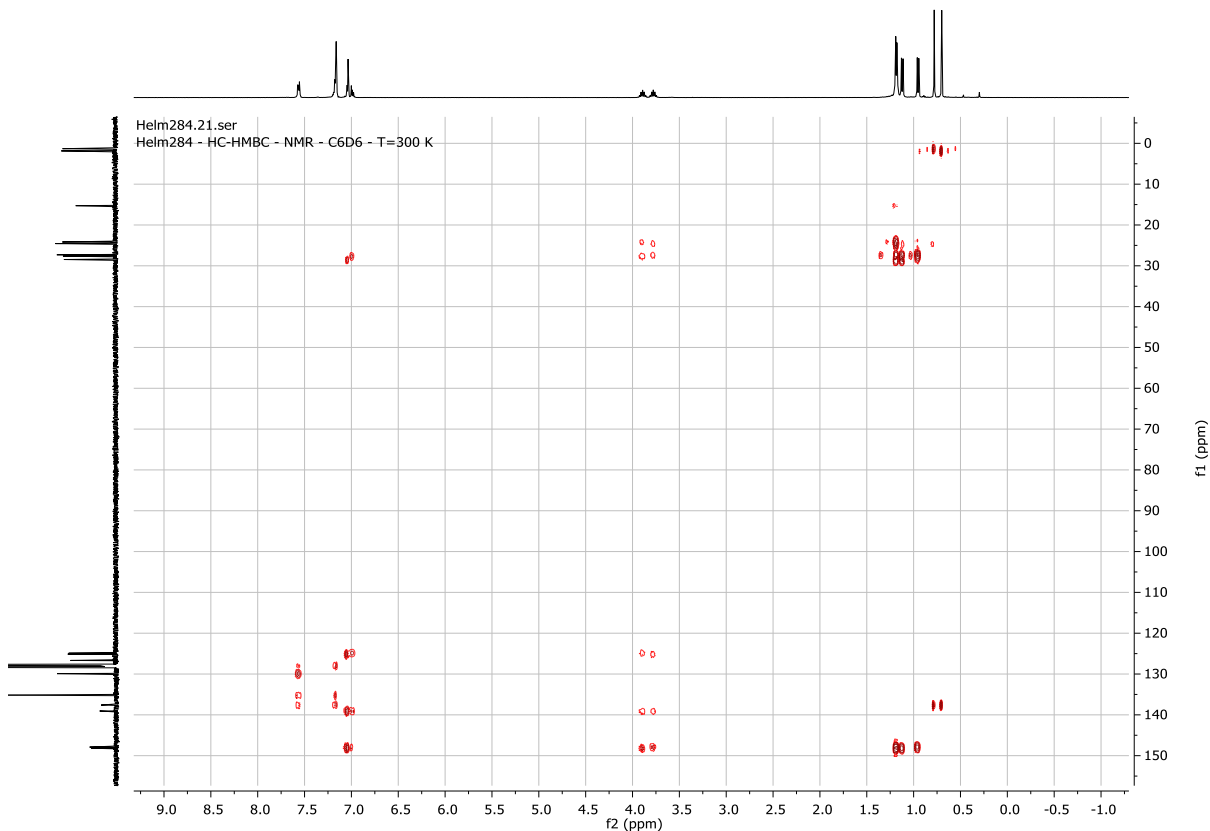


Figure S40. ¹H, ¹³C-HMBC-NMR spectrum (C_6D_6 , 300 K) of **8**.

Helm284.11.fid
Helm284 - $^{29}\text{Si}\{\text{H}\}$ Dept19.5 - NMR - C6D6 - T=300 K

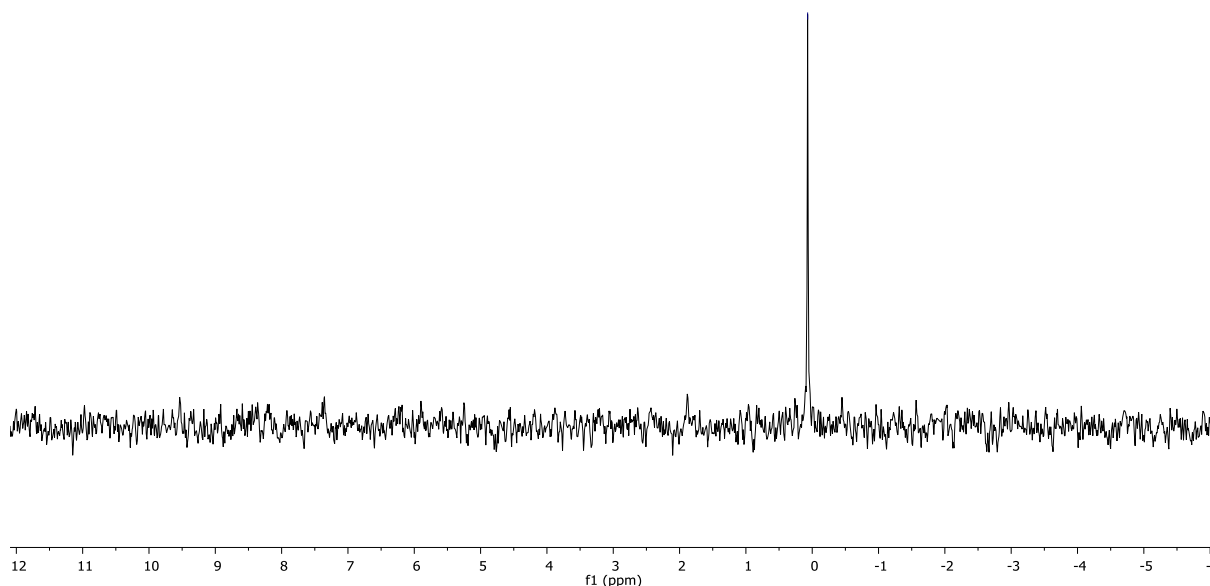


Figure S41. $^{29}\text{Si}\{^1\text{H}\}$ -DEPT19.5-NMR spectrum (C_6D_6 , 300 K, 80 MHz) of **8**.

Helm284.13.fid
Helm284 - $^{29}\text{Si}\{\text{H}\}$ IG - NMR - C6D6 - T=300 K

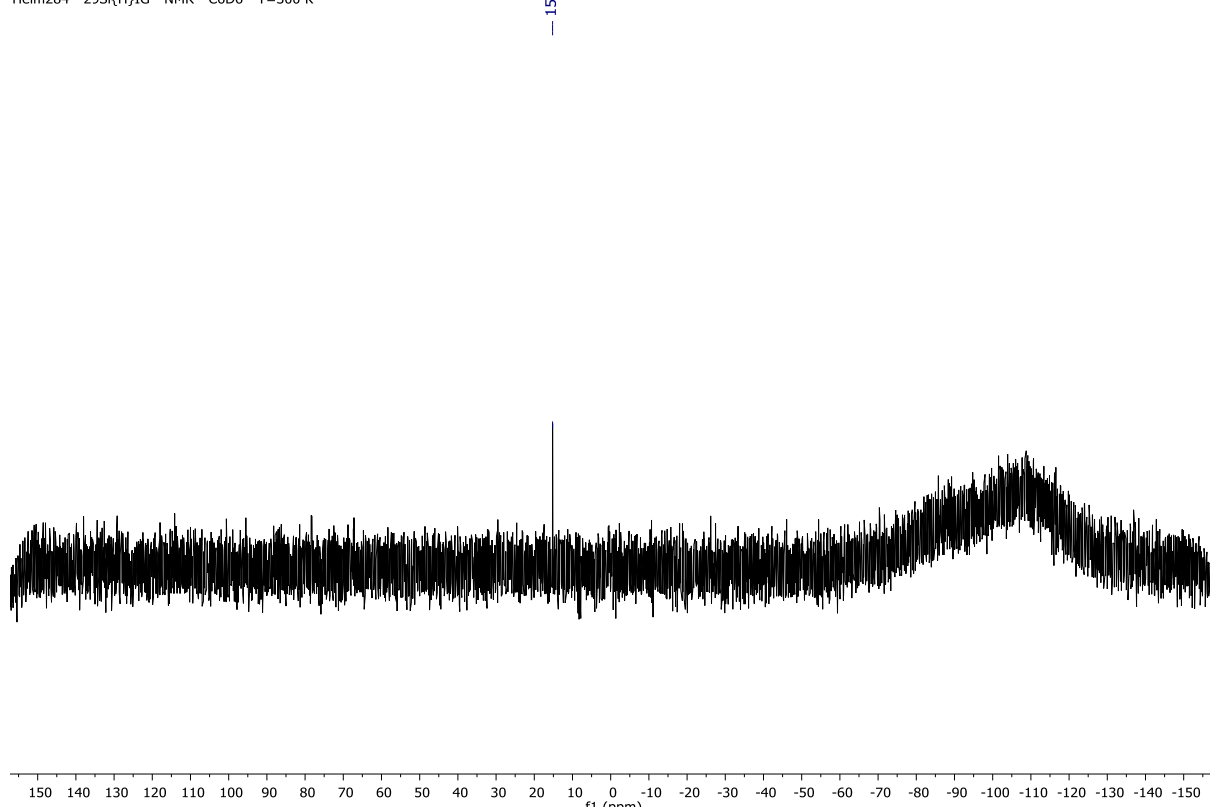


Figure S42. $^{29}\text{Si}\{^1\text{H}\}$ -IG-NMR spectrum (C_6D_6 , 300 K, 80 MHz) of **8**.

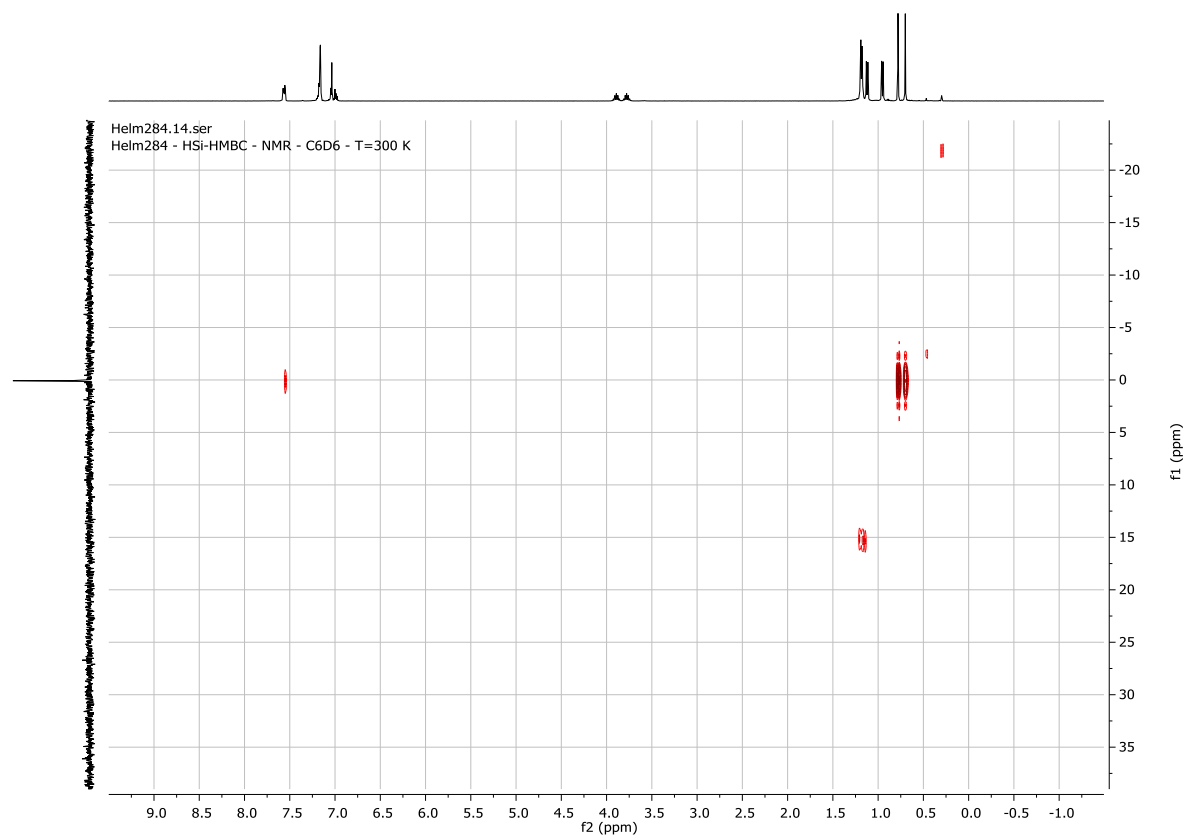


Figure S43. ^1H , ^{29}Si -HMBC-NMR spectrum (C_6D_6 , 300 K) of **8**.

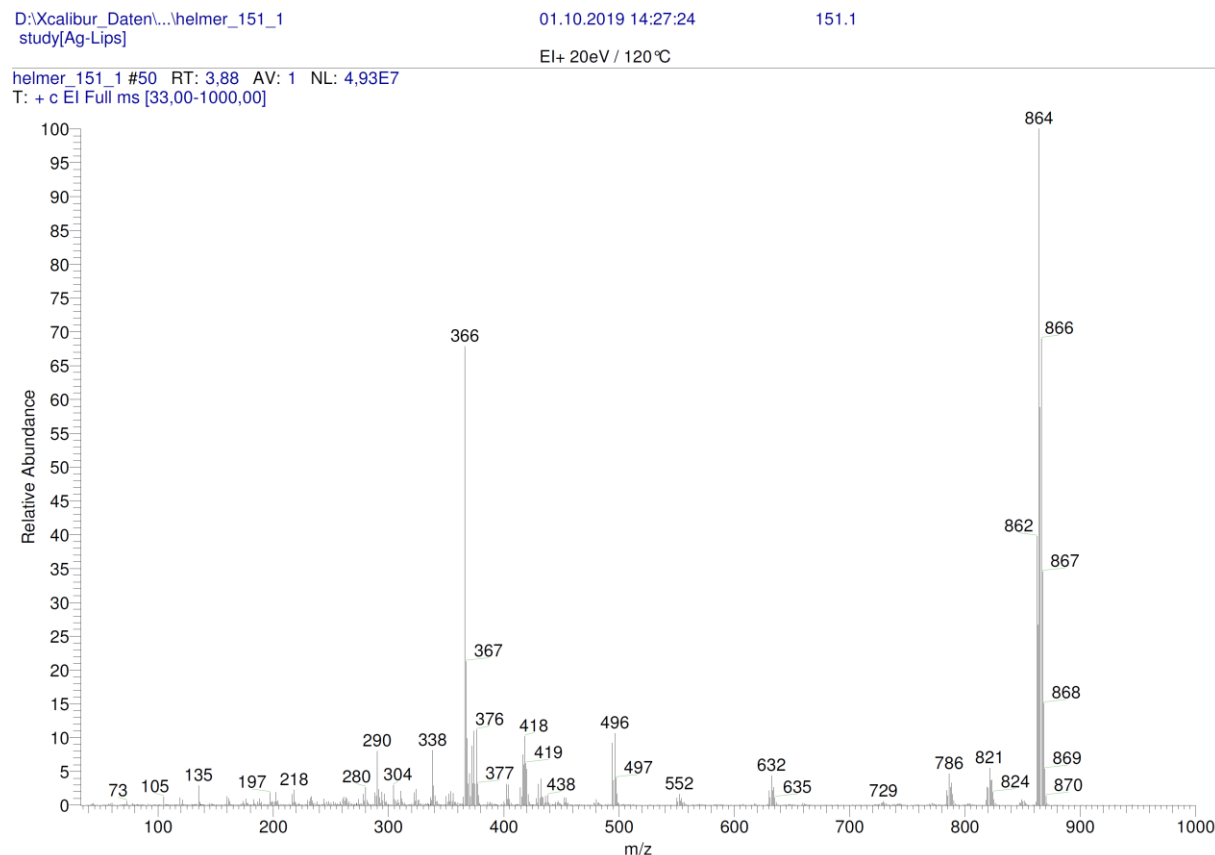


Figure S44. EI-MS spectrum of **8**.

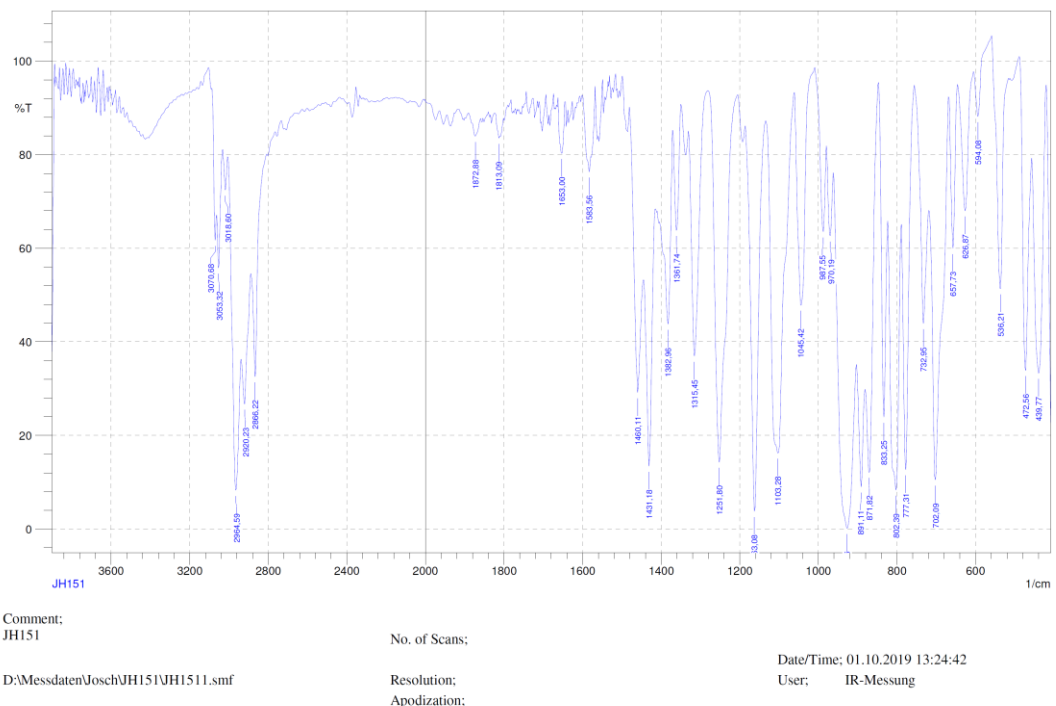
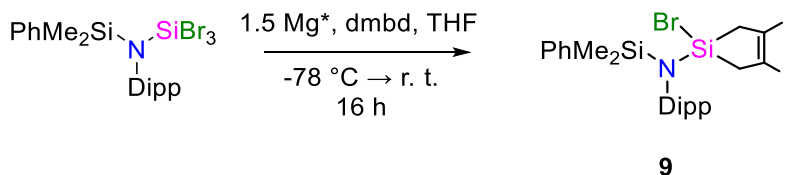


Figure S45. IR spectrum (KBr pellet) of **8**.

2.5. Synthesis and Characterization of 9



$[\text{N}\{\text{SiMe}_2\text{Ph}\}\text{Dipp}]\text{SiBr}_3$ **2** (2.000 g, 3.5 mmol, 1.0 equiv.) was dissolved in THF (30 ml) and slowly added to a suspension of Mg^* (0.126 g, 5.2 mmol, 1.5 equiv.) in THF (20 ml) at -78°C . 2,3-Dimethyl-1,3-butadiene (dmbd; 1.95 ml, 1.422 g, 17.3 mmol, 5.0 equiv.) was then added *via* syringe. The reaction mixture was allowed to warm to room temperature and stirred for 16 h. After addition of 1,4-dioxane (3.0 ml, 33.4 mmol, 9.5 equiv.), the solution was stirred for 1 h at room temperature. The suspension was filtrated, and all volatiles were removed *in vacuo*. The bright yellow residue was extracted with *n*-hexane (3 x 20 ml) and filtrated to obtain **9** (0.491 g, 0.98 mmol, 28%) in form of a colourless powder.

$^1\text{H-NMR}$ (C_6D_6 , 300 K, 400 MHz): δ [ppm] = 7.65–7.63 (2H, m, *ortho*- H_{Ph}), 7.21–7.17 (3H, m, *meta/para*- H_{Ph}), 7.08–7.02 (3H, m, *meta/para*- H_{Dipp}), 3.61 (2H, sept, $^3J_{\text{H-H}} = 6.9$ Hz, $\text{CH}(\text{CH}_3)_2$), 1.53 (2H, d, $^2J_{\text{H-H}} = 17.8$ Hz, SiCH_2), 1.46 (2H, d, $^2J_{\text{H-H}} = 17.8$ Hz, SiCH_2), 1.39 (6H, s, $\text{CH}_2\text{C}(\text{CH}_3)$), 1.12 (6H, d, $^3J_{\text{H-H}} = 6.9$ Hz, $\text{CH}(\text{CH}_3)_2$), 1.10 (6H, d, $^3J_{\text{H-H}} = 6.9$ Hz, $\text{CH}(\text{CH}_3)_2$), 0.57 (6H, s, $\text{Si}(\text{CH}_3)_2\text{Ph}$).

$^{13}\text{C-NMR}$ (C_6D_6 , 300 K, 101 MHz): δ [ppm] = 147.5 (*ortho*- C_{Dipp}), 140.7 (*ipso*- C_{Dipp}), 137.3 (*ipso*- C_{Ph}), 135.0 (*ortho*- C_{Ph}), 130.0 (*para*- C_{Ph}), 129.4 ($(\text{CH}_3)\text{C}=\text{C}(\text{CH}_3)$), 128.0 (*meta*- C_{Ph}), 126.4 (*para*- C_{Dipp}), 124.6 (*meta*- C_{Dipp}), 30.0 (CH_2), 28.4 ($\text{CH}(\text{CH}_3)_2$), 25.5 ($\text{CH}(\text{CH}_3)_2$), 24.3 ($\text{CH}(\text{CH}_3)_2$), 18.7 ($(\text{CH}_3)\text{C}=\text{C}(\text{CH}_3)$), 0.2 ($\text{Si}(\text{CH}_3)_2\text{Ph}$).

$^{29}\text{Si}\{^1\text{H}\}$ -DEPT19.5-NMR (C_6D_6 , 300 K, 80 MHz): δ [ppm] = 0.1 ($\text{Si}(\text{CH}_3)_2\text{Ph}$).

$^{29}\text{Si}\{^1\text{H}\}$ -IG-NMR (C_6D_6 , 300 K, 80 MHz): δ [ppm] = 19.4 (NSi-Br), 0.1 ($\text{Si}(\text{CH}_3)_2\text{Ph}$).

IR (KBr pellet): $\tilde{\nu}$ [cm^{-1}] (intensity) = 446(vw), 471(vw), 542(w), 598(vw), 656(vw), 677(vw), 702(m), 735(w), 779(s), 808(vs), 831(m), 876(m), 899(s), 949(vs), 1045(vw), 1109(s), 1173(vs), 1254(s), 1316(w), 1366(vw), 1385(w), 1435(s), 1458(w), 1655(vw), 2340(vw), 2369(vw), 2868(m), 2926(m), 2965(vs), 3051(vw).

EI-MS: m/z = 420 $[\text{N}\{(\cdot\text{SiMe}_2)\text{Dipp}\}\{\text{CH}_2\text{C}(\text{CH}_3)\}_2\text{SiBr}]$, 501

$[\text{N}\{(\text{SiMe}_2\text{Ph})\text{Dipp}\}\{\text{CH}_2\text{C}(\text{CH}_3)\}_2\text{SiBr}]$.

Elemental analysis: Calc.: H: 7.65, C: 62.37, N: 2.80; Found: H: 7.63, C: 62.26, N: 2.69.

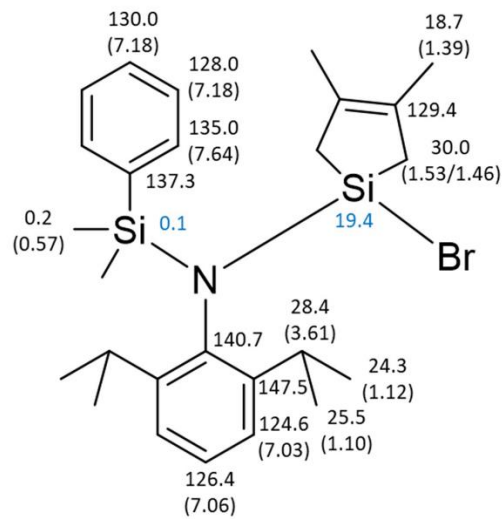


Figure S46. Assignment of chemical shifts to **9**; ^1H (in brackets), ^{13}C (black), and ^{29}Si (blue).

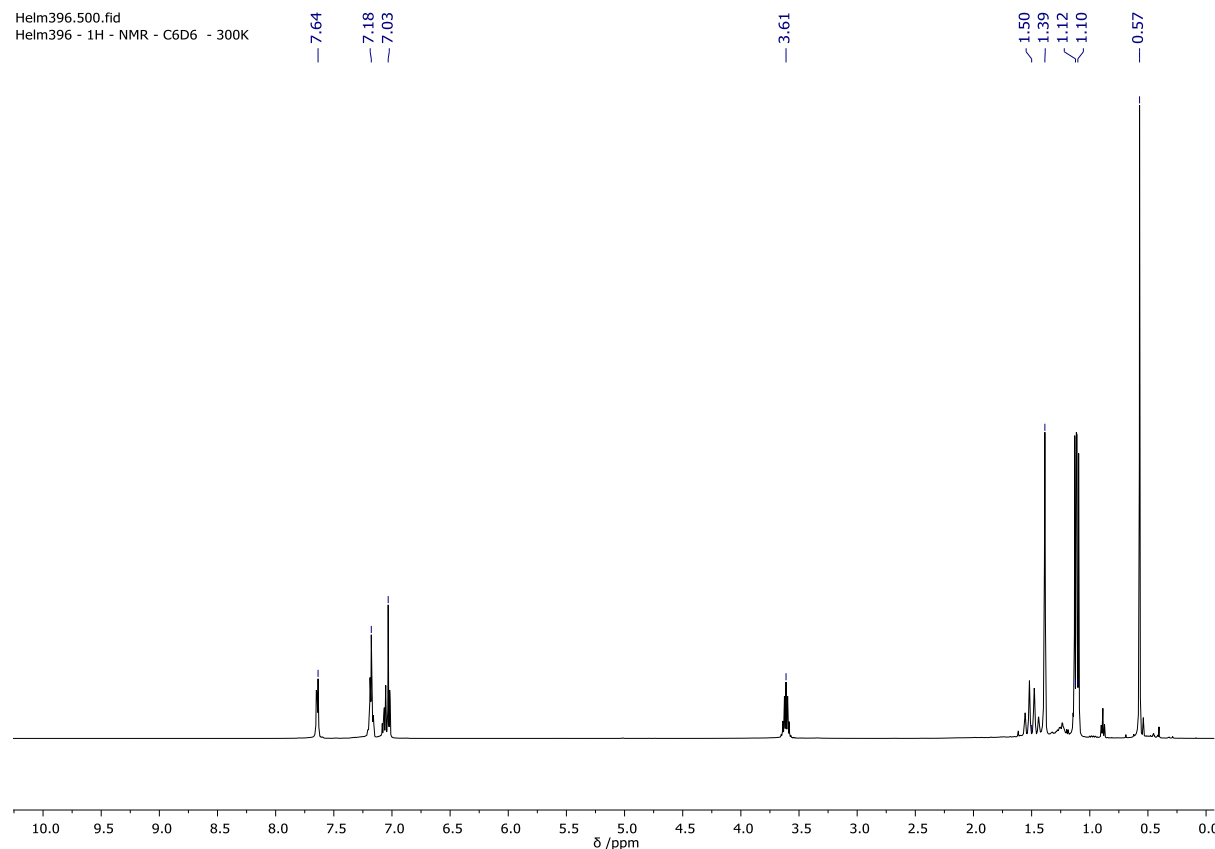


Figure S47. ^1H -NMR spectrum (C_6D_6 , 300 K, 400 MHz) of **9**.

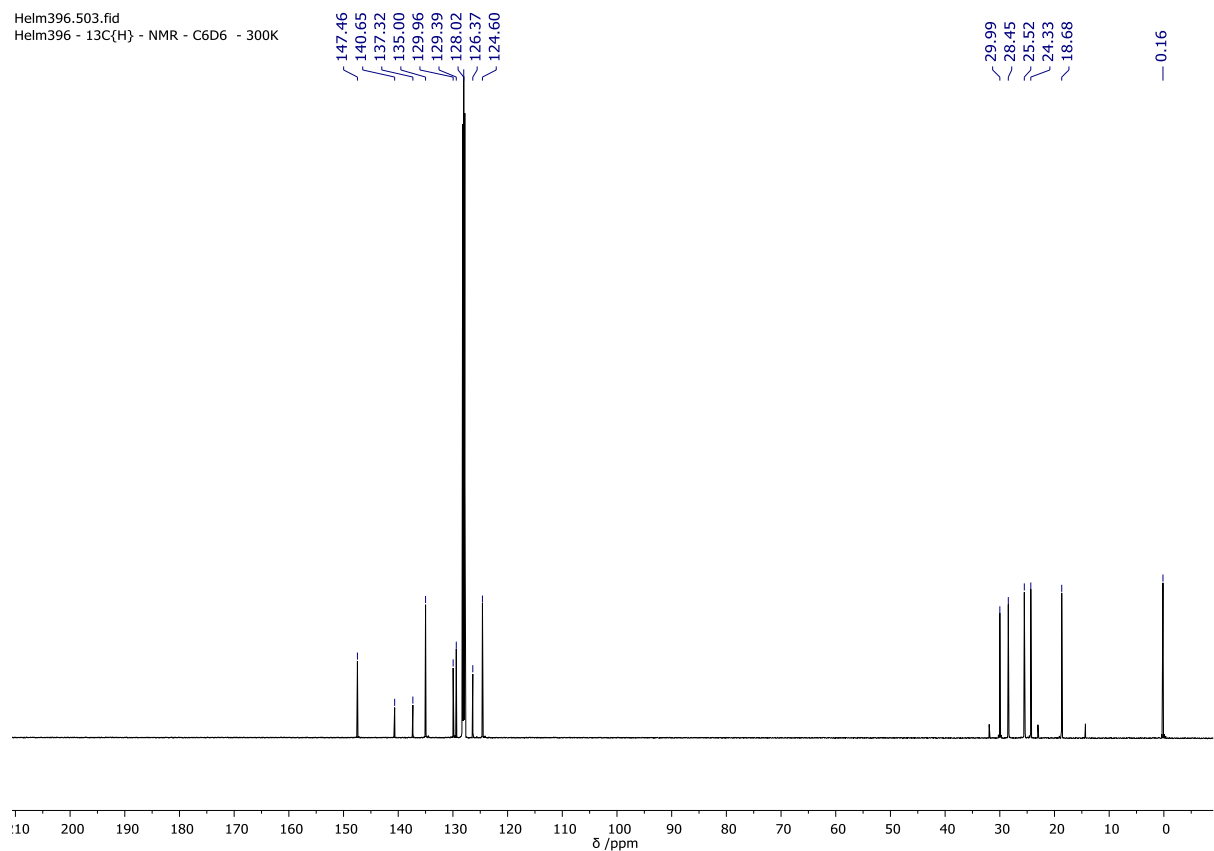


Figure S48. $^{13}\text{C}\{\text{H}\}$ -NMR spectrum (C₆D₆, 300 K, 100 MHz) of **9**.

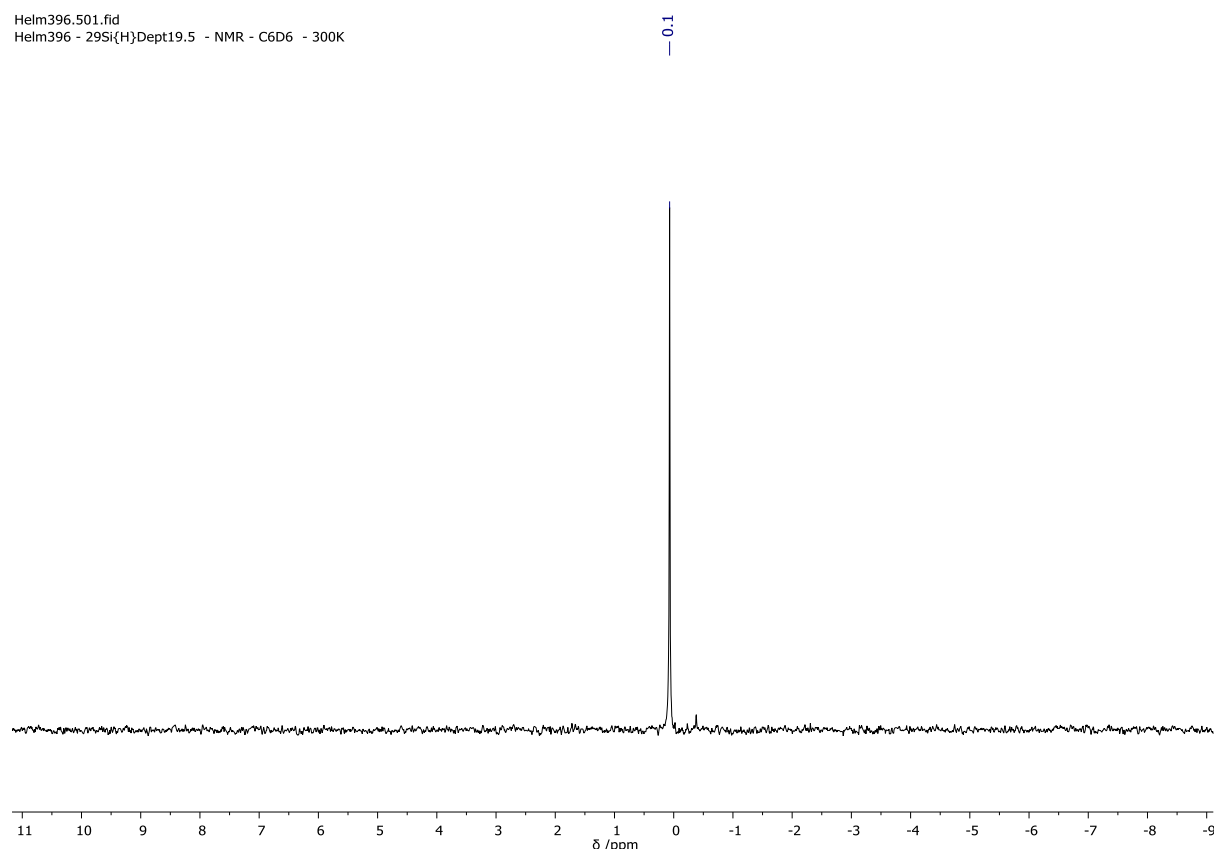


Figure S49. $^{29}\text{Si}\{\text{H}\}$ -DEPT19.5-NMR spectrum (C₆D₆, 300 K, 80 MHz) of **9**.

Helm396.502.fid
Helm396 - 029Si{H}IG(zgig30) - NMR - C6D6 - 300K

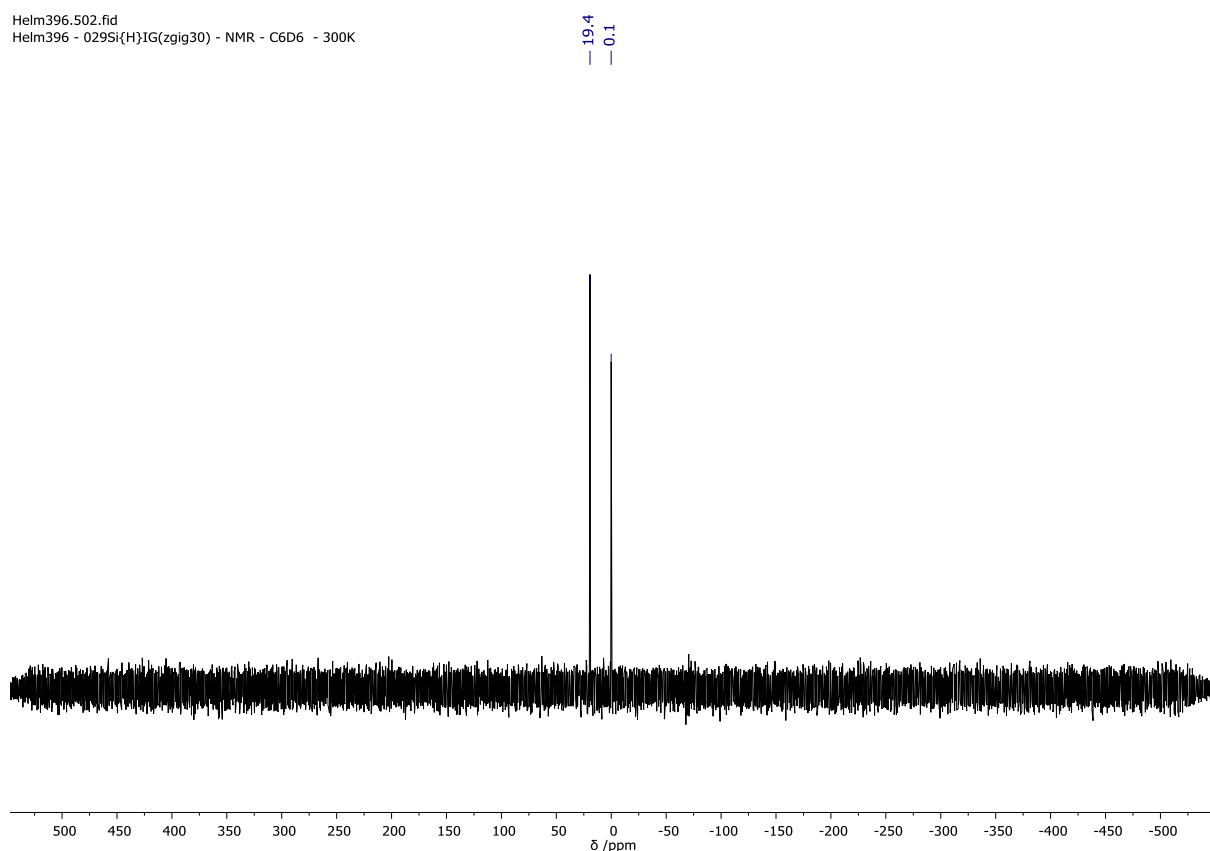


Figure S50. $^{29}\text{Si}\{\text{H}\}$ -IG-NMR spectrum ($C_6\text{D}_6$, 300 K, 80 MHz) of **9**.

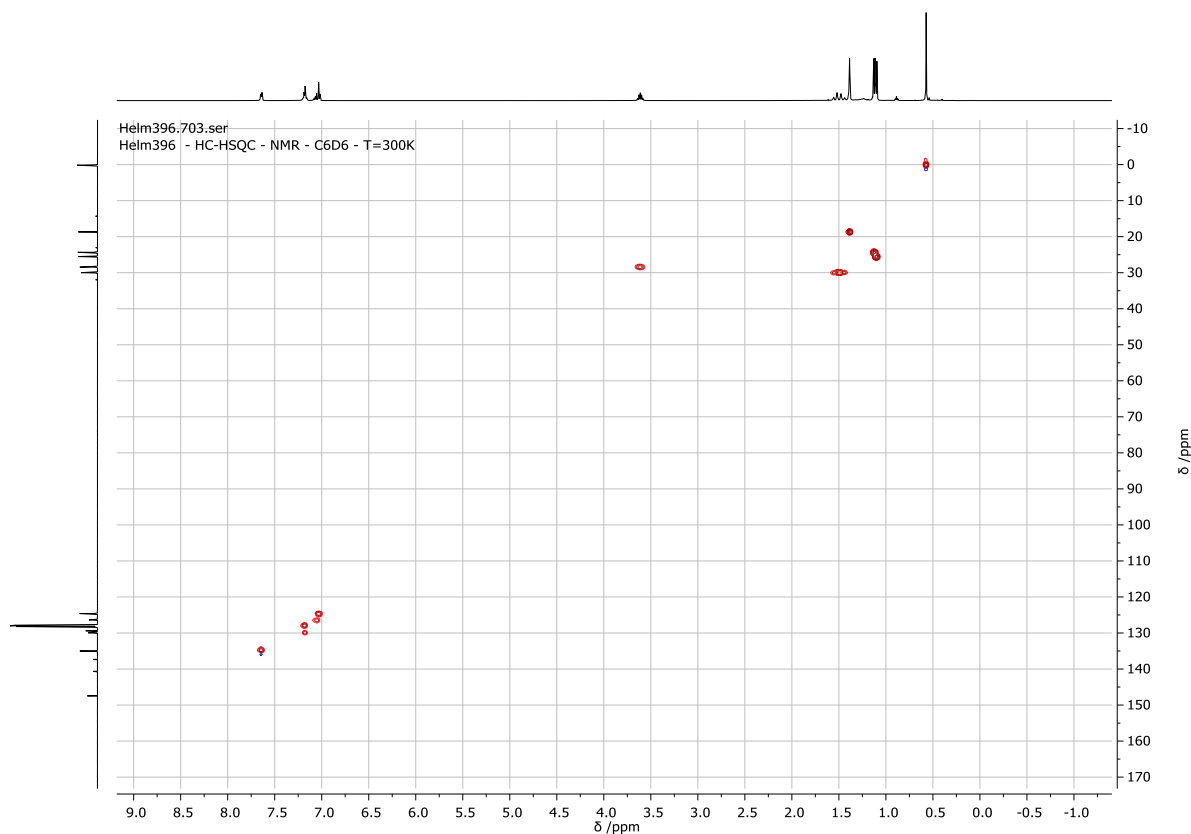


Figure S51. $^1\text{H}, ^{13}\text{C}$ -HSQC-NMR spectrum ($C_6\text{D}_6$, 300 K) of **9**.

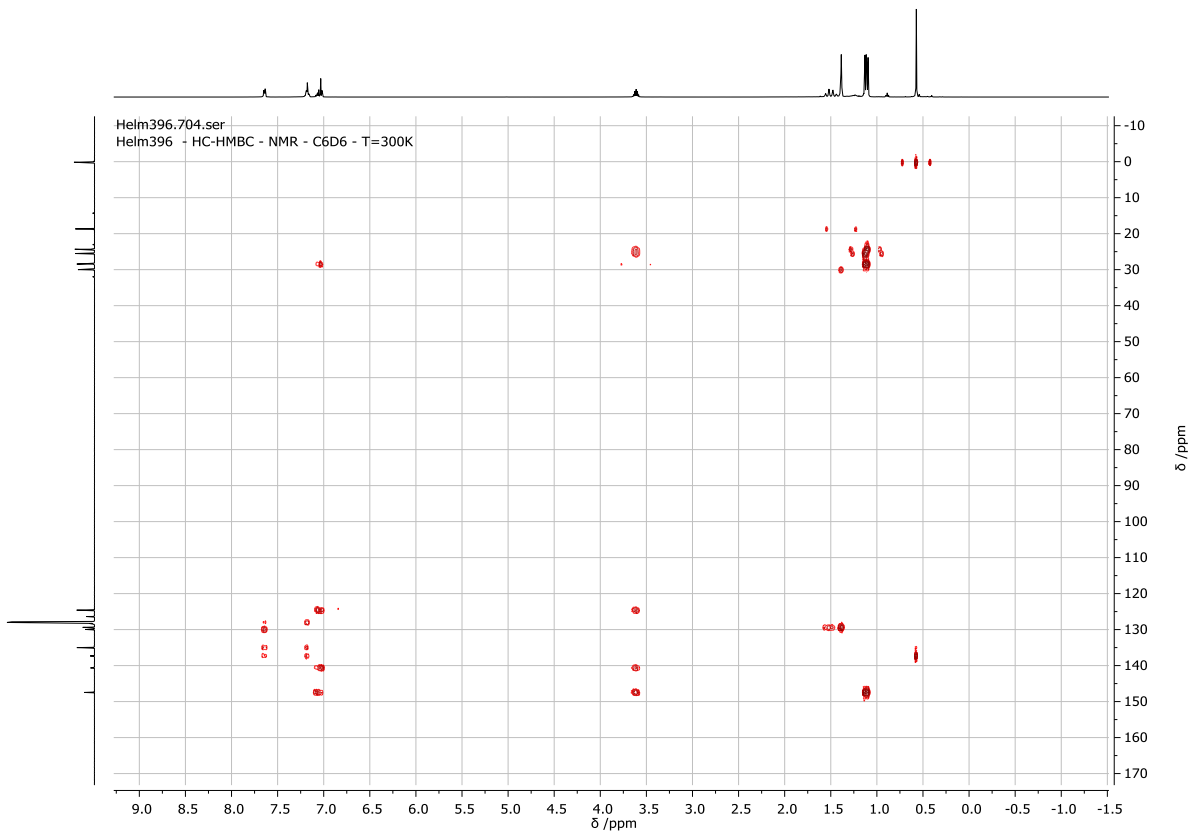


Figure S52. ^1H , ^{13}C -HMBC-NMR spectrum (C_6D_6 , 300 K) of **9**.

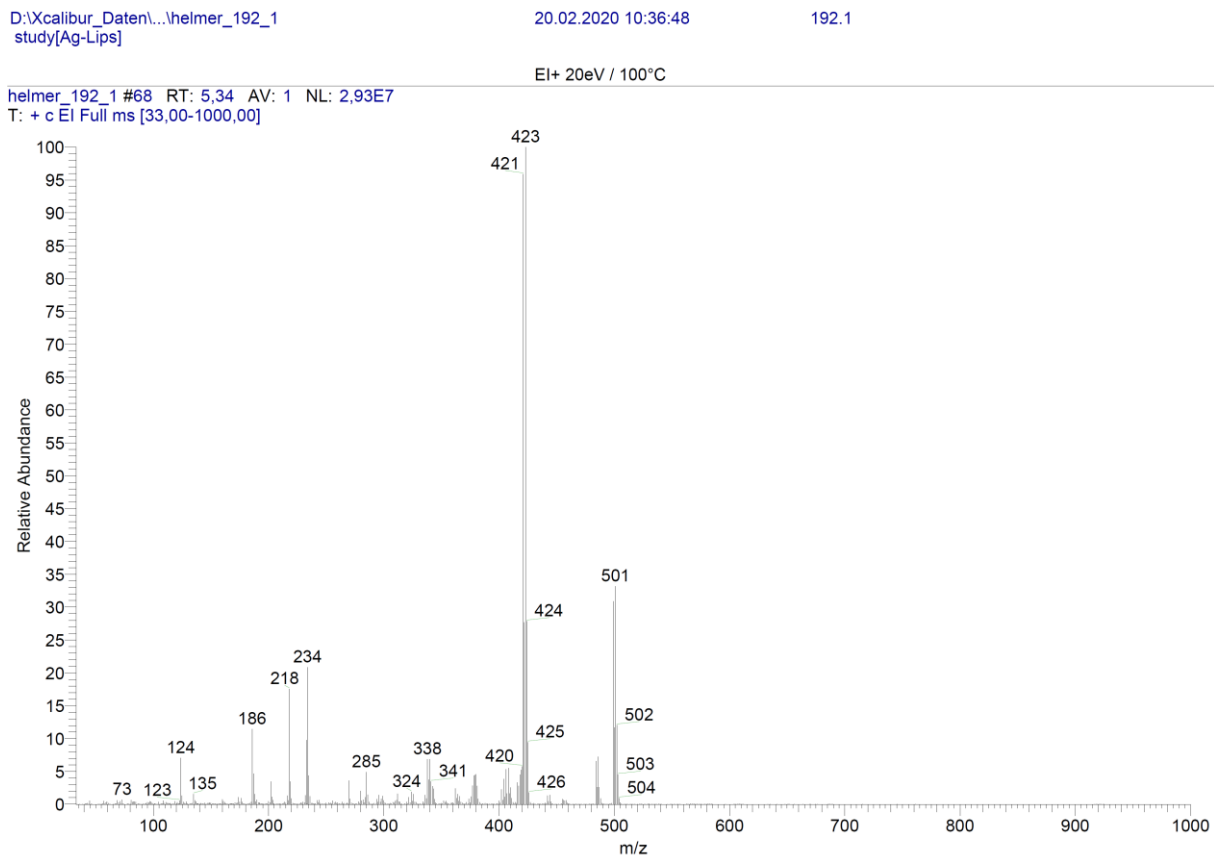
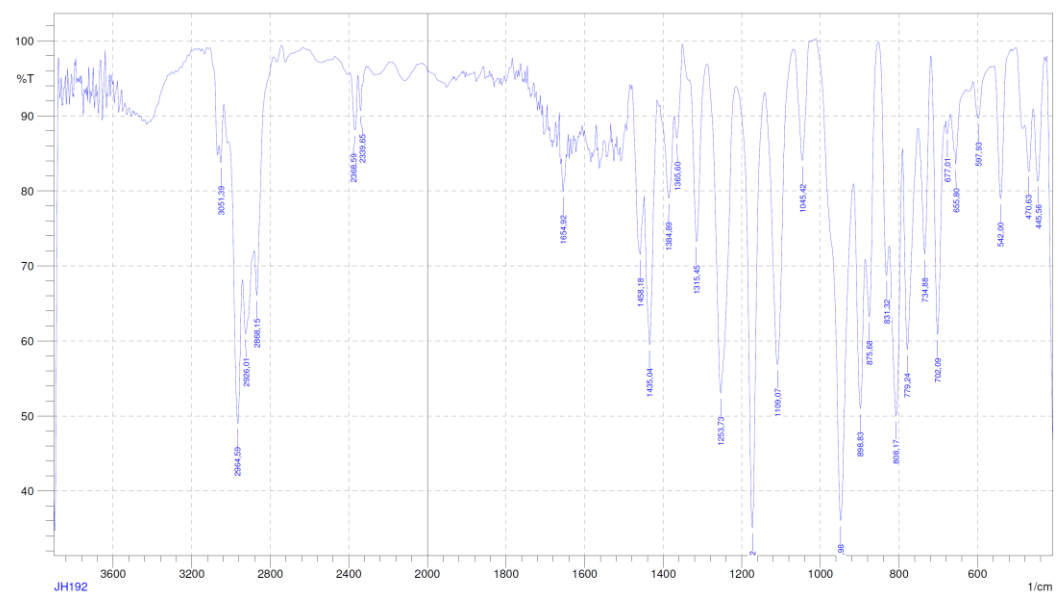


Figure S53. EI-MS spectrum of **9**.



Comment;
JH192

No. of Scans;

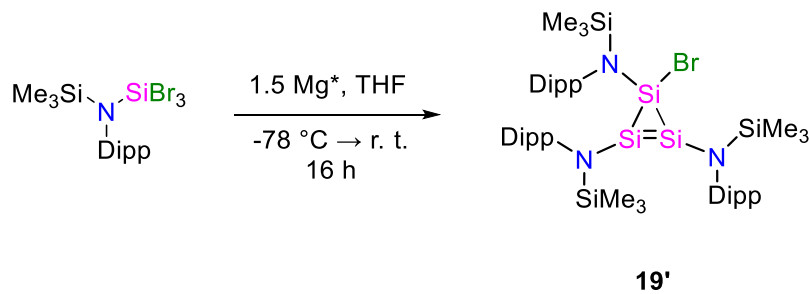
Date/Time; 20.02.2020 10:39:57
User; IR-Messung

D:\Messdaten\Josch\JH1922.smf

Resolution;
Apodization;

Figure S54. IR spectrum (KBr pellet) of **9**.

2.6. Synthesis and Characterization of **19'**



$\{\text{N}(\text{SiMe}_3)\}\text{Dipp}\}$ SiBr₃ (2.000 g, 3.87 mmol, 1.0 equiv.) was dissolved in THF (370 mL) and slowly added to a suspension of Mg* (0.141 g, 5.81 mmol, 1.5 equiv.) in THF (15 mL) at -78 °C. The reaction mixture was stirred for 16 h and allowed to warm to room, whereupon it turned red. 1,4-Dioxane (1.3 mL, 1.30 g, 14.5 mmol, 2.5 equiv.) was added and the mixture was stirred at room temperature for one hour. The red suspension was filtrated, and all volatile components were removed *in vacuo*. The obtained red powder was suspended in *n*-hexane (10 mL) and filtrated. The red solution was stored at room temperature for 16 hours to yield Si₄{N(SiMe₃)Dipp}₄ (0.268 g, 0.24 mmol, 25%) as red crystals. The orange red supernatant solution was separated from the crystals using a cannula. After further storage at room temperature of this solution for two weeks [Si₃{N(SiMe₃)Dipp}]₃]Br **19'** (0.045 g, 0.05 mmol, 4%) was obtained as orange crystals.

¹H-NMR (C₆D₆, 300K, 400 MHz): δ [ppm] = 7.14–7.10 (3H, m, *meta/para*-H_{Dipp}), 7.06–6.96 (6H, m, *meta/para*-H_{Dipp}), 3.65 (2H, sept, ³J_{H-H} = 6.8 Hz, CH(CH₃)₂), 3.56 (4H, sept, ³J_{H-H} = 6.8 Hz, CH(CH₃)₂), 1.45 (6H, d, ³J_{H-H} = 6.8 Hz, CH(CH₃)₂), 1.34 (6H, d, ³J_{H-H} = 6.8 Hz, CH(CH₃)₂), 1.24 (6H, d, ³J_{H-H} = 6.8 Hz, CH(CH₃)₂), 1.20 (12H, d, ³J_{H-H} = 6.8 Hz, CH(CH₃)₂), 1.17 (6H, d, ³J_{H-H} = 6.8 Hz, CH(CH₃)₂), 0.49 (9H, s, Si(CH₃)₃), 0.20 (18H, s, Si(CH₃)₃).

¹³C{¹H}-NMR (C₆D₆, 300K, 100.6 MHz): δ [ppm] = 146.6 (*ortho*-C_{Dipp}), 146.2 (*ortho*-C_{Dipp}), 146.0 (*ortho*-C_{Dipp}), 144.1 (*ipso*-C_{Dipp}), 138.8 (*ipso*-C_{Dipp}), 126.3 (*para*-C_{Dipp}), 125.8 (*para*-C_{Dipp}), 124.7 (*meta*-C_{Dipp}), 124.3 (*meta*-C_{Dipp}), 124.2 (*meta*-C_{Dipp}), 29.0 (CH(CH₃)₂), 28.8 (CH(CH₃)₂), 28.8 (CH(CH₃)₂), 25.7 (CH(CH₃)₂), 25.6 (CH(CH₃)₂), 24.8 (CH(CH₃)₂), 24.5 (CH(CH₃)₂), 24.0 (CH(CH₃)₂), 24.0 (CH(CH₃)₂), 3.7 (Si(CH₃)₃), 1.7 (Si(CH₃)₃).

¹H,¹⁵N-HMBC-NMR (C₆D₆, 300K, 41 MHz): δ [ppm] = 84, 83.

²⁹Si{¹H}-DEPT19.5-NMR (C₆D₆, 300K, 79.5 MHz): δ [ppm] = 9.9 (Si(CH₃)₃), 9.1 (Si(CH₃)₃).

²⁹Si{¹H}-IG-NMR (C₆D₆, 300K, 79.5 MHz): δ [ppm] = 9.9 (Si(CH₃)₃), 9.1 (Si(CH₃)₃), -7.5 (Si(Si₂)N), -16.8 (Si(Si₂)(N)Br).

IR (KBr pellet): $\tilde{\nu}$ [cm⁻¹] (intensity) = 440(vw), 500(w), 538(w), 598(vw), 642(vw), 687(vw), 714(vw), 750(w), 797(vs), 837(vs), 872(vs), 889(vs), 914(vs), 966(w), 1017(vw), 1045(w), 1101(m), 1169(s), 1248(vs), 1316(m), 1362(vw), 1381(vw), 1435(m), 1462(m), 1562(vw), 1584(vw), 1655(vw), 1927(vw), 2868(m), 2928(m), 2963(vs), 3017(vw), 3053(vw).

EI-MS: m/z = 552 [$\{\text{N}(\text{SiMe}_3)\text{Dipp}\}\text{Si}\equiv\text{Si}\{\text{N}(\text{SiMe}_3)\text{Dipp}\}\cdot$], 830 [$\text{Si}_3\{\text{N}(\text{SiMe}_3)\text{Dipp}\}_3$], 909 [$\text{Si}_3\{\text{N}(\text{SiMe}_3)\text{Dipp}\}_3\text{Br}$].

UV-Vis ($6.60 \cdot 10^{-5}$ mol/L in *n*-hexane): λ [nm] (ε [$\text{L} \cdot \text{mol}^{-1} \cdot \text{cm}^{-1}$]) = 279 (4776), 334 (1058), 438 (439).

Melting point: 210 °C.

Elemental analysis: Calc.: H: 8.64, C: 59.42, N: 4.62; Found: H: 8.67, C: 58.99, N: 4.46.

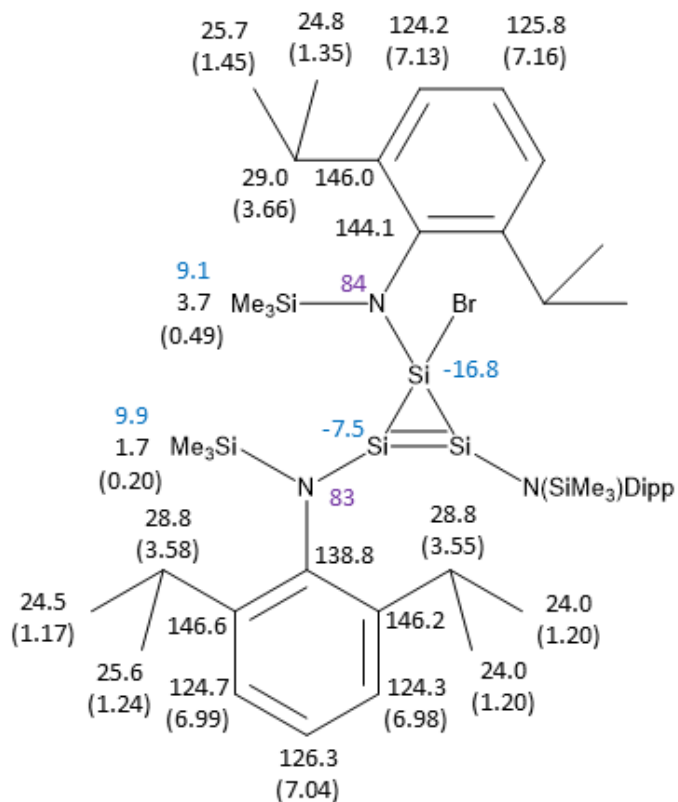


Figure S55. Assignment of chemical shifts to **19'**; ^1H (in brackets), ^{13}C (black), ^{15}N (purple), and ^{29}Si (blue).

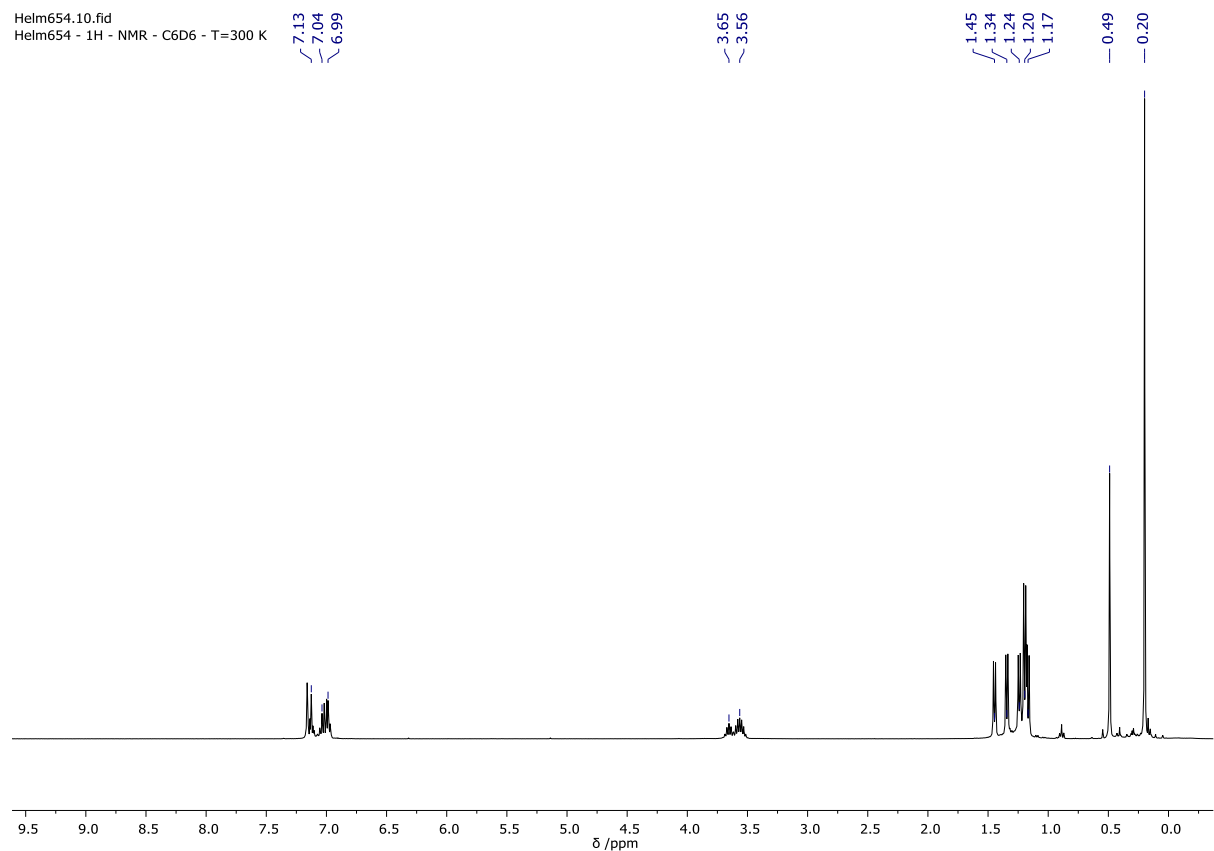


Figure S56. ^1H -NMR spectrum (C_6D_6 , 300 K, 400 MHz) of **19'**.

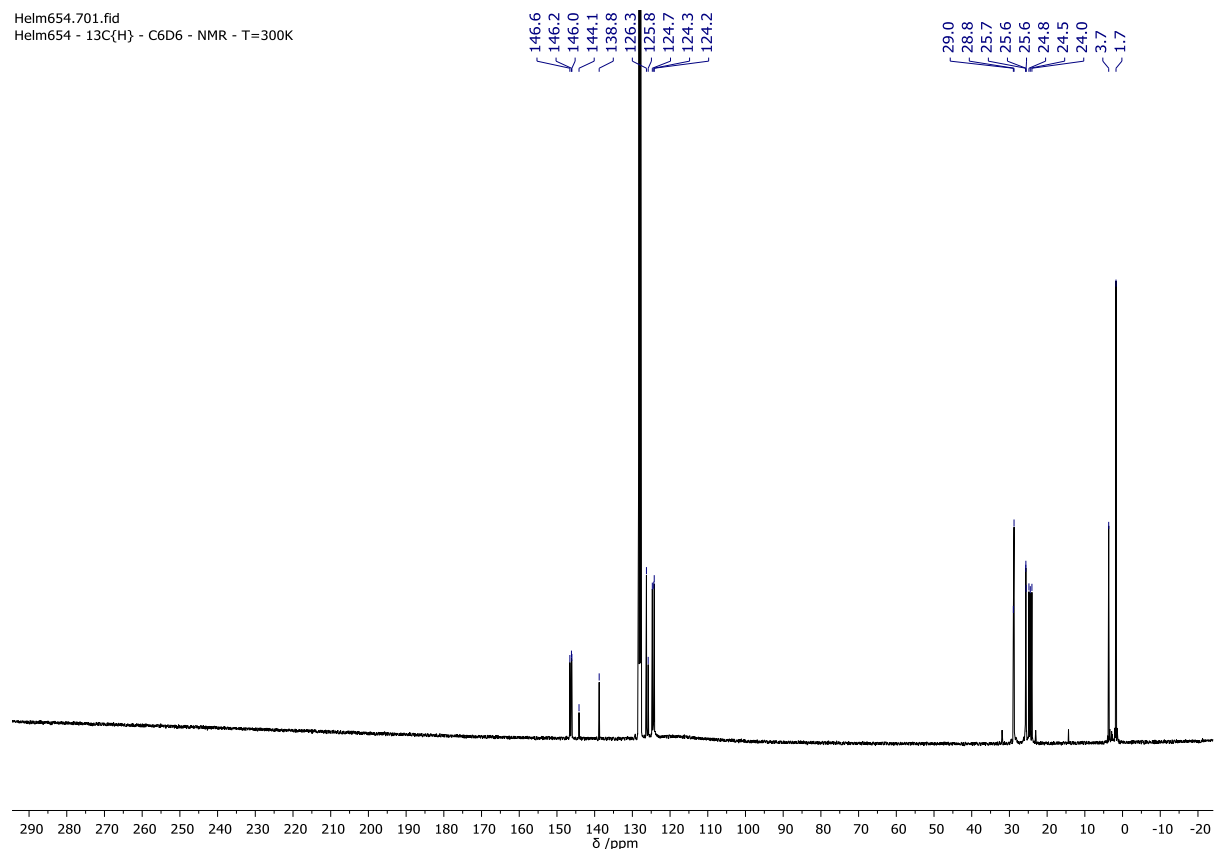


Figure S57. $^{13}\text{C}\{^1\text{H}\}$ -NMR spectrum (C_6D_6 , 300 K, 100 MHz) of **19'**.

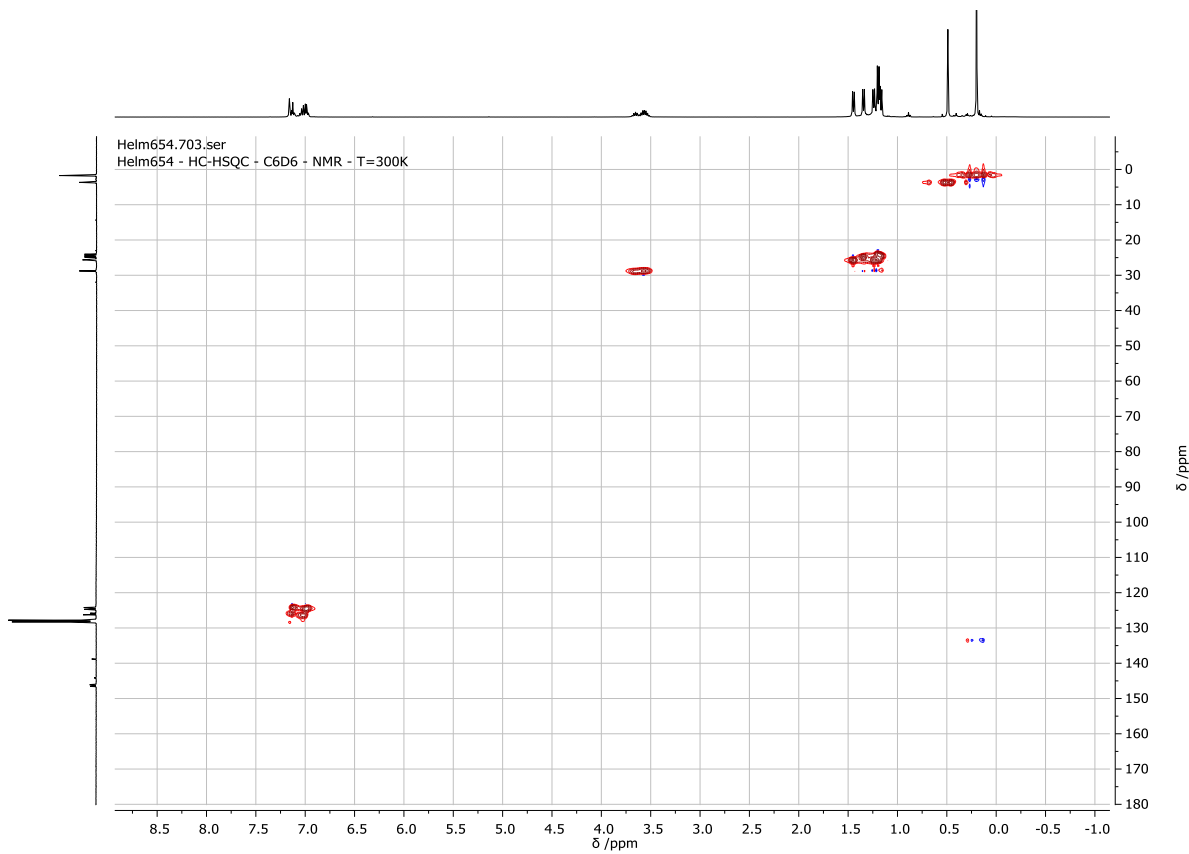


Figure S58. ^1H - ^{13}C -HSQC-NMR spectrum (C_6D_6 , 300 K) of **19'**.

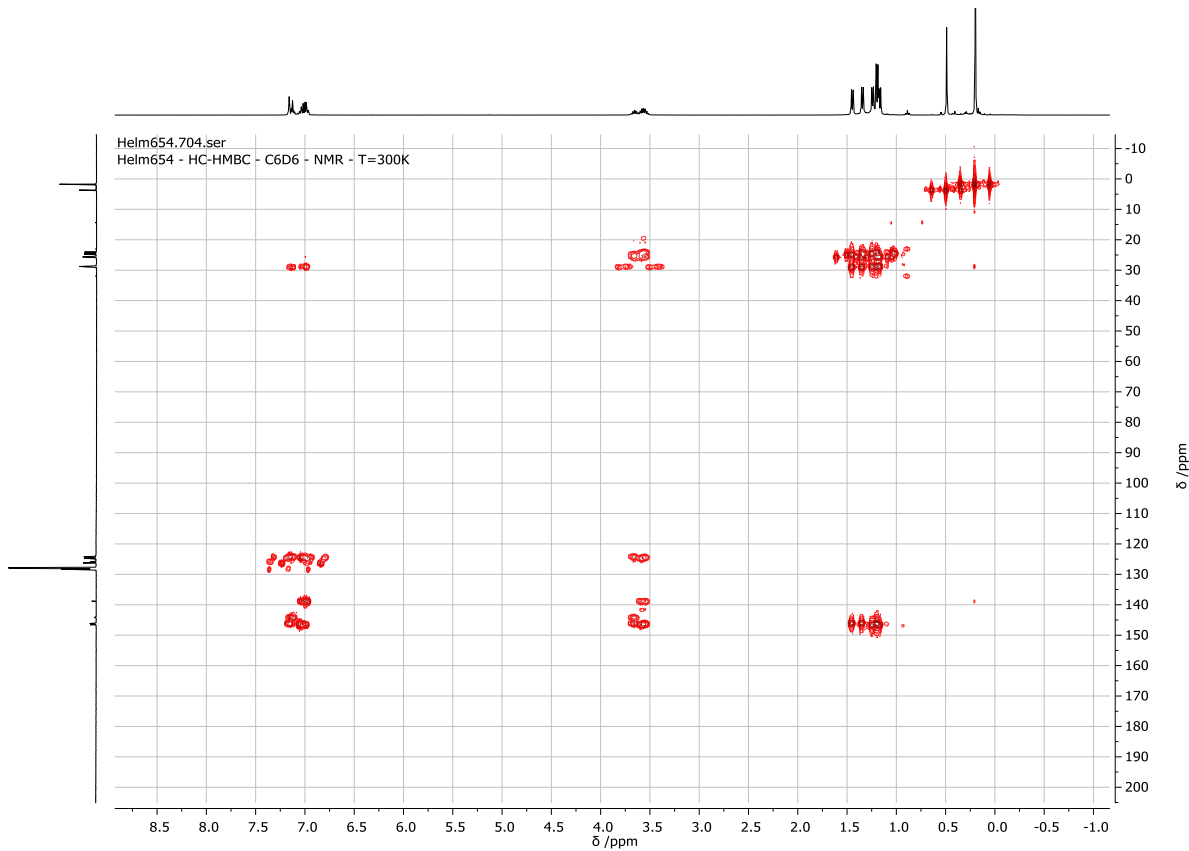


Figure S59. ^1H , ^{13}C -HMBC-NMR spectrum (C_6D_6 , 300 K) of **19'**.

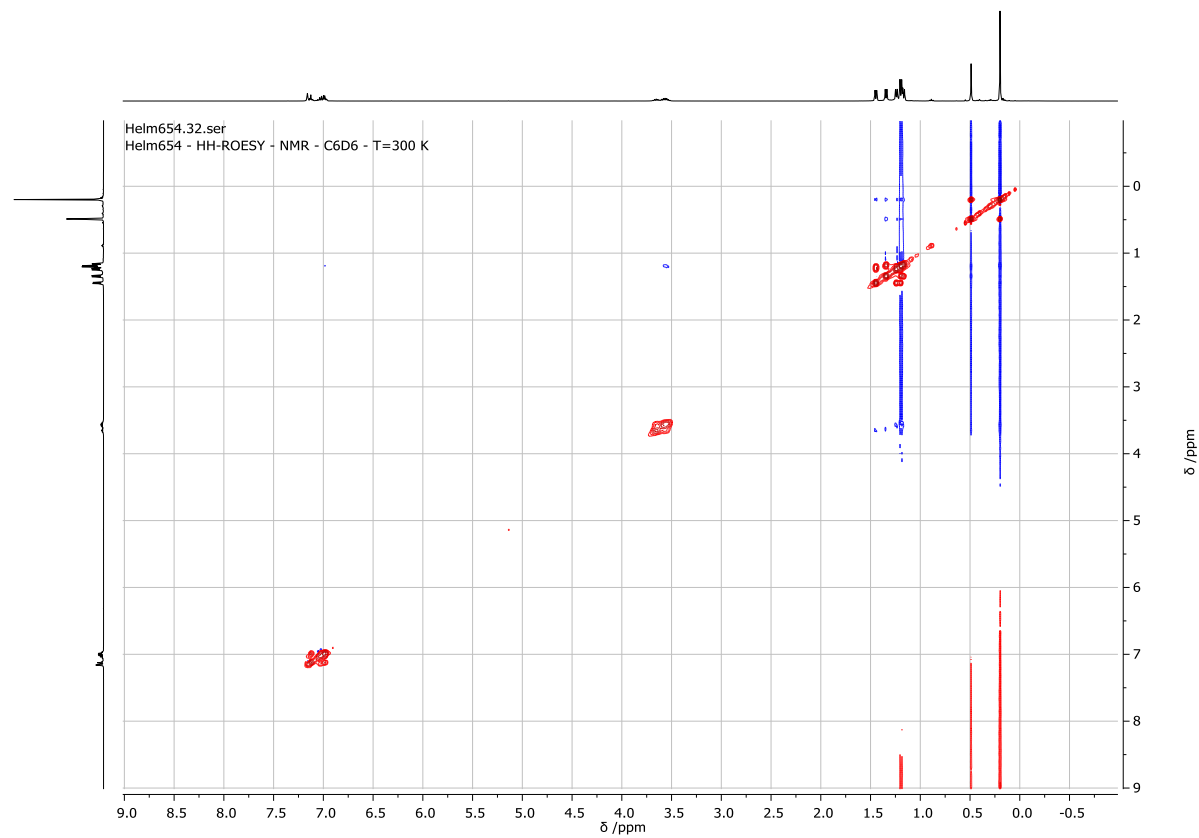


Figure S60. ^1H , ^1H -ROESY-NMR spectrum (C_6D_6 , 300 K) of **19'**.

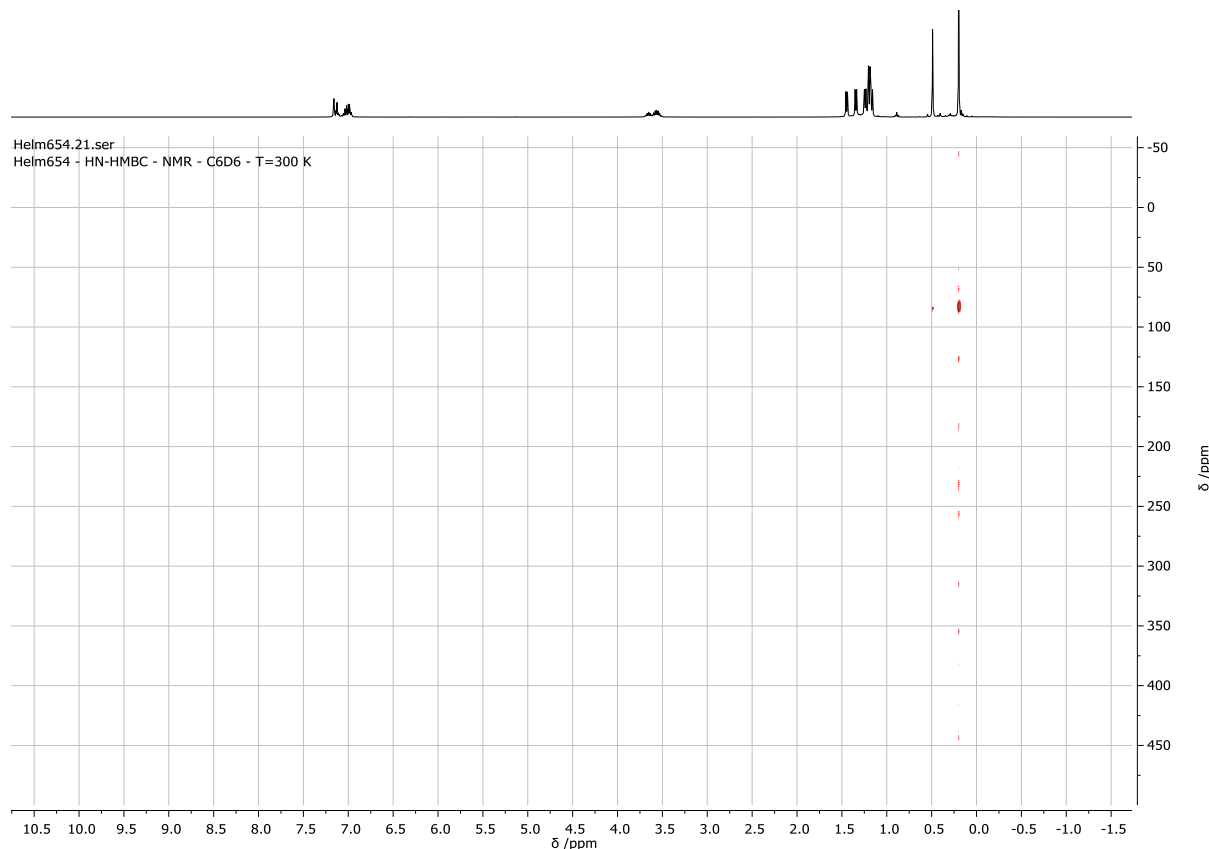


Figure S61. ^1H , ^{15}N -HMBC-NMR spectrum (C_6D_6 , 300 K) of **19'**.

Helm654.11.fid
Helm654 - 29Si{H}Dept19.5 - NMR - C6D6 - T=300 K

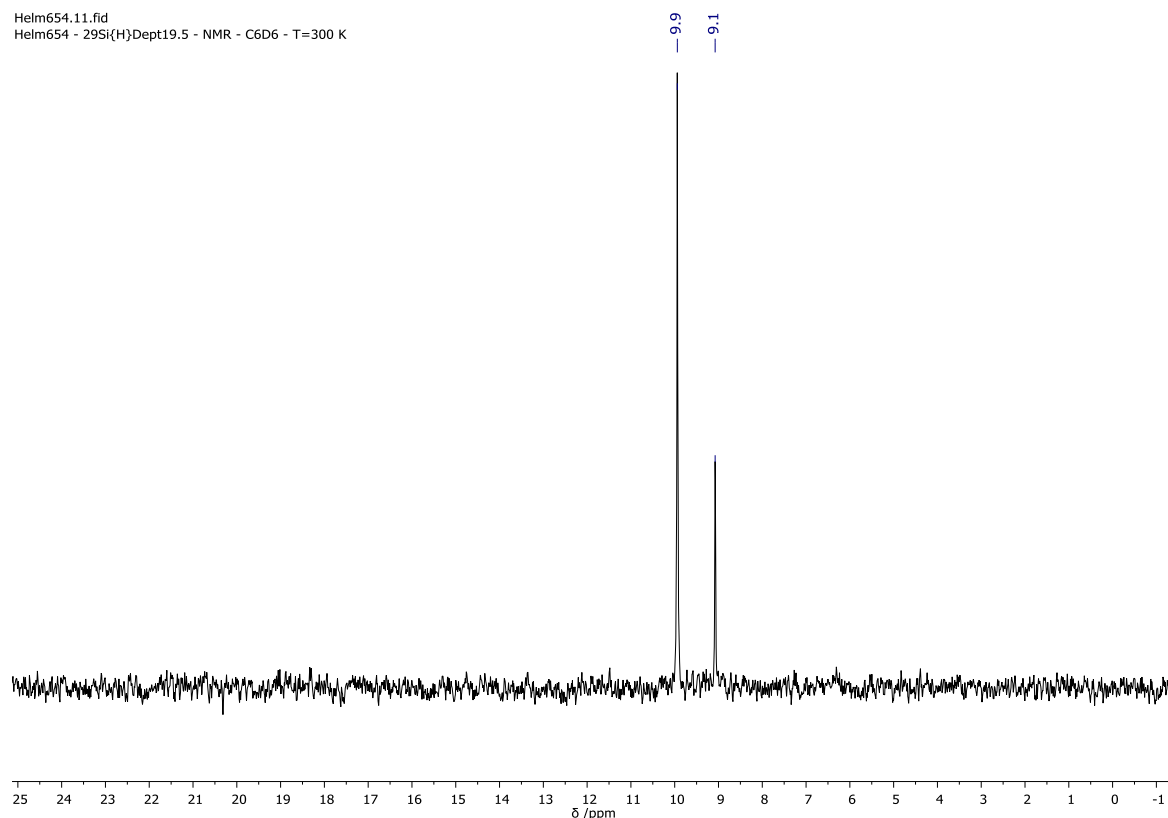


Figure S62. $^{29}\text{Si}\{\text{H}\}$ -DEPT19.5-NMR spectrum (C_6D_6 , 300 K, 80 MHz) of **19'**.

Helm654.13.fid
Helm654 - 29Si{H}IG - NMR - C6D6 - T=300 K - d1=20sec

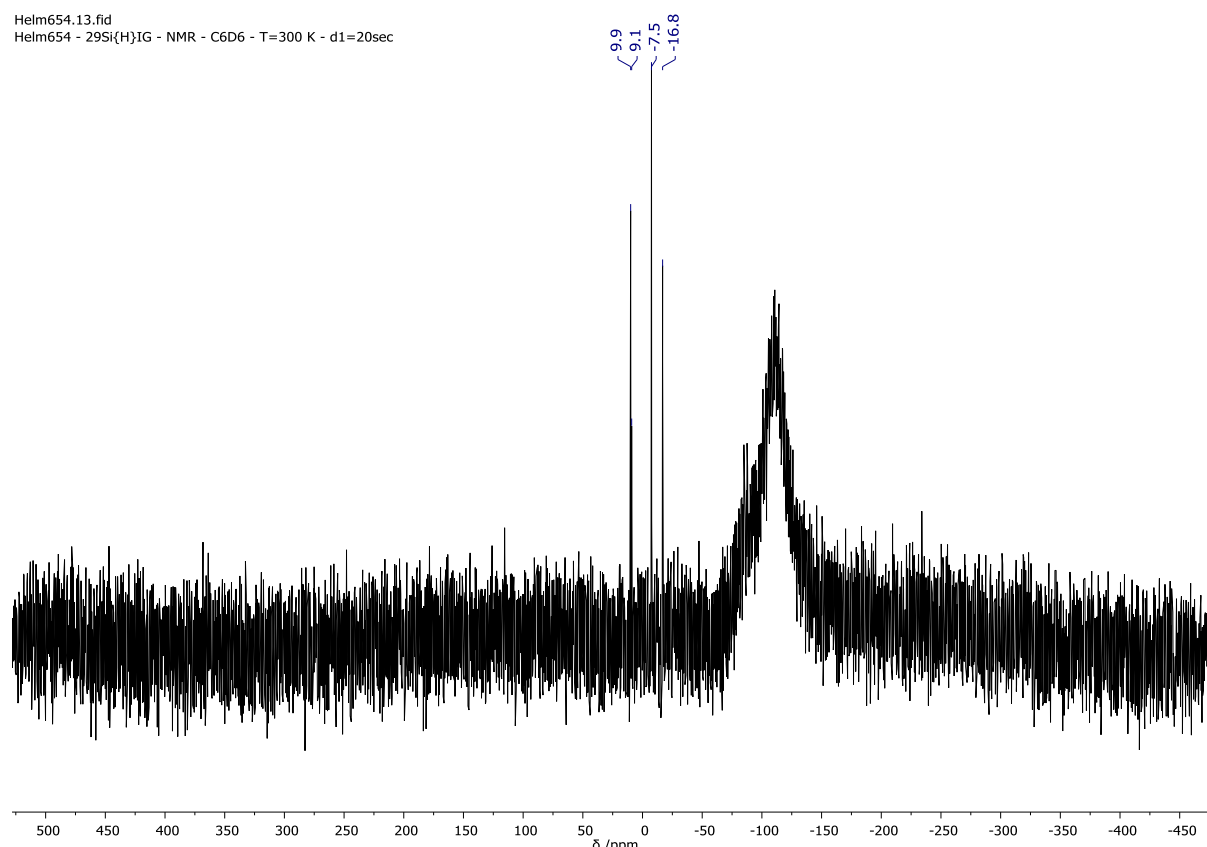


Figure S63. $^{29}\text{Si}\{\text{H}\}$ -IG-NMR spectrum (C_6D_6 , 300 K, 80 MHz) of **19'**.

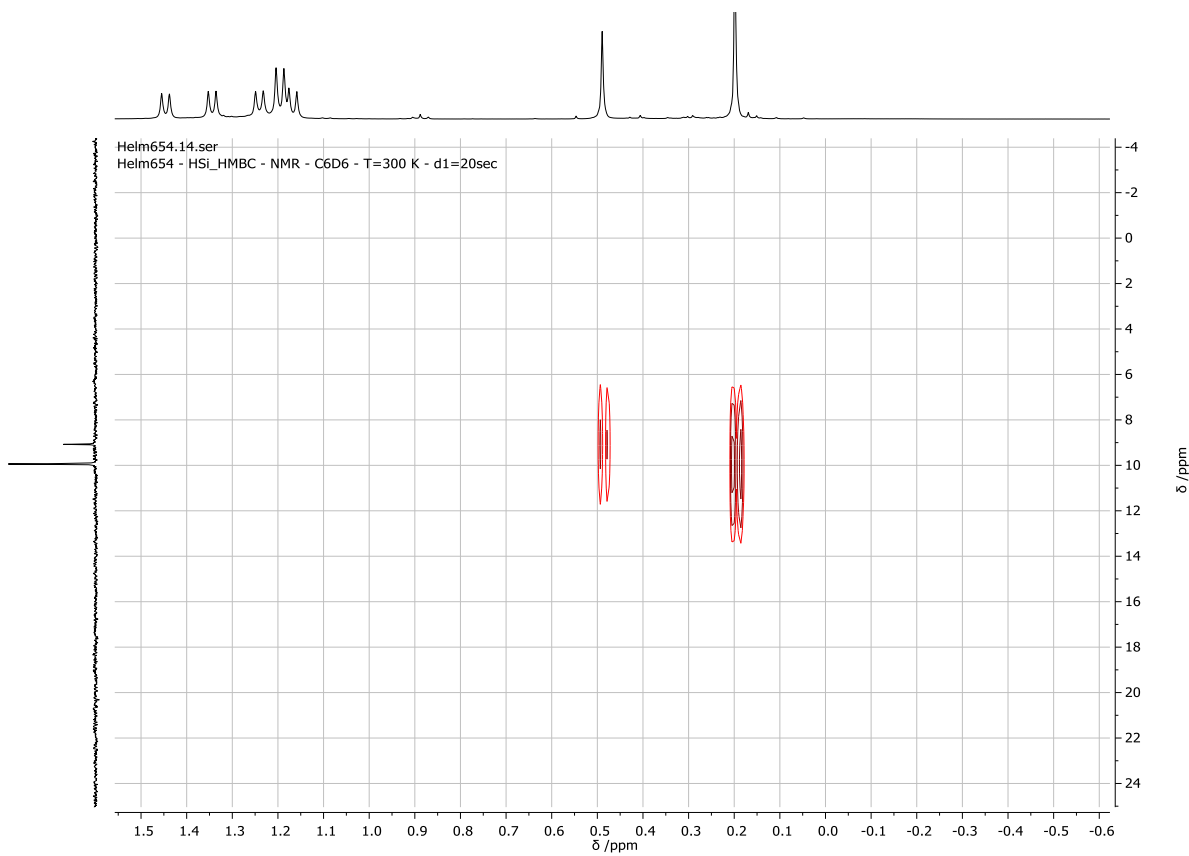


Figure S64. ^1H , ^{29}Si -HMBC-NMR spectrum (C_6D_6 , 300 K) of **19'**.

SHIMADZU

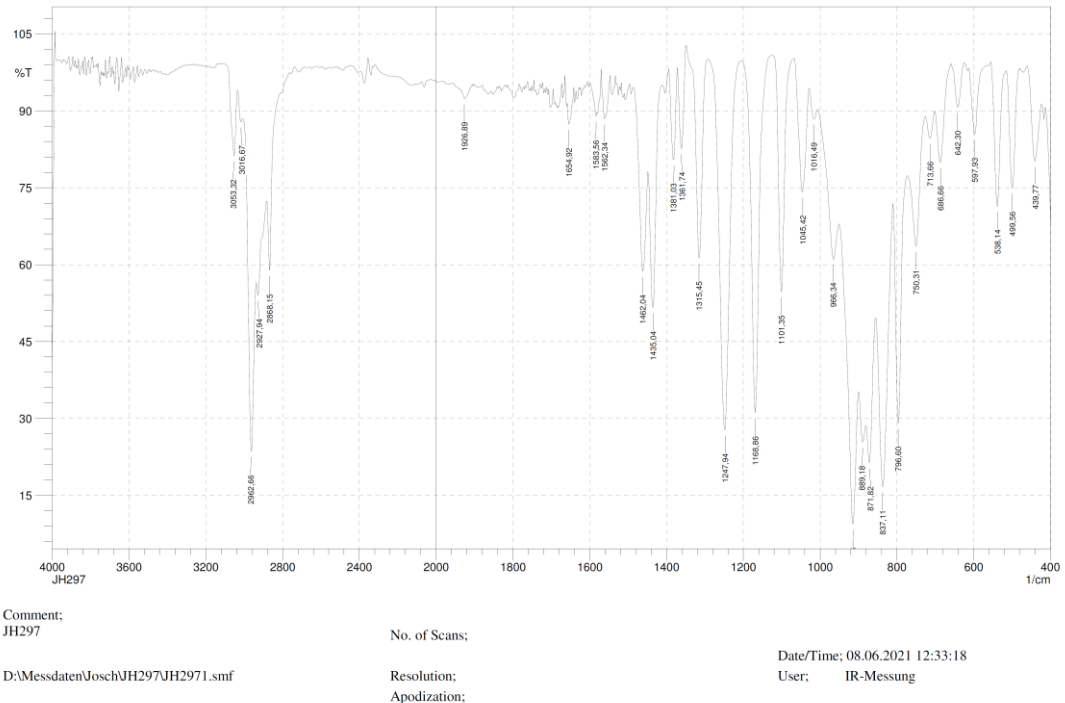


Figure S65. IR spectrum (KBr pellet) of **19'**.

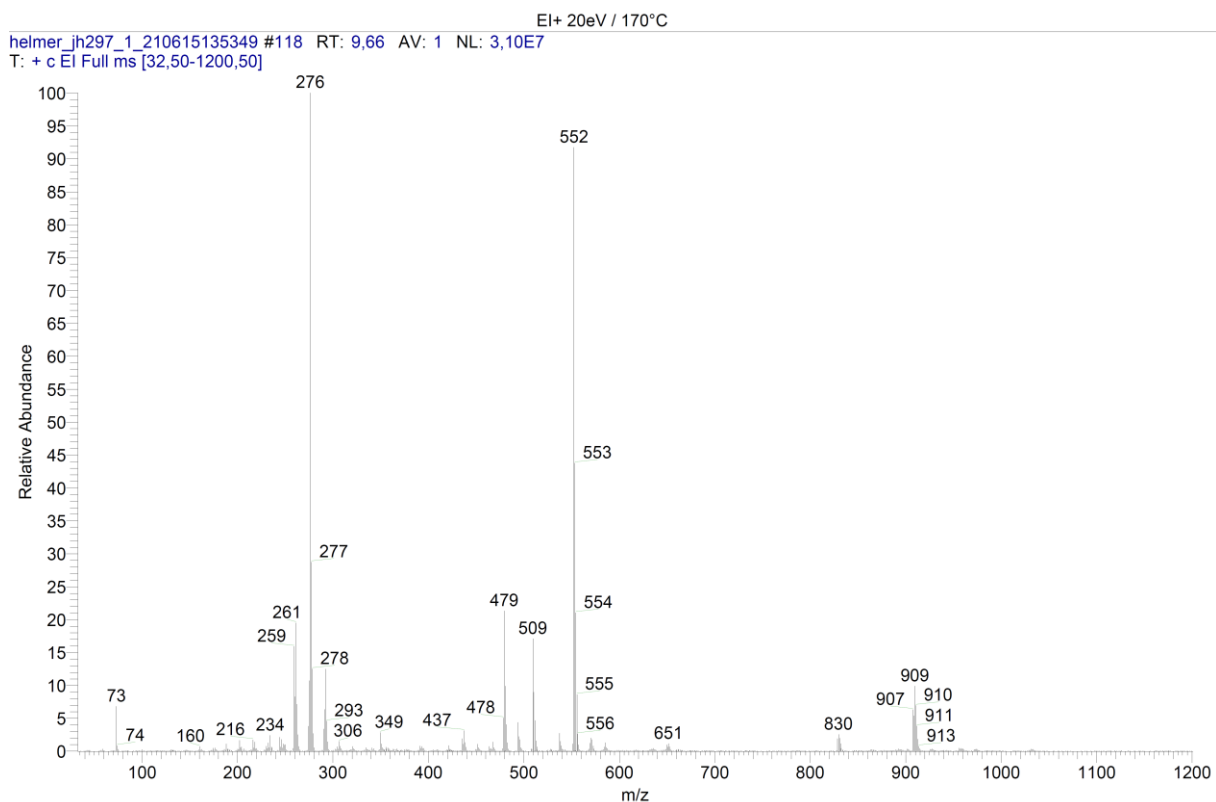


Figure S66. EI-MS spectrum of **19'**.

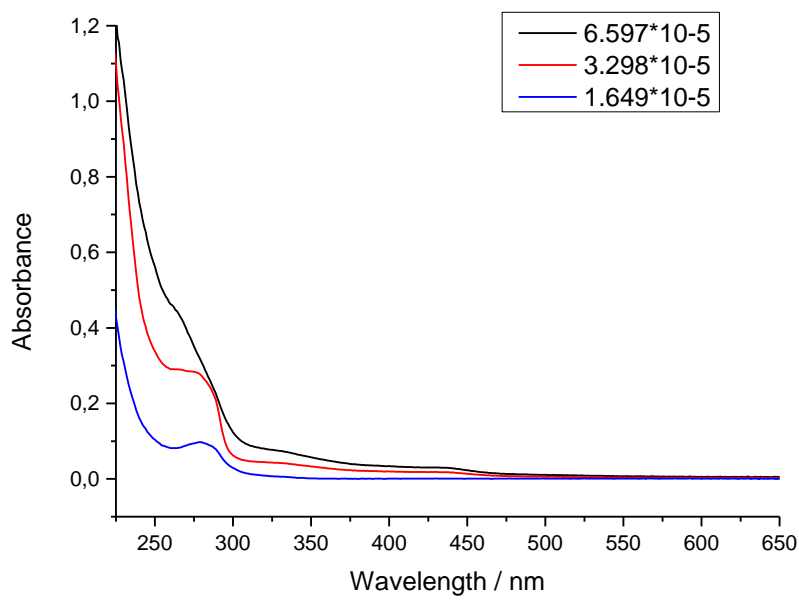
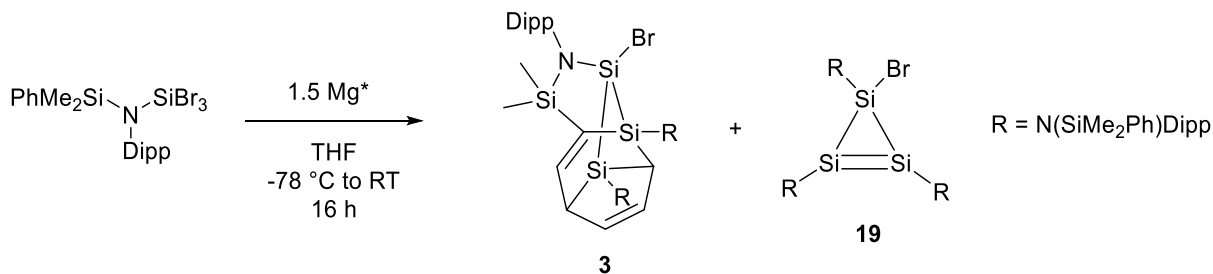


Figure S67. UV-Vis spectrum (*n*-hexane) of **19'**.

2.7. Synthesis and Characterization of 19



$\{N(SiMe_2Ph)Dipp\}SiBr_3$ (**2**) (1.157 g, 2.0 mmol, 1.0 equiv.) was dissolved in THF (185 ml) and slowly added to a suspension of Mg* (0.073 g, 3.0 mmol, 1.5 equiv.) in THF (15 ml) at $-78^\circ C$. The reaction mixture was allowed to warm to room temperature and stirred for 16 h. After addition of 1,4-dioxane (0.66 ml, 7.5 mmol, 3.75 equiv.), the deep yellow suspension was stirred for one hour and was filtrated. All volatile components were removed *in vacuo* and the yellow residue was extracted with *n*-hexane (50 ml) and filtrated. Storage of a concentrated solution at $-32^\circ C$ yielded **3** (0.094 g, 0.09 mmol, 13%). Crystallization attempts of **19** were met with failure. The orange solution was evaporated to dryness and redissolved in C_6D_6 as well as d_8 -THF to obtain NMR spectra.

¹H-NMR (C_6D_6 , 300 K, 400 MHz): δ [ppm] = 0.54 (6H, s), 0.38 (6H, s), 0.21 (6H, s).

²⁹Si{¹H}DEPT19.5-NMR (C₆D₆, 300 K, 79.5 MHz): δ [ppm] = 1.2, 0.3.

$^{29}\text{Si}\{^1\text{H}\}$ IG-NMR (C_6D_6 , 300 K, 80 MHz): δ [ppm] = -5.1, -10.9.

¹H-NMR (d_8 -THF, 300K, 400 MHz): δ [ppm] = 7.69–7.65 (2H, m, *ortho*-H_{Ph}), 7.61 - 7.58 (4H, m, *ortho*-H_{Ph}), 7.34–7.20 (9H, m, *meta/para*-H_{Ph}), 7.09– 6.89 (9H, m, *meta/para*-H_{Dipp}), 3.47 (2H, sept, 3 J_{H-H} = 6.8 Hz, CH(CH₃)₂), 3.43 (2H, sept, 3 J_{H-H} = 6.8 Hz, CH(CH₃)₂), 3.31 (2H, sept, 3 J_{H-H} = 6.8 Hz, CH(CH₃)₂), 1.18 (6H, d, 3 J_{H-H} = 6.8 Hz, CH(CH₃)₂), 1.14 (6H, d, 3 J_{H-H} = 6.8 Hz, CH(CH₃)₂), 1.02 (6H, d, 3 J_{H-H} = 6.8 Hz, CH(CH₃)₂), 0.94 (6H, d, 3 J_{H-H} = 6.8 Hz, CH(CH₃)₂), 0.90 (3H, d, 3 J_{H-H} = 6.8 Hz, CH(CH₃)₂), 0.86 (3H, d, 3 J_{H-H} = 6.8 Hz, CH(CH₃)₂), 0.37 (6H, s, Si(CH₃)₃), 0.31 (6H, s, Si(CH₃)₃), 0.10 (6H, s, Si(CH₃)₃).

¹³C{¹H}-NMR (C_6D_6 , 300K, 100.6 MHz): δ (ppm) = 147.3 (*ortho*-CDipp), 146.9 (*ortho*-CDipp), 146.8 (*ortho*-CDipp), 144.4 (*ipso*-CDipp), 139.3 (*ipso*-CPh), 139.0 (*ipso*-CDipp), 138.5 (*ipso*-CPh), 136.6(*ortho*-CPh), 135.1 (*ortho*-CPh), 130.0 (*meta*-CPh), 130.0 (*para*-CPh), 129.9 (*para*-CPh), 128.3 (*meta*-CPh), 126.8 (*para*-CDipp), 126.3 (*para*-CDipp), 125.3 (*meta*-CDipp), 124.7 (*meta*-CDipp), 124.7 (*meta*-CDipp), 29.4 ($CH(CH_3)_2$), 29.2 ($CH(CH_3)_2$), 29.2 ($CH(CH_3)_2$), 26.6 ($CH(CH_3)_2$), 26.1 ($CH(CH_3)_2$), 26.1 ($CH(CH_3)_2$), 25.0 ($CH(CH_3)_2$), 24.7 ($CH(CH_3)_2$), 23.3 ($CH(CH_3)_2$), 2.9 ($Si(CH_3)_3$), 0.9 ($Si(CH_3)_3$), 0.9 ($Si(CH_3)_3$).

$^{15}\text{N},^1\text{H}$ -HMBC-NMR (d_8 -THF, 300 K, 41 MHz): δ (ppm) = 84, 81.

$^{29}\text{Si}\{^1\text{H}\}$ -DEPT19.5-NMR (d_8 -THF, 300 K, 79.5 MHz): δ (ppm) = 1.1 ($Si(\text{CH}_3)_2\text{Ph}$), 0.1 ($Si(\text{CH}_3)_2\text{Ph}$).

$^{29}\text{Si}\{^1\text{H}\}$ -IG-NMR (d_8 -THF, 300 K, 80 MHz): δ (ppm) = -5.4 ($Si(\text{Si}_2)\text{N}$), -11.9 ($Si(\text{Si}_2)(\text{N})\text{Br}$).

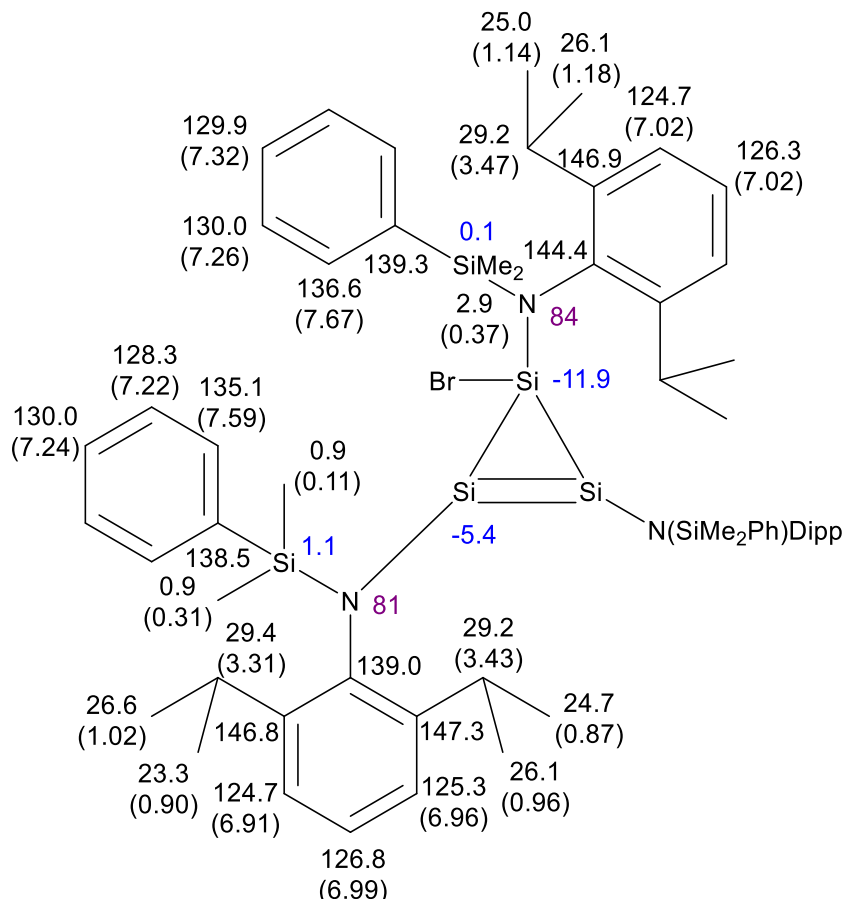


Figure S68. Assignment of chemical shifts to **19**; ^1H (in brackets), ^{13}C black, ^{15}N (purple), and ^{29}Si (blue).

Comment to Figure S80:

Signals labeled with * in Figure S80 could not clearly assigned to **19** due to line broadening of **19** at 210 K. Figure S77 shows the ^{29}Si NMR spectrum at 300 K were both signals of **3** and **19** were identified.

Helm596.700.fid
Helm596 - 1H - C6D6 - NMR - T=300K

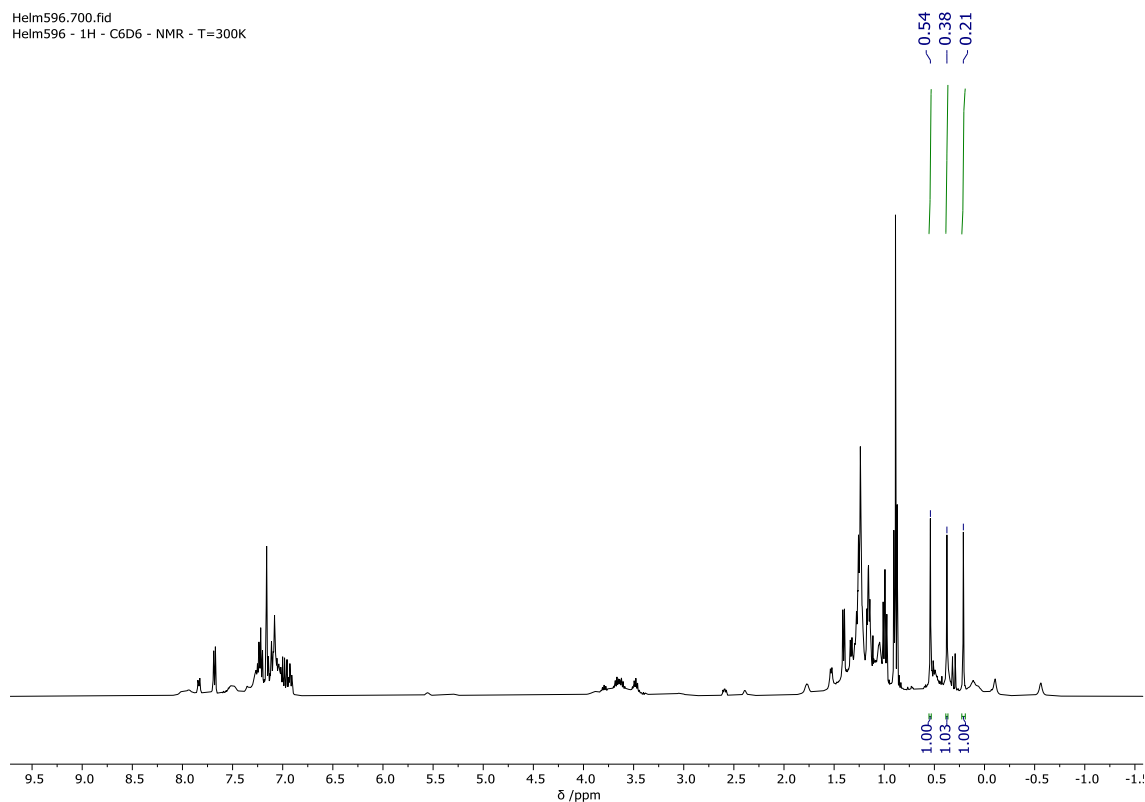


Figure S69. ¹H-NMR spectrum (C₆D₆, 300 K, 400 MHz) of reductive dehalogenation of **2** with Mg*.

Helm596.701.fid
Helm596 - 29Si{H}Dept19.5 - C6D6 - NMR - T=300K

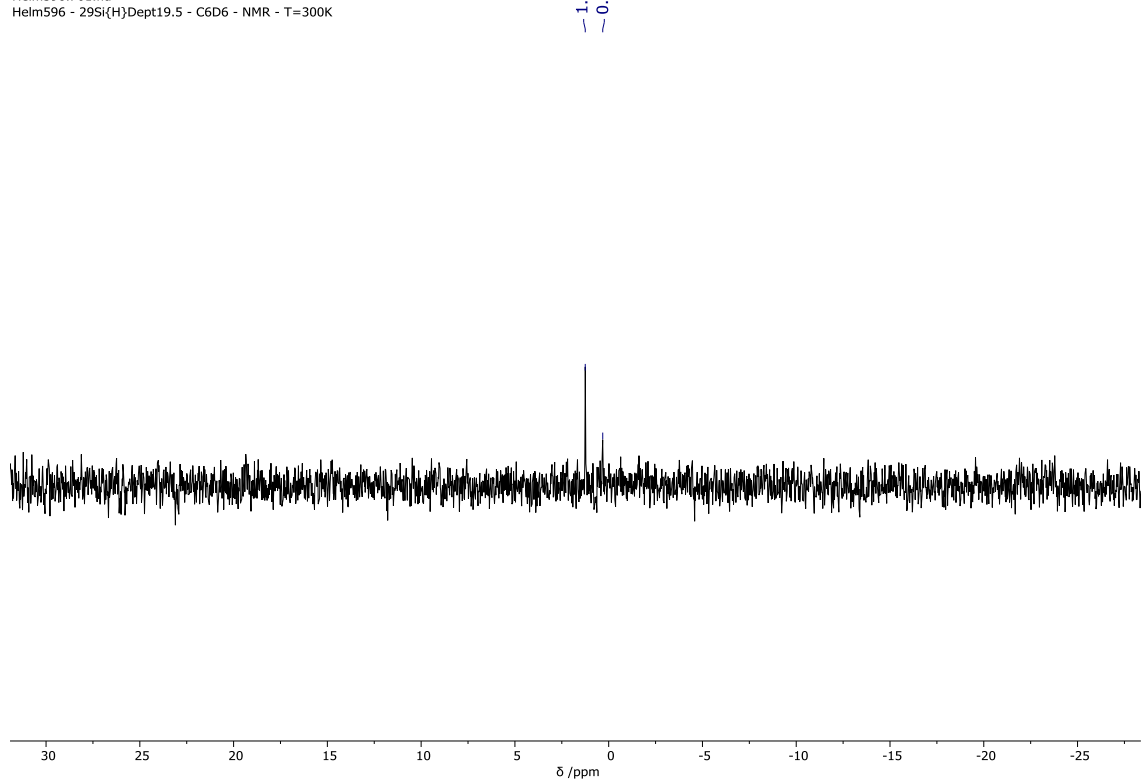


Figure S70. ²⁹Si{¹H}DEPT19.5-NMR spectrum (C₆D₆, 300 K, 80 MHz) of reductive dehalogenation of **2** with Mg*.

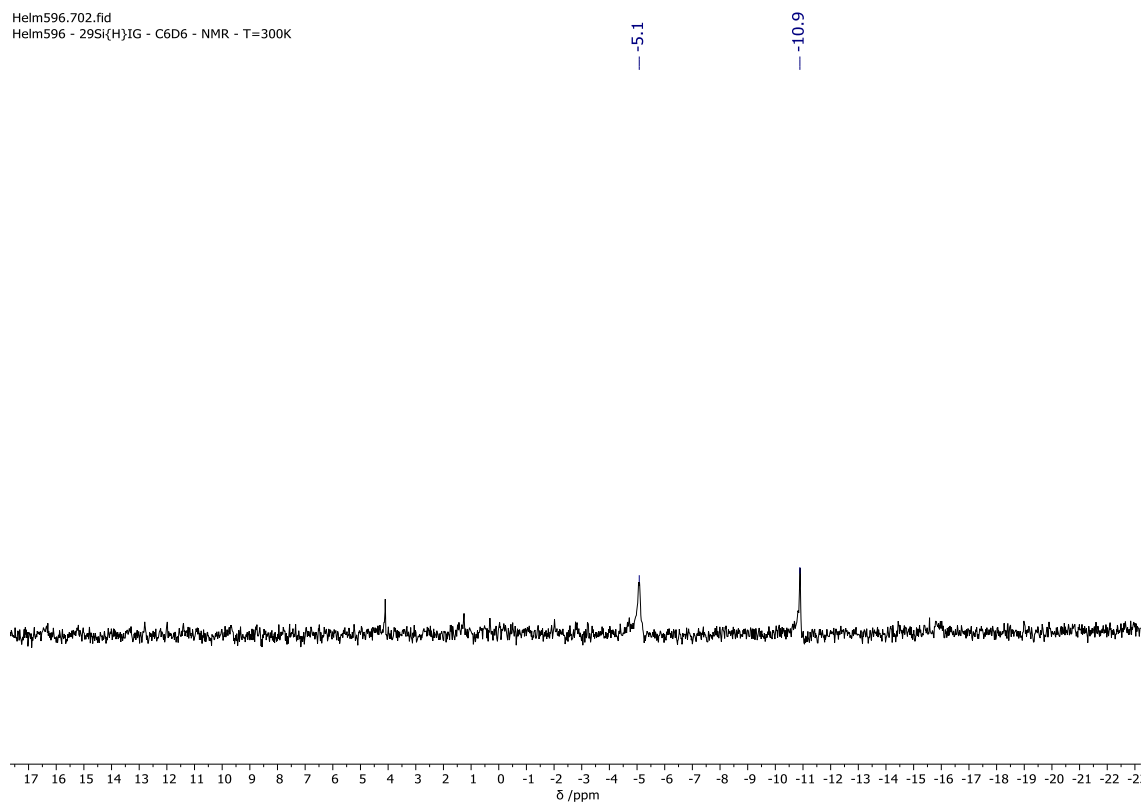


Figure S71. $^{29}\text{Si}\{\text{H}\}$ -NMR spectrum (C_6D_6 , 300 K, 80 MHz) of reductive dehalogenation of **2** with Mg^* .

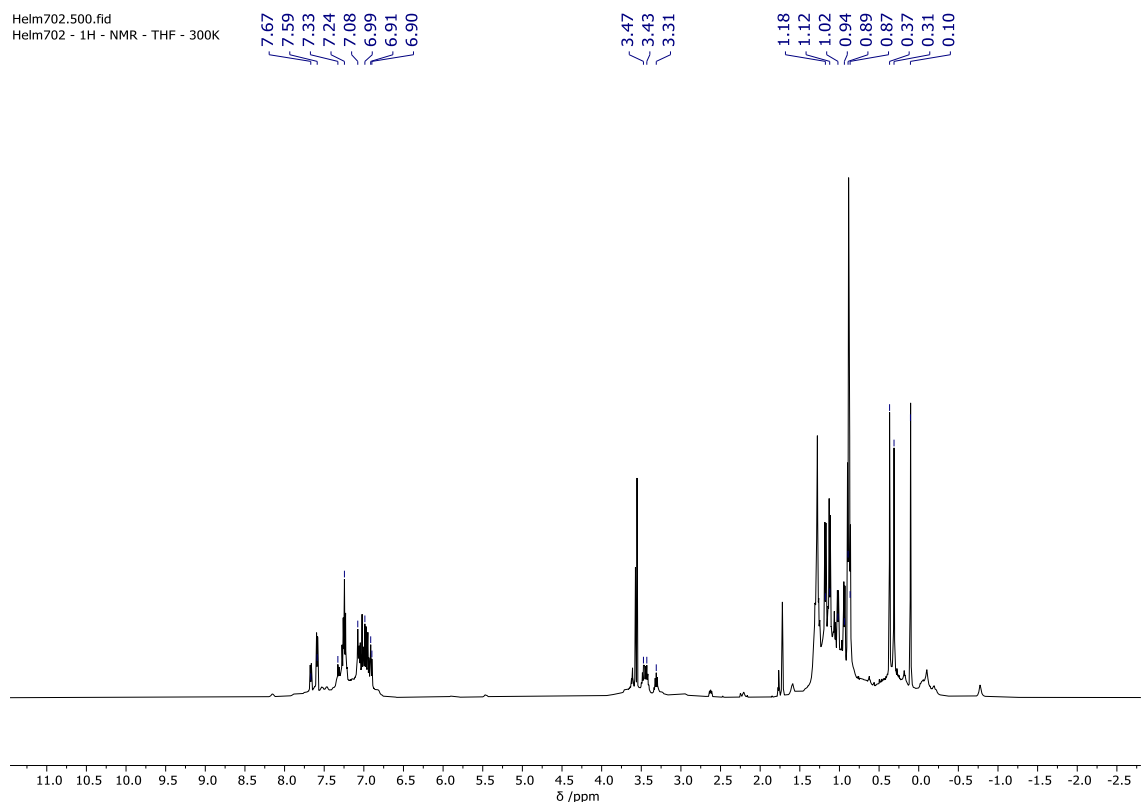


Figure S72. ^1H -NMR spectrum (d_8 -THF, 300 K, 400 MHz) of reductive dehalogenation of **2** with Mg^* .

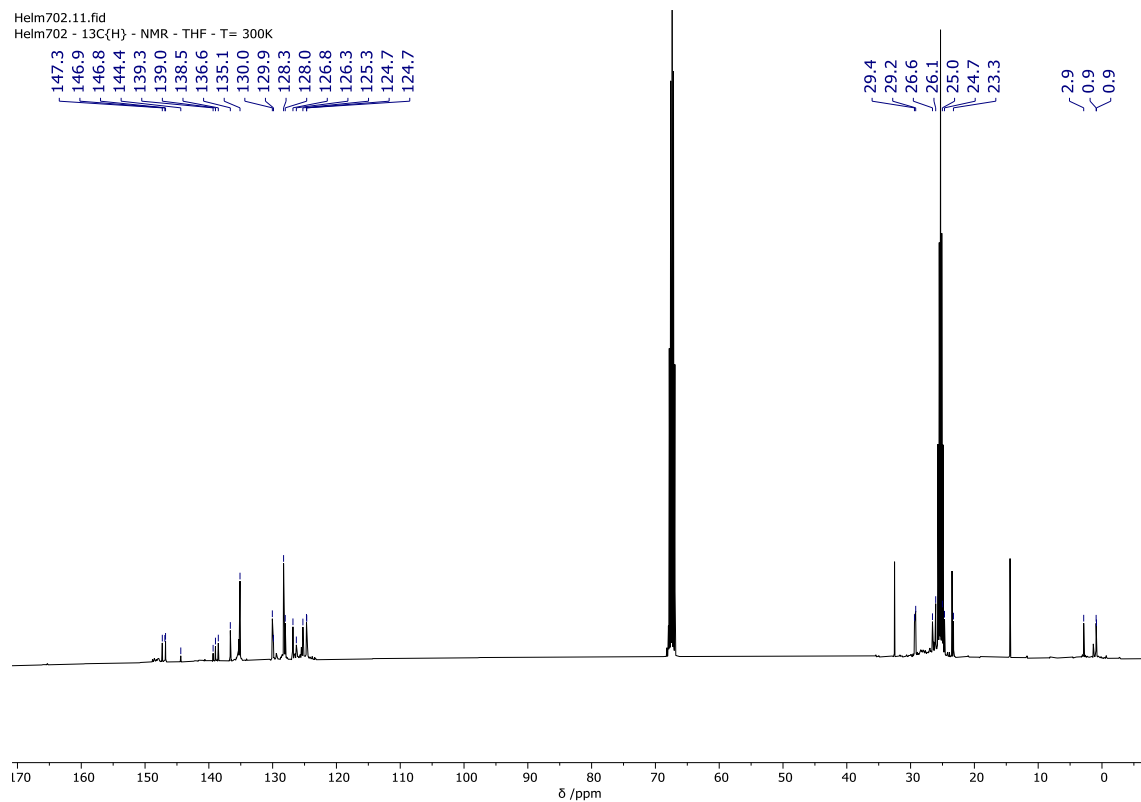


Figure S73. $^{13}\text{C}\{\text{H}\}$ -NMR spectrum (d_8 -THF, 300 K, 100 MHz) of reductive dehalogenation of **2** with Mg*.

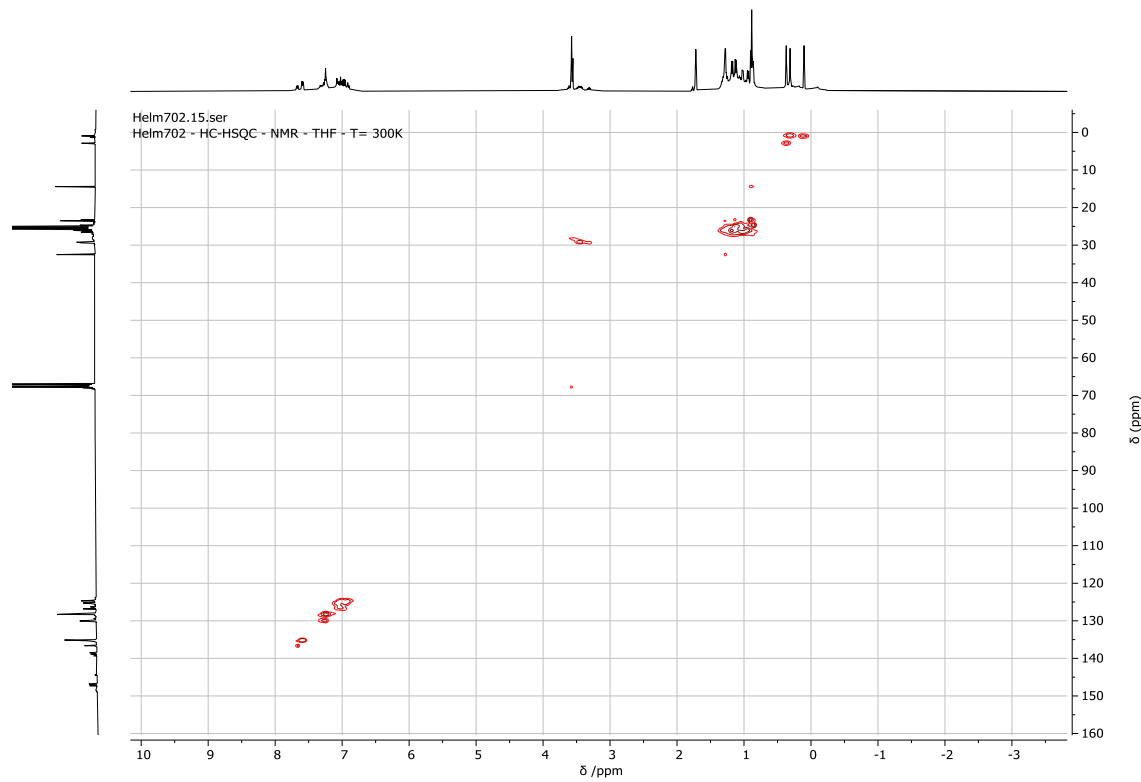


Figure S74. $^1\text{H}, ^{13}\text{C}$ -HSQC-NMR spectrum (d_8 -THF, 300 K) of reductive dehalogenation of **2** with Mg*.

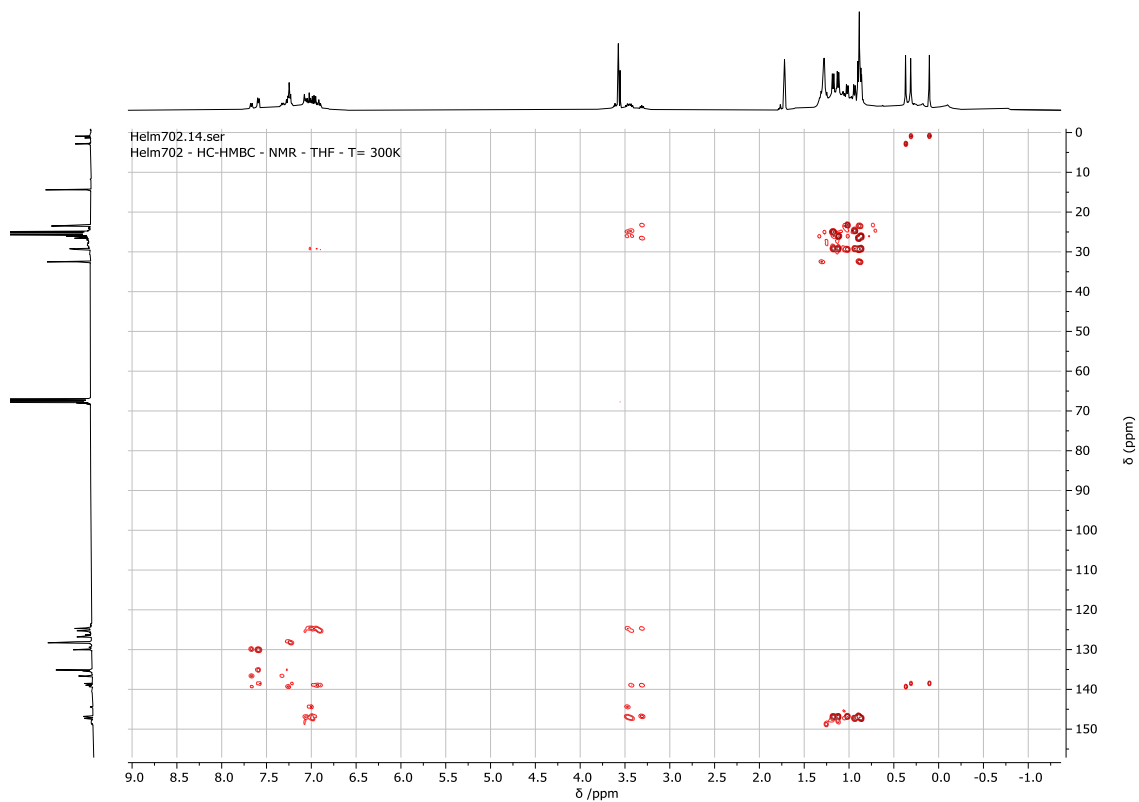


Figure S75. ^1H , ^{13}C -HMBC-NMR spectrum (d_8 -THF, 300 K) of reductive dehalogenation of **2** with Mg^* .

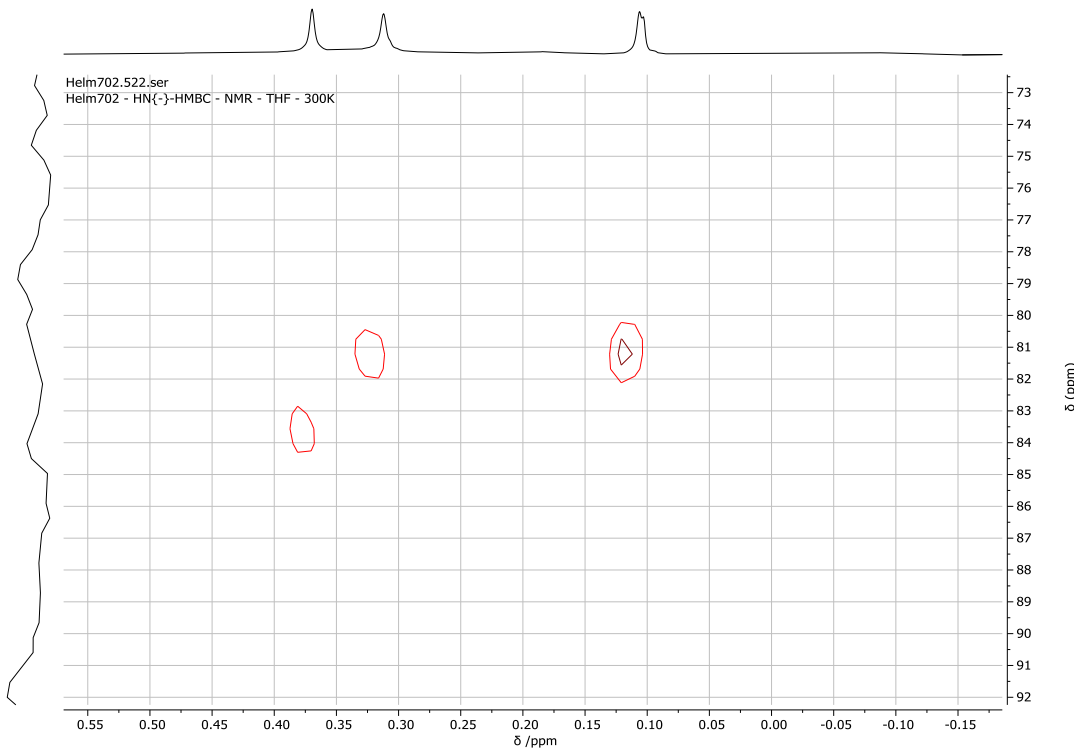


Figure S76. ^1H , ^{15}N -HMBC-NMR spectrum (d_8 -THF, 300 K) of reductive dehalogenation of **2** with Mg^* .

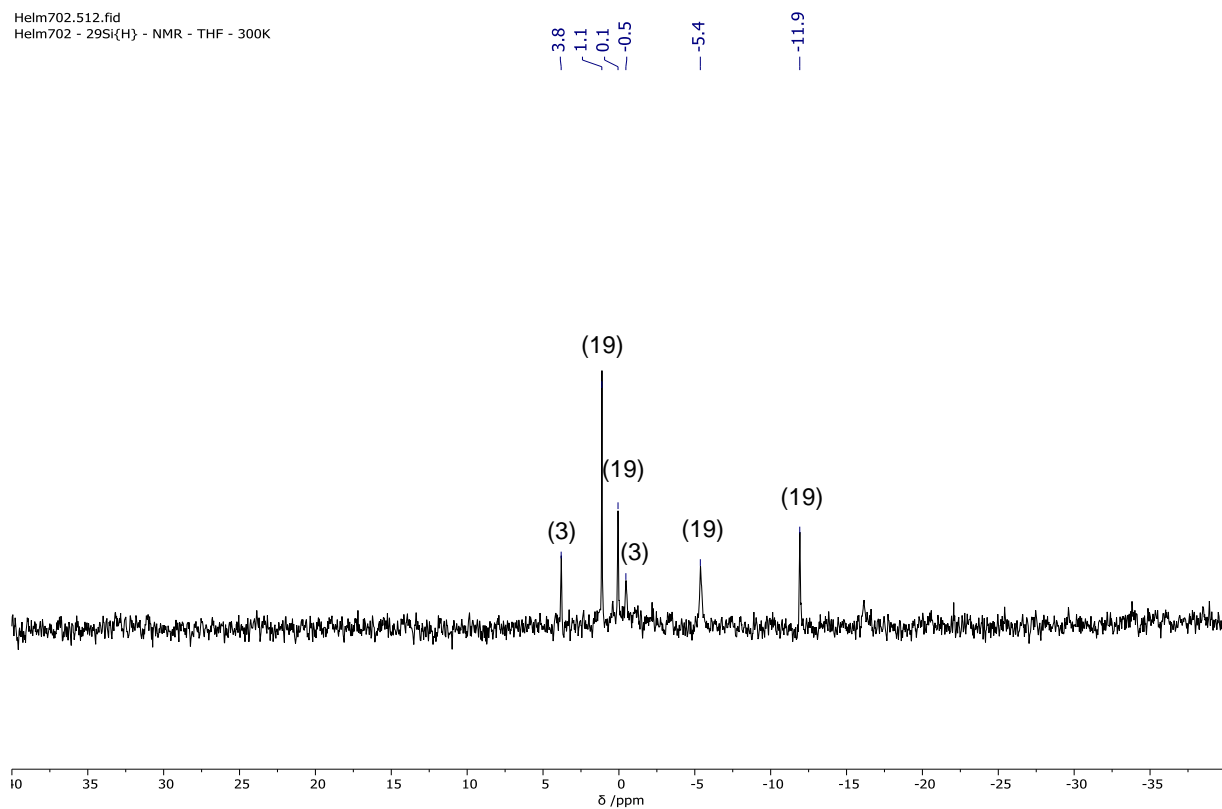


Figure S77. $^{29}\text{Si}\{\text{H}\}$ -NMR spectrum (d_8 -THF, 300 K, 80 MHz) of reductive dehalogenation of **2** with Mg*.

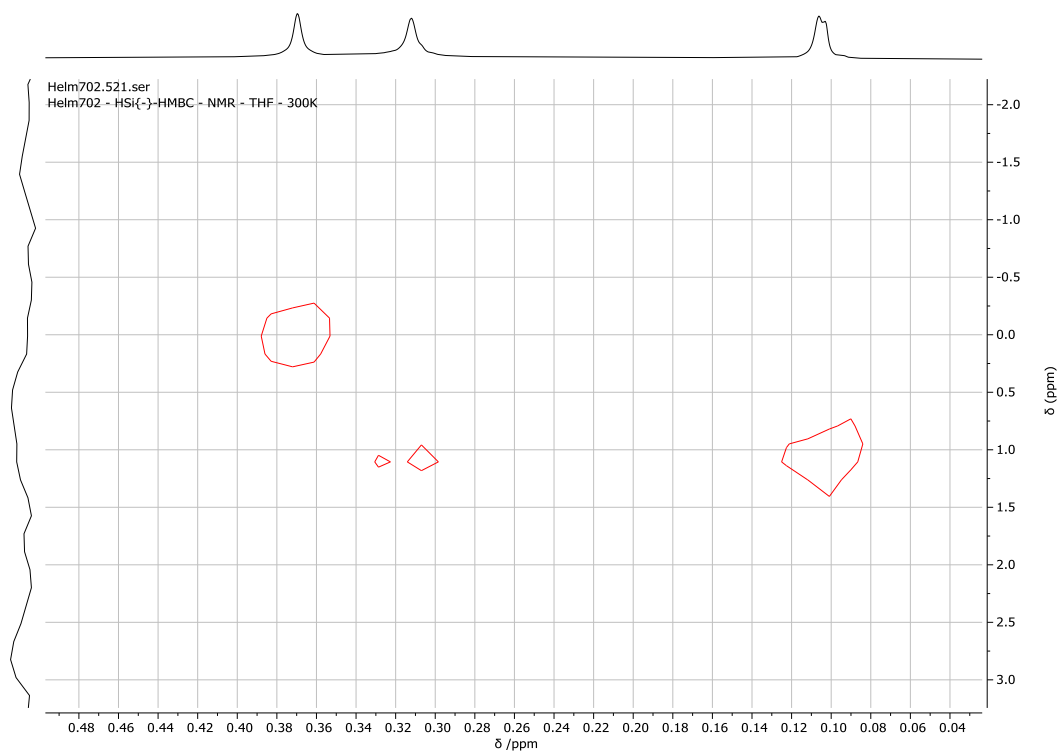


Figure S78. $^1\text{H}, ^{29}\text{Si}$ -HMBC-NMR spectrum (d_8 -THF, 300 K) of reductive dehalogenation of **2** with Mg*.

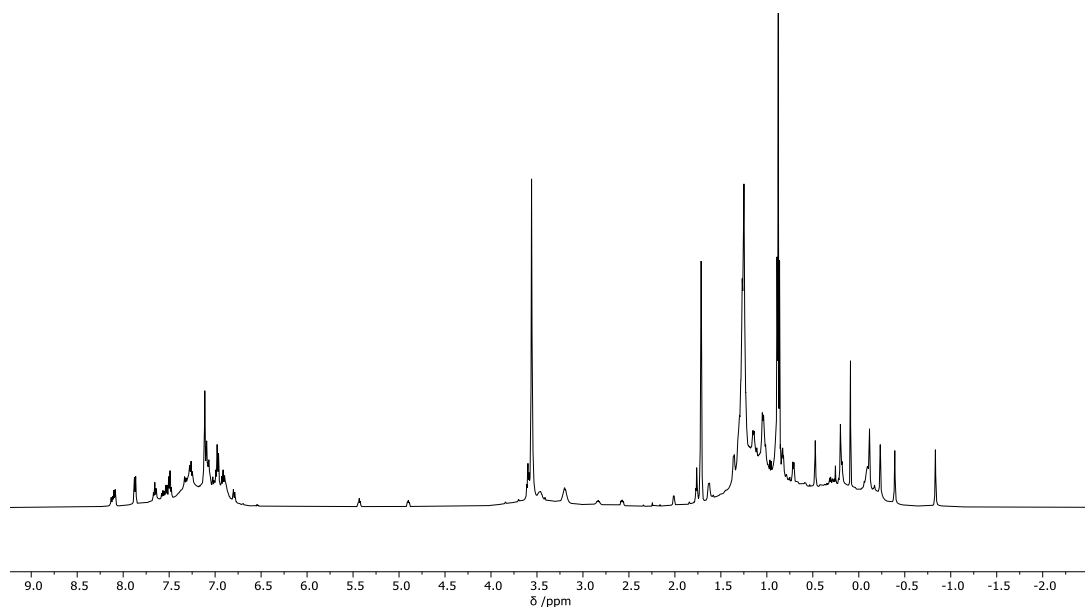


Figure S79. ¹H-NMR spectrum (*d*₈-THF, 210 K, 400 MHz) of reductive dehalogenation of **2** with Mg*.

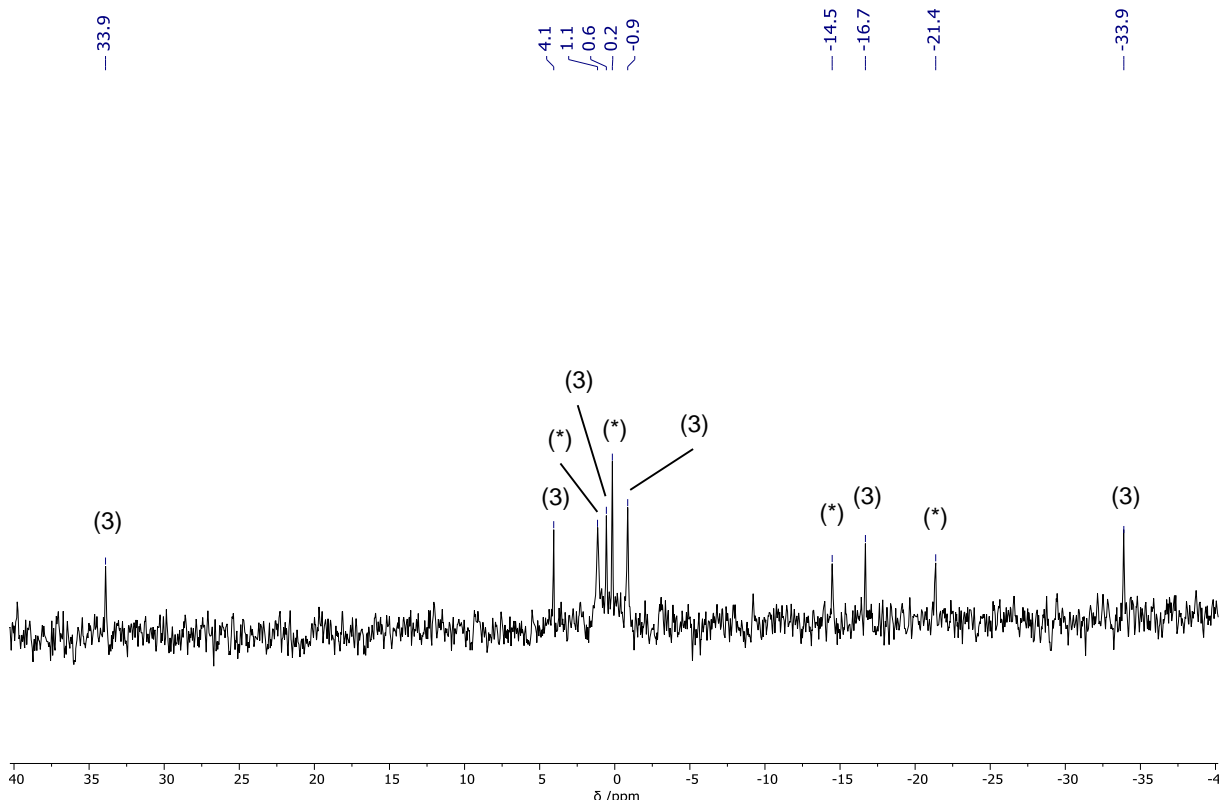


Figure S80. ²⁹Si{¹H}-IG-NMR spectrum (*d*₈-THF, 210 K, 80 MHz) of reductive dehalogenation of **2** with Mg*.

3. Details of Single Crystal X-ray Diffraction Analyses

Crystals of **1**, **2**, **3**·(1.5 PhMe), **8**, and **19'** were removed from a Schlenk tube under an argon atmosphere and covered with a layer of hydrocarbon oil. A suitable crystal was selected, attached to a glass fiber, and quickly placed in a low temperature argon stream. The data were collected^{S4} at 100 K on a Bruker Venture with Mo K α radiation ($\lambda = 0.71073 \text{ \AA}$) and corrected for Lorentz and polarization effects with SAINT^{S4} and absorption using Blessing's method^{S5} as incorporated into the program SADABS.^{S6,S7} Crystal structures were solved by using the SHELXTL program package to determine the space group based upon intensity statistics.^{S8} The structure was determined by direct methods with a majority of the non-hydrogen atoms from the molecule of interest being located directly using the program SHELXS.^{S9} Refinement of the structure was achieved using the program SHELXL with all non-hydrogen atoms refined anisotropically.^{S10} Difference-Fourier least-squares refinement cycles were required to locate all non-hydrogen atoms.

3.1. Refinement Details

For compounds **1**, **2**, **8**, and **19'**, no constraints or restraints were used in the refinement. However, compound **3** co-crystallises with the solvent toluene (PhMe). One of the solvent molecules is located next to a symmetry element and was treated with PART-1, SIMU, and DELU instructions. In addition, three reflexes were omitted because they were affected by the beam stopper.

Table S1. Crystal Data and Structure Refinement for **1**, **2**, and **3·(1.5PhMe)**

Compound	1	2	3·(1.5PhMe)
Empirical formula	C ₄₀ H ₅₆ Li ₂ N ₂ Si ₂	C ₂₀ H ₂₈ Br ₃ NSi ₂	C ₁₄₁ H ₁₉₂ Br ₂ N ₆ Si ₁₂
Formula weight [g·mol ⁻¹]	634.92	578.34	2467.89
Crystal colour, shape	colourless, block	colourless, plate	yellow, rod
Crystal size [mm ³]	0.347 × 0.366 × 0.539	0.299 × 0.488 × 0.490	0.136 × 0.249 × 0.594
Crystal system	monoclinic	monoclinic	triclinic
Space group	P2 ₁ /n	Cc	P-1
<i>a</i> [Å]	11.5185(4)	17.261(2)	12.7757(5)
<i>b</i> [Å]	12.5920(5)	8.5278(11)	13.7788(5)
<i>c</i> [Å]	12.8943(5)	16.840(2)	21.0655(8)
α [°]	90	90	104.3480(10)
β [°]	91.9280(10)	106.535(5)	103.6750(10)
γ [°]	90	90	100.7350(10)
<i>V</i> [Å ³]	1869.14(12)	2376.3(5)	3370.6(2)
<i>Z</i>	2	4	1
<i>T</i> [K]	116(2)	100(2)	100(2)
Compl. to θ 25.24° [%]	99.9	99.9	99.7
ρ _{calc} [g·cm ⁻³]	1.128	1.617	1.216
μ(Mo) [mm ⁻¹]	0.124	5.199	0.759
2θ range [°]	4.52–54.33	5.05–54.25	4.40–54.31
Reflections measured	15883	18654	43534
Independent reflections	4123	5127	14872
<i>R</i> (int)	0.0332	0.0506	0.0377
Ind. reflections (<i>I</i> > 2σ(<i>I</i>))	3565	5004	13265
Parameters	208	236	746
Restraints	—	—	57
<i>R</i> ₁ (<i>I</i> > 2σ(<i>I</i>))	0.0433	0.0224	0.0444
<i>wR</i> ₂ (all data)	0.1275	0.0531	0.1168
<i>GooF</i> (all data)	1.011	1.033	1.049
Max. peak/hole [e ⁻¹ ·Å ⁻³]	0.356 / -0.329	0.448 / -0.487	2.078 / -0.754
Absorption correction	multi-scan	multi-scan	multi-scan
Min. / Max. transmission	0.5909 / 0.7455	0.3020 / 0.7455	0.6264 / 0.7455

Table S2. Crystal Data and Structure Refinement for **8** and **19'**

Compound	8	19'
Empirical formula	C ₄₂ H ₆₀ Br ₂ N ₂ Si ₄	C ₄₅ H ₇₈ BrN ₃ Si ₆
Formula weight [g·mol ⁻¹]	865.10	909.55
Crystal colour, shape	colourless, plate	orange, plate
Crystal size [mm ³]	0.159 × 0.427 × 0.681	0.370 × 0.403 × 0.619
Crystal system	monoclinic	monoclinic
Space group	P2 ₁ /c	C2/c
<i>a</i> [Å]	18.4502(16)	43.0170(13)
<i>b</i> [Å]	8.4359(7)	13.5024(4)
<i>c</i> [Å]	27.821(2)	20.2693(7)
α [°]	90	90
β [°]	93.700(2)	117.158(2)
γ [°]	90	90
<i>V</i> [Å ³]	4321.1(6)	10475.1(6)
<i>Z</i>	4	8
<i>T</i> [K]	100(2)	150(2)
Compl. to θ 25.24° [%]	99.4	99.9
ρ_{calc} [g·cm ⁻³]	1.330	1.153
$\mu(\text{Mo})$ [mm ⁻¹]	2.018	0.953
2 <i>θ</i> range [°]	3.79–54.28	3.20–54.88
Reflections measured	34664	67843
Independent reflections	9488	11861
<i>R</i> (int)	0.0345	0.0487
Ind. reflections (<i>I</i> > 2 σ (<i>I</i>))	8399	8618
Parameters	463	517
Restraints	0	0
<i>R</i> ₁ (<i>I</i> > 2 σ (<i>I</i>))	0.0440	0.0541
<i>wR</i> ₂ (all data)	0.0983	0.1540
<i>GooF</i> (all data)	1.227	1.042
Max. peak/hole [e ⁻¹ ·Å ⁻³]	1.073 / -0.563	0.920 / -0.338
Absorption correction	multi-scan	multi-scan
Min. / Max. transmission	0.5155 / 0.7455	0.6413 / 0.7455

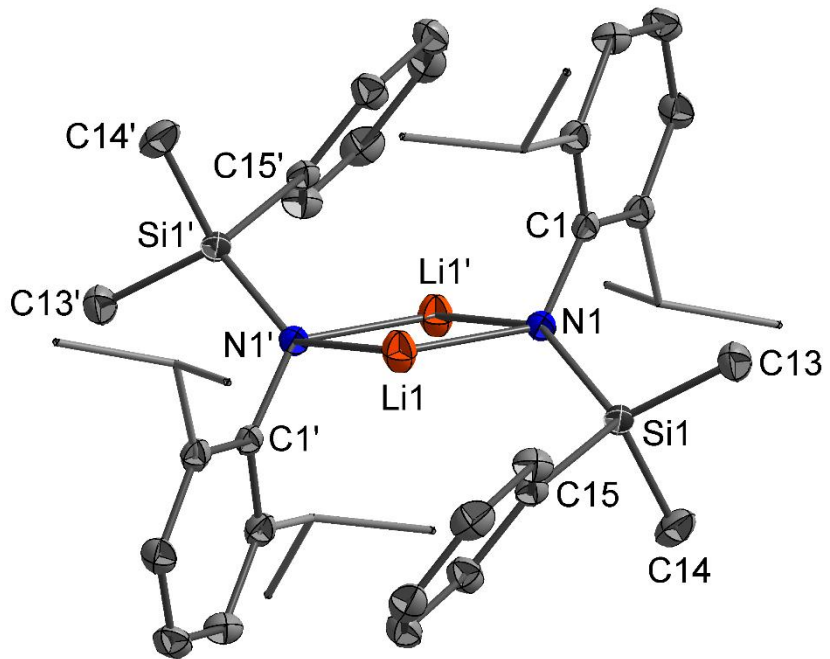


Figure S81. Molecular structure of **1** in the solid state. Thermal ellipsoids are drawn at 50% probability level and hydrogen atoms are omitted for clarity. Selected bond lengths [Å] and angles [°]: Li1–Li1' 2.4143(1), Li1–Ni1 2.0204(1), Li1–N1' 1.9888(1), C1–N1 1.4191(0), Si1–N1 1.7094(0), Si1–C13 1.8706(1), Si1–C14 1.8831(1), Si1–C15 1.8928(1), Li1–N1–Li1' 74.048(1), C1–N1–Si1 119.520(2), C13–Si1–C14 105.741(1), C14–Si1–C15 104.959(1), C13–Si1–C15 108.536(1), C13–Si1–N1 112.826(1), C14–Si1–N1 117.675(1), C15–Si1–N1 106.573(2), C1–N1–L1 90.899(1), C1–N1–Li1' 127.006(2), S1–N1–Li1' 103.104(1).

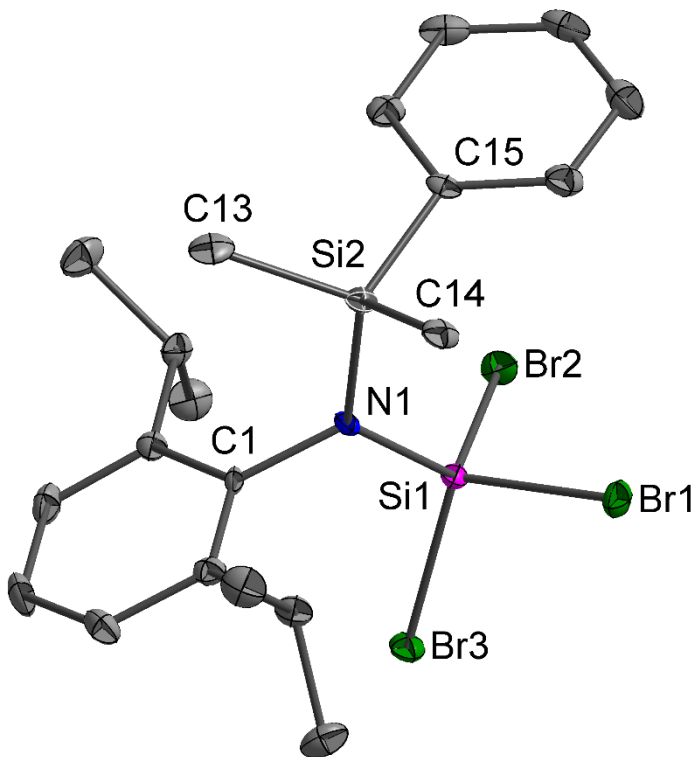


Figure S82. Molecular structure of **2** in the solid state. Thermal ellipsoids are drawn at 50% probability level and hydrogen atoms are omitted for clarity. Selected bond lengths [Å] and angles [°]: Br1–Si1 2.2065(10), Br2–Si1 2.2056(10), Br3–Si1 2.2004(10), Si1–N1 1.696(3), Si2–N1 1.785(3), Si2–C14 1.880(4), Si2–C13 1.882(4), Si2–C15 1.891(4), N1–C1 1.461(4), N1–Si1–Br3 110.55(11), N1–Si1–Br2 115.31(11), Br3–Si1–Br2 106.28(4), N1–Si1–Br1 111.71(11), Br3–Si1–Br1 106.86(4), Br2–Si1–Br1 105.61(4), N1–Si2–C14 112.53(16), N1–Si2–C13 107.94(15), C14–Si2–C13 107.98(18), N1–Si2–C15 107.18(14), C14–Si2–C15 109.65(16), C13–Si2–C15 111.59(17), C1–N1–Si1 117.7(2), C1–N1–Si2 117.9(2), Si1–N1–Si2 124.34(17).

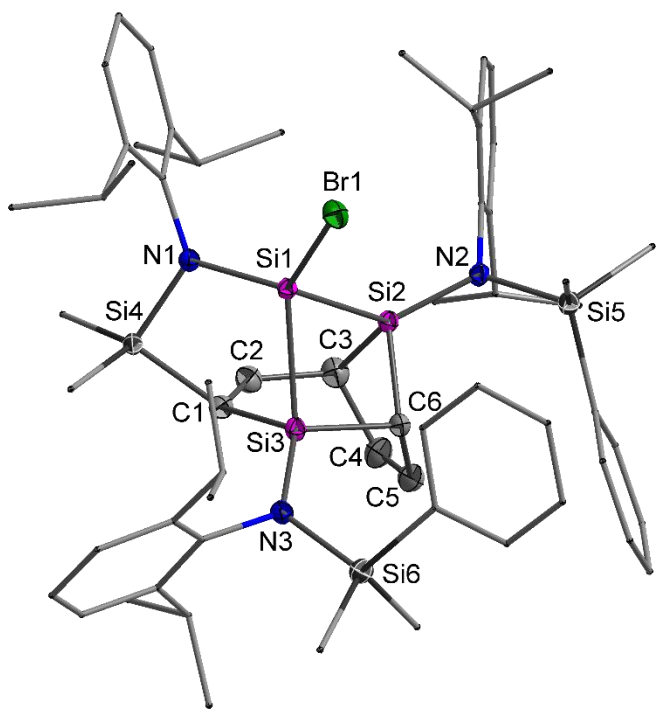


Figure S83. Molecular structure of **3** in the solid state. Thermal ellipsoids are drawn at 50% probability level and hydrogen atoms are omitted for clarity. Selected bond lengths [Å] and angles [°]: Br1–Si1 2.2478(6), Si1–Si2 2.4201(8), Si1–Si3 2.3486(8), Si2–Si3 2.8181(8), Si2–C6 1.906(2), Si2–C3 1.947(3), Si3–C1 1.886(2), Si3–C6 1.889(2), Si4–C1 1.898(2), C1–C2 1.370(3), C2–C3 1.517(3), C3–C4 1.519(3), C4–C5 1.329(4), C5–C6 1.508(3), Si1–N1 1.7374(19), Si2–N2 1.7354(19), Si3–N3 1.7408(19), Si4–N1 1.7747(19), Si5–N2 1.7639(19), Si6–N3 1.7591(19), N1–Si1–Br1 109.98(7), N1–Si1–Si3 108.49(7), Br1–Si1–Si3 124.44(3), N1–Si1–Si2 125.14(7), Br1–Si1–Si2 112.93(3), Si3–Si1–Si2 72.43(3), N2–Si2–C6 113.16(9), N2–Si2–C3 117.36(10), C6–Si2–C3 88.37(11), N2–Si2–Si1 128.72(7), C6–Si2–Si1 89.60(7), C3–Si2–Si1 108.13(8), N2–Si2–Si3 149.51(7), C6–Si2–Si3 41.80(7), C3–Si2–Si3 83.94(8), Si1–Si2–Si3 52.61(2), N3–Si3–C1 119.97(10), N3–Si3–C6 112.44(9), C1–Si3–C6 108.21(10), N3–Si3–Si1 139.06(7), C1–Si3–Si1 78.59(7), C6–Si3–Si1 92.20(7), N3–Si3–Si2 154.05(7), C1–Si3–Si2 80.89(7), C6–Si3–Si2 42.27(7), Si1–Si3–Si2 54.96(2), C2–C1–Si3 118.84(18), C2–C1–Si4 109.93(17), Si3–C1–Si4 113.65(11), C1–C2–C3 128.0(2), C2–C3–C4 113.4(2), C2–C3–Si2 102.99(16), C4–C3–Si2 101.16(17), C5–C4–C3 116.2(2), C4–C5–C6 117.1(2), C5–C6–Si3 114.21(16), C5–C6–Si2 101.91(16), Si3–C6–Si2 95.93(10).

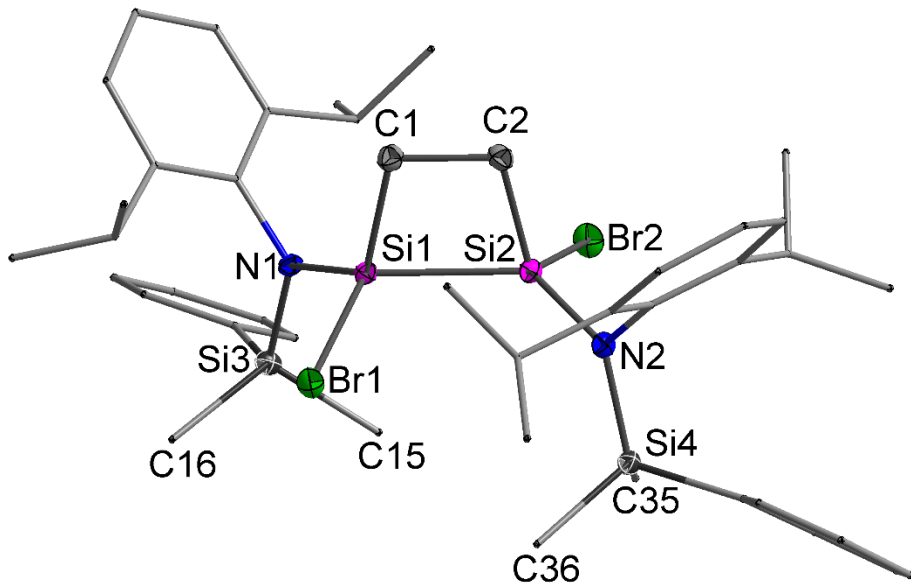


Figure S84. Molecular structure of **8** in the solid state. Thermal ellipsoids are drawn at 50% probability level and hydrogen atoms are omitted for clarity. Selected bond lengths [Å] and angles [°]: C1–C2 1.573(4), Si1–C1 1.888(3), Si2–C2 1.893(3), Si1–Si2 2.3547(11), Br1–Si1 2.2585(8), Br2–Si2 2.2610(8), Si1–N1 1.726(2), Si2–N2 1.723(2), Si3–N1 1.760(3), Si4–N2 1.768(3), N1–C3 1.460(4), N2–C23 1.468(4), C2–C1–Si1 102.02(19), C1–C2–Si2 101.84(19), N1–Si1–C1 114.70(13), N1–Si1–Br1 108.62(9), C1–Si1–Br1 112.25(10), N1–Si1–Si2 129.31(9), C1–Si1–Si2 78.13(10), Br1–Si1–Si2 110.39(4), N2–Si2–C2 115.13(13), N2–Si2–Br2 111.02(9), C2–Si2–Br2 110.04(10), N2–Si2–Si1 127.26(9), C2–Si2–Si1 77.99(9), Br2–Si2–Si1 110.74(4), N1–Si3–C15 106.78(13), N1–Si3–C16 113.51(14), C15–Si3–C16 108.97(16), N1–Si3–C17 111.15(12), C15–Si3–C17 109.72(15), C16–Si3–C17 106.68(15), N2–Si4–C35 110.78(13), N2–Si4–C36 111.53(13), C35–Si4–C36 107.04(14), N2–Si4–C37 110.38(12), C35–Si4–C37 108.98(14), C36–Si4–C37 108.01(13), C3–N1–Si1 117.88(19), C3–N1–Si3 120.51(19), Si1–N1–Si3 121.13(14), C23–N2–Si2 116.29(19), C23–N2–Si4 117.53(18), Si2–N2–Si4 126.13(14).

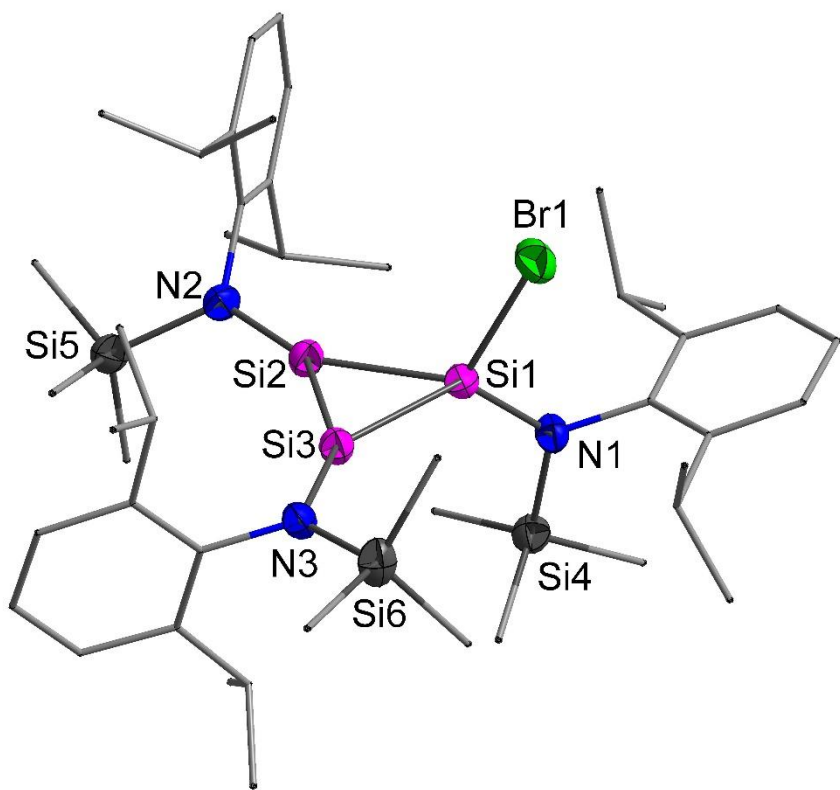


Figure S85. Molecular structure of **19'** in the solid state. Thermal ellipsoids are drawn at 50% probability level and hydrogen atoms are omitted for clarity. Selected bond lengths [Å] and angles [°]: Br1–Si1 2.2580(8), Si1–N1 1.724(2), Si1–Si2 2.2780(10), Si1–Si3 2.2852(10), Si2–N2 1.713(2), Si2–Si3 2.1346(10), Si3–N3 1.709(2), Si4–N1 1.772(2), Si4–C13 1.853(3), Si4–C15 1.853(3), Si4–C14 1.859(3), Si5–N2 1.762(2), Si5–C29 1.845(3), Si5–C30 1.849(3), Si5–C28 1.859(3), Si6–N3 1.759(2), Si6–C45 1.840(4), Si6–C44 1.851(4), Si6–C43 1.854(3), N1–C1 1.455(3), N2–C16 1.455(4), N3–C31 1.452(3), N1–Si1–Br1 103.46(8), N1–Si1–Si2 129.67(8), Br1–Si1–Si2 116.86(4), N1–Si1–Si3 131.16(9), Br1–Si1–Si3 114.51(4), Si2–Si1–Si3 55.78(3), N2–Si2–Si3 147.33(9), N2–Si2–Si1 150.04(9), Si3–Si2–Si1 62.28(3), N3–Si3–Si2 150.46(8), N3–Si3–Si1 147.38(8), Si2–Si3–Si1 61.94(3), N1–Si4–C13 111.60(13), N1–Si4–C15 108.46(13), C13–Si4–C15 107.32(17), N1–Si4–C14 111.52(13), C13–Si4–C14 108.43(17), C15–Si4–C14 109.41(16), N2–Si5–C29 107.94(14), N2–Si5–C30 110.49(13), C29–Si5–C30 109.38(17), N2–Si5–C28 109.03(14), C29–Si5–C28 111.73(17), C30–Si5–C28 108.28(18), N3–Si6–C45 108.45(15), N3–Si6–C44 107.67(15), C45–Si6–C44 111.9(2), N3–Si6–C43 110.93(13), C45–Si6–C43 108.61(19), C44–Si6–C43 109.28(17), C1–N1–Si1 122.44(17), C1–N1–Si4 115.82(17), Si1–N1–Si4 121.67(13), C16–N2–Si2 115.80(17), C16–N2–Si5 120.96(17), Si2–N2–Si5 122.60(13), C31–N3–Si3 115.53(17), C31–N3–Si6 122.31(18), Si3–N3–Si6 122.11(13).

4. Computational Details

The geometries of compounds **5–7** and **10–19** along with those of the associated transition states, were optimised in the gas phase with density functional theory using the PBE1PBE functional,^{S11–S14} def2-TZVP basis sets,^{S15} and Grimme's D3 dispersion correction with Becke-Johnson damping,^{S16,S17} and employing the Gaussian 16-C.01 program suite.^{S18} The structures were confirmed to be either minima or first order transition states on the potential energy hypersurface *via* calculation of the associated vibrational frequencies (all positive or one imaginary, respectively). The nature of all transition states found was further confirmed by following the reaction coordinate to both forward and reverse directions. Table S3 includes the Gibbs free energies of all investigated species, while their structures are provided in a separate coordinate file in standard xyz-format.

Table S3. Calculated Gibbs Free and Relative Energies [kJ mol⁻¹] of **5–7** and **10–19**

Compound	Gibbs Free Energy	Relative Energy
5	-7970.947205	—
6_{long}	-2823.072150	—
6_{short}	-2823.061687	—
7	-3985.469978	—
6_{long} + 7	-6808.542128	0
10	-6808.552671	-28
TS 10-11	-6808.530344	31
11	-6808.542330	-1
TS 11-12	-6808.527235	39
12	-6808.568659	-70
TS 12-13	-6808.550730	-23
13	-6808.568921	-70
TS 13-14	-6808.564036	-58
14	-6808.604935	-165
TS 14-15	-6808.592014	-131
15	-6808.592984	-134
TS 15-16	-6808.587758	-120
16	-6808.602633	-159
TS 16-17	-6808.586553	-117
3	-6808.625636	-219
TS 6-17	-2823.056969	40
17	-2823.078936	-18
TS 17-18	-2823.058538	36
18	-2823.084939	-34
TS 10-19	-6808.537936	11
19	-6808.611084	-181

5. References

- [S1] R. D. Rieke, *Science*, 1989, **246**, 1260.
- [S2] R. D. Rieke, *Acc. Chem. Res.*, 1977, **10**, 301.
- [S3] A. V. Protchenko, K. H. Birjkumar, D. Dange, A. D. Schwarz, D. Vidovic, C. Jones, N. Kaltsoyannis, P. Mountford and S. Aldridge, *J. Am. Chem. Soc.*, 2012, **134**, 6500.
- [S4] Bruker SMART APEX (2012-10.6) and SAINT (Version 8.27a), Bruker AXS Inc.: Madison, Wisconsin, USA, 2012.
- [S5] R. H. Blessing, *Acta Cryst.*, 1995, **A51**, 33.
- [S6] SADABS, An empirical absorption correction program, part of the SAINTPlus NT version 5.0 package, Bruker AXS Inc.: Madison, Wisconsin, USA, 1998.
- [S7] G. M. Sheldrick, SADABS-2012/1 ‘Siemens Area Detector Absorption Correction’, Universität Göttingen: Göttingen, Germany, 2012.
- [S8] G. M. Sheldrick, SHELLXTL 6.1, Siemens Analytical X-ray Instruments Inc.: Madison, Wisconsin, USA, 2002.
- [S9] G. M. Sheldrick, SHELLXS97, Universität Göttingen: Göttingen, Germany, 1997.
- [S10] G. M. Sheldrick, SHELLXL2014 Program for refinement of Crystal structures, Universität Göttingen: Göttingen, Germany, 2014.
- [S11] J. P. Perdew, K. Burke and M. Ernzerhof, *Phys. Rev. Lett.*, 1996, **77**, 3865.
- [S12] J. P. Perdew, K. Burke and M. Ernzerhof, *Phys. Rev. Lett.*, 1996, **78**, 1396.
- [S13] C. Adamo and V. Barone, *J. Chem. Phys.*, 1999, **110**, 6158.
- [S14] M. Ernzerhof and G. E. Scuseria, *J. Chem. Phys.*, 1999, **110**, 5029.
- [S15] F. Weigend and R. Ahlrichs, *Phys. Chem. Chem. Phys.*, 2005, **7**, 3297.
- [S16] S. Grimme, J. Antony, S. Ehrlich and H. Krieg, *J. Chem. Phys.*, 2010, **132**, 154104.
- [S17] S. Grimme, S. Ehrlich and L. Goerigk, *J. Comput. Chem.* 2011, **32**, 1456.
- [S18] Gaussian 16, Revision C.01, M. J. Frisch, G. W. Trucks, H. B. Schlegel, G. E. Scuseria, M. A. Robb, J. R. Cheeseman, G. Scalmani, V. Barone, G. A. Petersson, H. Nakatsuji, X. Li, M. Caricato, A. V. Marenich, J. Bloino, B. G. Janesko, R. Gomperts, B. Mennucci, H. P. Hratchian, J. V. Ortiz, A. F. Izmaylov, J. L. Sonnenberg, D. Williams-Young, F. Ding, F. Lipparini, F. Egidi, J. Goings, B. Peng, A. Petrone, T. Henderson, D. Ranasinghe, V. G. Zakrzewski, J. Gao, N. Rega, G. Zheng, W. Liang, M. Hada, M. Ehara, K. Toyota, R. Fukuda, J. Hasegawa, M. Ishida, T. Nakajima, Y. Honda, O. Kitao, H. Nakai, T. Vreven, K. Throssell, J. A. Montgomery, Jr., J. E. Peralta, F. Ogliaro, M. J. Bearpark, J. J. Heyd, E. N. Brothers, K. N. Kudin, V. N. Staroverov, T. A. Keith, R. Kobayashi, J. Normand, K.

Raghavachari, A. P. Rendell, J. C. Burant, S. S. Iyengar, J. Tomasi, M. Cossi, J. M. Millam, M. Klene, C. Adamo, R. Cammi, J. W. Ochterski, R. L. Martin, K. Morokuma, O. Farkas, J. B. Foresman and D. J. Fox, Gaussian, Inc.: Wallingford Connecticut, USA, 2016.